ANALYTICAL MODELLING OF BACTERIAL MIGRATION AND ACCUMULATION WITH RATE-LIMITED SORPTION IN DISCRETE FRACTURES

MELIHA BEYZA YAZICIOGLU, BSc.

A thesis submitted to the
Department of Earth Sciences
Brock University,
St.Catharines, Ontario

in partial fulfillment of the requirements for
the degree of Master of Science.

I dedicate this Masters' Thesis to the memory of beloved grandparents...

Ibrahim Ethem Kirman (1918-2000) and

Muzeyyen Kirman (1926-1999)

&

Mustafa Yazicioglu (1902-1969) and

Meliha Yazicioglu (1914-1967)

ABSTRACT

An analytical model for bacterial accumulation in a discrete fracture has been developed. The transport and accumulation processes incorporate into the model include advection, dispersion, rate-limited adsorption, rate-limited desorption, irreversible adsorption, attachment, detachment, growth and first order decay both in sorbed and aqueous phases. An analytical solution in Laplace space is derived and numerically inverted. The model is implemented in the code BIOFRAC which is written in Fortran 99.

The model is derived for two phases, Phase I, where adsorption-desorption are dominant, and Phase II, where attachment-detachment are dominant. Phase I ends when enough bacteria to fully cover the substratum have accumulated. The model for Phase I was verified by comparing to the Ogata-Banks solution and the model for Phase II was verified by comparing to a non-Homogenous version of the Ogata-Banks solution. After verification, a sensitivity analysis on the input parameters was performed. The sensitivity analysis was conducted by varying one input parameter while all others were fixed and observing the impact on the shape of the curve describing bacterial concentration versus time.

Increasing fracture aperture allows more transport and thus more accumulation, which diminishes the duration of Phase I. The larger the bacteria size, the faster the substratum will be covered. Increasing adsorption rate, was observed to increase the duration of Phase I.

Contrary to the assumption of uniform biofilm thickness, the accumulation starts from the inlet, and the bacterial concentration in aqueous phase moving towards the outlet declines, slowing the accumulation at the outlet. Increasing the desorption rate, reduces the duration of Phase I, speeding up the accumulation. It was also observed that Phase II is of longer duration than Phase I. Increasing the attachment rate lengthens the accumulation period. High rates of detachment speeds up the transport. The growth and decay rates have no significant effect on transport, although increases the concentrations in both aqueous and sorbed phases are observed. Irreversible adsorption can stop accumulation completely if the values are high.

TABLE OF CONTENTS

LIST OF FIGURES

LIST OF TABLES

LIST OF SYMBOLS AND ABBREVIATIONS

v: Advective fluid velocity (L/T)

c: Concentration of bacteria in the fluid (M/L^3)

x: Coordinate direction taken along the direction of flow

t: Time

D: Coefficient of hydrodynamic dispersion (L^2/T)

α: Longitduinal dispersivity (L)

D*: Coefficient of molecular diffusion (L^2/T)

G: Mass adsorbed over unit volume of media times time ($M \times T/L^3$)

θ: Porosity

CH: Cell height (L)

CL: Cell length (L)

CW: Cell width (L)

ρ_b: Dry bulk density of solids in porous media (M/L^3)

s: Concentration of adsorbed bacteria (M/L^3)

λ: Decay constant of bacteria (1/T)

μ: Specific growth rate of bacteria (1/T)

S: Substrate concentration (M/L^3)

Ks: Monod half velocity coefficient (M/L^3)

μ_{max}: Maximum specific growth rate of bacteria (1/T)

k_p: Irreversible adsorption constant (1/L)

k_1: Rate-limited adsorption coefficient (1/T)

k_2: Rate-limited desorption coefficient (1/T)

k_{at}: Attachment coefficient (1/T)

k_{det}: Detachment coefficient (1/T)

A: Surface area to void space volume ratio (1/L)

SA: Surface area (L^2)

V: Void space volume (L^3)

W: Fracture width (L)

L: Fracture length (L)

2b: Fracture aperture (L)

τ: Time when attachment-detachment dominates adsorption-desorption (T)

c_τ: Concentration at τ (M/L^3)

c_0: Source concentration (M/L^3)

H(t-t'): Heaviside step function

t': Duration of constant input (T)

B: Decay constant

NLL: Number of layers of biofilm

p: Laplace variable

NFL: Fracture length (L)

XFW: Fracture width (L)

XCHECK: Number of bacterial cells that are necessary to cover both fracture walls

AVSORB: Average sorbed bacterial concentration in fracture (M/L^3)

XCMASS: Mass of one bacterial cell (M)

ROWTOT: Average concentration in the fracture at a certain time (M/L^3)

TSTOP: Duration of simulation (T)

XGAP: Time when attachment-detachment dominates adsorption-desorption in the code (T)

ACKNOWLEDGEMENTS

I would like to sincerely thank my supervisor, Kent Novakowski, for his assistance, guidance and advice throughout this thesis. Without the incredible academic and financial support he has supplied, as well as his patience during editing, this work would not have been possible. I also would like to acknowledge his mentorship during my studies.

I would like to thank Pat Lapcevic for her support during the initial stages of this study. I would like to acknowledge Nathalie Ross (National Water Resources Institute) for helping me understand the biological processes and sharing her experimental data.

I appreciate the tireless efforts of my life long friend Zeynep Akyol (University of Iowa, Biological Sciences Department) and would like to acknowledge her great help with my research with growth and decay rates. I would also like to thank Volkan Celik (Canada Life Insurance Co.) for his emotional support as well as his technical support with math and coding.

Many thanks to my brother I. Murat Yazicioglu for helping me with geology, being a great friend and always making me laugh.

I also would like to thank Mike Lozon for helping me draw several figures and Diane Gadoury for always being nice and ready to help me.

Thanks to Jennifer Hopkins for her support and friendship and understanding what it is to write a thesis. Thanks to John Taylor for always being ready for a chat or a coffee walk.

I would like to acknowledge Ezgi Unal, whom I always consider myself very lucky to have met, and would like to thank her for her unconditional friendship and help throughout my studies.

I would like to thank my life long friends Elif Idil Keser, Metin Talat Guleryuzlu and Sener Kozakoglu for not letting the distance affect our friendship and for providing support.

I appreciate all the efforts and friendship of Chris Cowman and the entire Cowman family, and would like to thank them for welcoming me to Canada and always helping.

Foremost, I owe a lot to my parents Nursel Yazicioglu and Osman Tarik Yazicioglu for continuously supporting me financially and emotionally, as well as trusting in me, always cheering me up on the phone and for making my life beautiful with their presence. I apologize for not being by their side during their hardest times and would like to thank them for their understanding.

1.0 INTRODUCTION

Bacteria are present in most natural subsurface settings. The population of bacteria in groundwater is small and their presence is innocuous in most cases. However, where conditions encourage growth, the population can enlarge to a point where the presence of the bacteria will clog pores and prevent flow. The accumulation of bacteria on the pore surface is commonly referred to as a biofilm (Baveye et al, 1998,Cunningham et al., 1991, Corapcioglu et al., 1997)

By definition, a biofilm is the structure that is composed of an immobilized, organic polymer matrix of cells attached to a solid surface (Characklis et al., 1990). Cunningham et al. (1991) define a biofilm as the entire deposit of cells and polymers, together with captured organic and inorganic particles. Taylor et al. (1990b) explain a biofilm as an accumulation of bacteria with low permeability, high specific surface, narrow and tortuous pores and containing hydrated ionic polymers. In nature, biofilms can grow to a thickness sufficient to completely fill pore spaces. Dennis et al. (1998) states that biofilms in porous media form when aquatic bacteria attach firmly to the soil particle surfaces. This processes occurs also in fractured media in the form where bacteria attach to fracture wall. According to Dennis et al. (1998), formation of biofilm in porous medium causes a reduction in permeability by decreasing the pore volume available for fluid transport. Similarly in fractured media, fluid transport is decreased by reduction of the fracture aperture (Ross et al., 2000).

The bacteria in the biofilm produce a layer of extracellular polymer substances (EPS) in which bacteria live. EPS helps bacteria to adhere to a surface, providing a protective environment. Bacteria can attach to any surface provided that the environment is aquatic. When the bacterial cell is attached, it can grow, reproduce, and decay. EPS extend from the bacterial

cell on the solid surface, forming a tangled matrix of fibers. This tangled matrix provides structure to the biofilm (Characklis et al., 1990). The bacterial cells grow near and at the interface between the water and solid phases and at the layer that biomass and EPS increase (Taylor et al. 1990c, Peyton, 1996).

Dennis et al. (1998) identified different types of bacteria that produce different types of biofilms and have different end products. The properties of the biofilm are highly dependent on the organism and the environment. For example, when a particular bacterium is fed with a nutrient, which has a high carbon-to-nitrogen ratio, the end product is EPS rich with glucuronic acid residues. The residue makes the bacteria more resistant to chemical, biological and physical attacks.

Biofilm production rates are dependent on the type of bacteria and aquatic conditions. Aerobic bacteria have a tendency to produce large quantities of EPS rapidly; however, anaerobic bacteria produce a more uniformly distributed biofilm at a slower rate. Some aerobic bacteria do not produce (EPS) at all when they are under anaerobic conditions; whereas they produce high quantities if dissolved oxygen is present.

A biofilm is composed of layers that can be as thick as 300 to 400 mm (Characklis et al., 1990). When biofilms are of such thickness, both aerobic and anaerobic bacteria may be present. Anaerobic conditions develop because of oxygen diffusion limitations within the biofilm. Thus, a biofilm may not be uniform in composition in time or space, as it is a surface accumulation. Bishop et al. (1995) reports biofilm thickness that range as wide as 52μm to 1710μm. Cunningham et al. (1991) observed biofilm thicknesses of 9μm, 14μm, 40μm and 63μm. Biofilms are usually adsorptive and porous and are greater than 95% water with less than 20% volatile mass (Characklis et al., 1990).

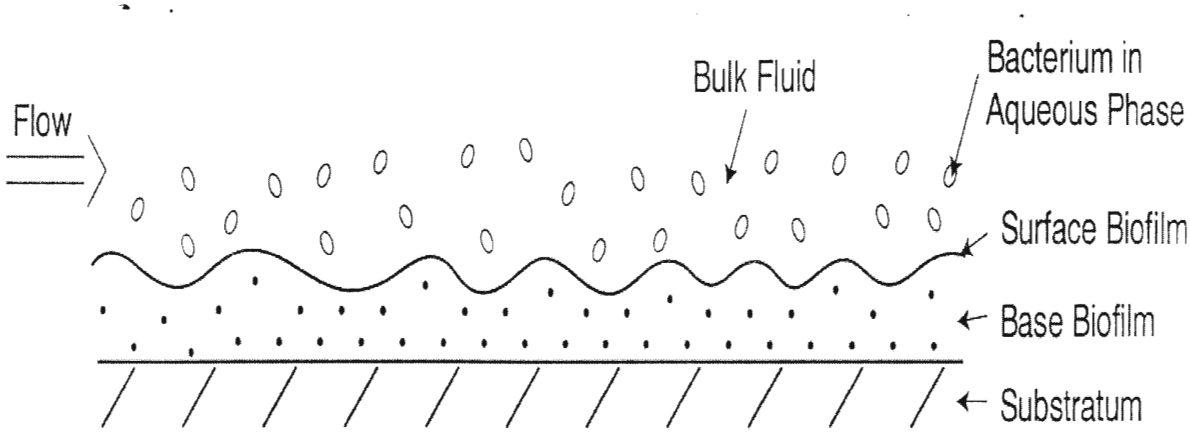

Figure 1.1 Biofilm System

Characklis et al. (1990) describes a biofilm system as a combination of the substratum on which the biofilm is immobilized, the biofilm, and the overlaying gas and/or liquid layer. Characklis et al. (1990) explains this system in five sections:

- The substratum: A solid-phase material, to which the biofilm attaches itself as can be seen in Figure 1.1. The substratum acts as a base upon which the biofilm builds. This compartment is important in the processes that occur during the early stages of accumulation. The composition of the substratum, which is usually an impermeable, non-porous material, may have an influence on the rate of cell accumulation and the initial distribution of cell population.
- The base film: Consists of a structured accumulation. The base film has well defined upper and lower boundaries compared to other sections. Molecular transport of bacteria is dominant in the base film.

- The surface film: Provides a transition between the bulk liquid and the base film. Change in the gradients of certain biofilm properties, in the direction away from the substratum occur in the surface film. For example, biofilm density decreases with distance from the substratum within the surface film. Surface film may exist or may not be present in a biofilm system, and sometimes may extend from bulk liquid compartment to the substratum. Advective transport of bacteria dominates the accumulation of surface film.
- The bulk liquid: A continuous liquid phase, which fills the biofilm and contains different dissolved and suspended particles.
- The gas phase: May be absent in most biofilm systems. This phase provides aeration and sometimes aids in the removal of gaseous products present in the biofilm that occur due to microbial reactions (Characklis et al., 1990). In most groundwater environments, the gas phase is absent. Behrendt et al. (1999) modeled the biofilm including the gas phase, which included gases like carbon dioxide and oxygen. In their study modeling of a fixed bed reactor, bulk liquid phase, gas phase, biofilm, gas reaction rates and alkalinity were described by separate equations.

Several types of processes occur in the biofilm, which lead to accumulation. These are adsorption, desorption, attachment, detachment, growth and decay. The transfer of a suspended particle from one biofilm phase to another (e.g. liquid to solid phase) is considered a transformation process (Characklis et al., 1990).

The initial process involved in biofilm accumulation is sorption. Sorption occurs where a molecule or cell moves from one phase to be accumulated in another, especially when the second phase is solid. This process includes both adsorption and absorption.

According to Characklis et al. (1990) adsorption of bacteria to the substratum is an interfacial transfer process, since the components leave the bulk liquid phase and become a part of the substratum. In the case of adsorption, molecules of a certain phase penetrate another phase and a solution with the second phase is formed. Absorption describes the interaction of water-based components with the biofilm. Adsorption is a two-dimensional process unlike absorption which is a three dimensional process. (Leitao et al., 1996, Wik, 1999, Carlson et al., 1998, Characklis, 1998, Characklis et al, 1990)

There are two types of adsorption. The first is physical adsorption, which is a reversible or equilibrium process. Reversible adsorption involves electro-chemical forces like van der Waals force, (hydrogen bonds between the molecules) and is characterized by low heat of adsorption per chemical bond (Characklis et al., 1990 Leitao et al., 1996, Wik, 1999, Carlson et al., 1998, Characklis, 1998).

The second type of adsorption is an irreversible process and is characterized by a high heat of adsorption per chemical bond. Reversible adsorption refers to an initially weak interaction of the cell with the substratum such that the cell can sometimes even exhibit Brownian motion (Characklis et al., 1990). In the case of irreversible adsorption, bacteria become permanently bonded to the substratum.

The inverse of adsorption is called desorption. Desorption is the movement of bacteria from the substratum back into the bulk liquid. Desorption is an interfacial transfer process consisting of the transfer of cells and other adsorbed components from the substratum compartment to the bulk liquid. The probability of desorption occurrence reduces with the increasing duration of the cell remaining reversibly adsorbed. Thus desorption and adsorption rates are closely related (Characklis et al., 1990).

In this study, sorption processes are assumed to be rate-limited. Many studies involving rate-limited mass transfer coefficients, which is held responsible for nonequilibrium by most researchers, can be found in the literature.

One of the earliest studies is by Lapidus and Amundson (1952) and has been referred to by many researchers. Lapidus and Amundson investigated the effect of longitudinal diffusion in chromatographic and ion exchange columns. They used the assumption of local equilibrium where sorption is much more rapid than advective-dispersive transport. According to Lapidus and Amundson, the equilibrium assumption is not realistic at flow rates commonly encountered in nature.

In a 1989 study by Brusseau et al., processes responsible for nonequilibrium are grouped into two cases. The first case is the transport related nonequilibrum, (also known as physical nonequilibrium), which occurs in the regions in the porous media where the advective flow is minimal. Authors indicate that diffusive mass transfer of solute between the nonadvective flow and advective flow regions results in the former behaving as distributed source and sink components. Early initial breakthrough resulting from rapid transport in the advective domain and tailing are typical in such cases. The mass transfer between mobile and immobile regions is by diffusion. The second case is sorption related nonequilibrium, which results from chemical nonequilibrium and intrasorbent diffusion where the main source is rate-limited sorption. Transport related and sorption related non-equilibrium are different since transport related non-equilibrium is more similar to a solid diffusion, whereas sorption related nonequilibrium is a pore diffusion process (Lindqvist et al. 1995).

Maraqa (2001), studied mass transfer rates for solute transport in porous media. He defines physical non-equilibrium as rate-limited mass transfer between sorbed and aqueous

phases. His study demonstrated that mass-transfer coefficients are dependent on several system parameters such as velocity, length, and retardation coefficients.

According to Fry et al.(1993), who modeled the advection-dispersion equation with rate-limited desorption and first order decay only in the aqueous phase, in some contaminated aquifers, contaminant desorption from sorbed phase to aqueous phase limits the remediation rate. Thus, Fry et al. (1993) finds rate-limited sorption models useful for modeling purposes.

In the literature, non equilibrium has been approached in various ways: either all the sorption sites are time dependent or part of the sorbed phase is in equilibrium with the sorbed phase and the other part is time dependent. Brusseau et al., (1991) indicated the importance of nonequilibrium processes and conducted his research using a two-compartment model where an initial, rapid phase of adsorption/desorption is followed by extended, much slower period. Brusseau (1995) modeled nonlinear, rate-limited sorption, which is essentially instantaneous for a fraction of sorbent and rate-limited for the rest. Brusseau (1995) indicates that when transformations occur in the solution mainly, rate-limited sorption processes can reduce the rate at which mass is transformed. He also added that the effects of rate-limited sorption are similar to nonlinear-instantaneous sorption where the only difference is that rate-limited sorption arrives earlier when relative concentration is plotted versus pore volumes. A third approach is given by expressing the non-equilibrium process as a diffusive transfer between the sorbed and aqueous phases. This can also be expressed using a spherical diffusion model where the concentration in the sorbed phase changes with the distance between the aqueous and sorbing phases. (Fry et al., 1993, Murali et al., 1983, Miller et al., 1984, vanGenuchten et al, 1981, Selim et al., 1988, vanGenuchten et al., 1976, Goltz et al., 1986, Lindstrom, 1976).

Brusseau et al. (1996) studied the effects of rate-limited mass transfer processes coupled with other mechanisms. Similarly, Karapanagioti et al. (2001) studied coupling of nonlinear and nonequilibrium sorption. Brusseau et al. (1996) tested the capability of a multiprocess nonequilibrium model to simulate transport by using data obtained from miscible displacement experiments. Brusseau et al. (1997a) have conducted several studies on a natural-gradient experiment conducted at the Borden aquifer with reactive solutes to investigate effects of sorption on transport. Brusseau et al. (1997b, 1989) conducted several research on non-ideal transport and sorption and discussed previous studies (Goltz et al., 1986), which have focused on rate-limited sorption as the cause of non-ideality. The term non-ideality, used both for transport and sorption, refers to dual porosity (advective-nonadvective together) media and two domain (instantaneous and rate-limited together) sorption, where sorption may be instantaneous or rate-limited in either of the two porosity domains (Brusseau et a. 1996). He concluded that rate-limited sorption had a relatively minor influence on transport. According to Brusseau et al. (1997a), the rate-limited sorption is responsible for the spreading behavior when coupled with non-linearity. Brusseau et al. (1997b) tried to identify factors causing nonideality by using flow interruption. They investigated specific process pairs, mainly the rate-limited processes such as rate-limited sorption, diffusional mass transfer, and transformation reactions. They found that rate-limited sorption can cause breakthrough curves to exhibit tailing. In his studies Brusseau indicated that in transport and sorption multiple factors and processes are involved and it is critical to consider possible interactions among them. Brusseau's transport and sorption studies were restricted strictly to porous media.

Goltz et al., 1991, investigated several rate-limited sorption approaches, such as a first-order rate model, a layered diffusion model, a cylindrical diffusion model and a spherical

diffusion model while searching for the reason of decline in the contaminant load discharged by extraction wells with time during aquifer cleanup via extraction wells. This behavior was related to rate-limited desorption of an organic contaminant from aquifer solids. It was concluded that a first-order rate model could be used to approximate both extraction well breakthrough concentrations and mass remaining in the aquifer simulated by the more complex diffusion models and showed that rate-limited sorption can have a significant impact upon aquifer remediation.

Similar with Fry et al. (1983), previous studies such as Lindstrom(1976) solved the advection-dispersion equation using rate-limited desorption and first order decay, however used different initial and boundary conditions. Huang et al. (2001) did similar research to Fry et al. (1983), but with dual porosity. Logan, 1996 studied rate-limited adsorption with periodic boundary conditions. Fortin et al., 1997 published their research on column flow experiments under saturated conditions to investigate the sorption behavior of simazine and the outflow results showed that there was a nonequilibrium, which they found, was due to the rate-limited sorption. Lindqvist et al., 1995 examined the contribution of cell characteristics to variation of sorption rate and transport of bacteria by using rate-limited sorption. They analyzed bacteria in saturated soil columns and found out that motile cells absorbed faster than non-motile cells, especially at a lower density around 6×10^6 cells ml^{-1}. Also, Lindqvist et al. observed that sorption rate increased and the peak effluent concentration decreased as high interstitial water velocities compressed the hydrodynamic boundary layer. Their conclusion was that sorption was limited by diffusive mass transfer.

Laboratory investigations suggest that transport of bacteria is a non-equilibrium process, controlled by non-equilibrium sorption. (Lindqvist et al., 1991, Hornberger et al., 1992,

Lindqvist et al. 1992b) Bacteria are transported to the substratum by diffusion over the hydrodynamic boundary later, in case of laminar flow, extending several microns beyond the substratum surface (Characklis et al., 1990). As indicated by Busscher et al (1987), closer to the surface, less than 50nm, the physical and chemical properties of the substratum and bacteria become rate-limiting. Thus in this study, rate-limited adsorption and desorption are used. An advantage of using rate-limited coefficients is that the effects of changing rates of adsorption-desorption can easily be compared to changing rates of attachment-detachment.

Attachment is the process where cells are captured by the biofilm, and refers to the advective and diffusive interaction of the bulk liquid with the biofilm. Attachment occurs after a biofilm is formed when the substratum is covered and there is no interaction between the bulk fluid and the substratum. The difference between adsorption and attachment is that adsorption occurs at the liquid-substratum interface, while attachment occurs at biofilm-liquid interface. (Characklis et al., 1990). Kornegay et al. (1968) explains the attachment kinetics as occurring in three phases. The first phase lasts until the active film thickness is reached and growth is logarithmic. When the active thickness is reached, substrate utilization reaches steady state. After that, the accumulation has no effect on active thickness. During the second phase, film growth is linear. Accumulation during the second phase continues until a plateau thickness is sustained. Then the third phase begins, when accumulation is equal to zero. The newly formed cells are carried away during this phase.

Detachment is the reverse of attachment and is defined as the transport of cells from a biofilm into the bulk liquid. As with attachment, detachment also occurs after the biofilm is formed, at the biofilm-liquid interface. Detachment is different from desorption, since desorption is loss of components from the substratum. Detachment can also be categorized as erosion,

which is the continuous loss of small portions of biofilm due to fluid dynamic conditions; sloughing, which is the rapid, massive loss of biofilm because of an artificial stimulus, and abrasion, which is the loss of biofilm due to repeated collisions. The erosion rate is usually a function of the particulate material concentration in the biofilm (Characklis et al., 1990, Morgenroth et al., 2000). Clement et al. (1997) state that no simple analytical expression has been found to accurately model the underlying phenomena that cause detachment and add that it is difficult to compute detachment rates.

A diagram showing adsorption, desorption, attachment and detachment is given in Figure 1.2.

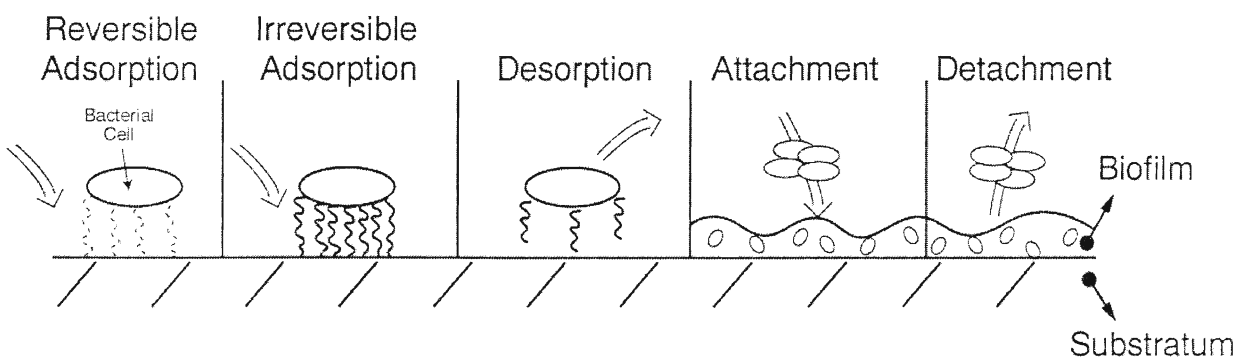

Figure 1.2 Accumulation processes

The detachment rate has a significant effect on biofilm accumulation. At steady state and with a negligible attachment rate, the net rate of biofilm detachment is equal to the net rate of biofilm growth and can be modeled as a first order function of biofilm thickness (Peyton et al., 1992). Once the biofilm is formed, attachment and detachment mechanisms become more important with respect to adsorption and desorption and have more effect on the biofilm accumulation. Attachment and detachment mechanisms are the main mechanisms that provide transport between the biofilm and the bulk fluid (Wanner et al., 1996).

In porous media, attachment and detachment mechanisms are influenced by hydrophobicity of the bacteria. In the continuous-flow column experiments with short-pulse inputs in porous media, McCaulou et al. (1994) observed that hydrophilic bacteria have slower attachment and detachment rates as opposed to hydrophobic bacteria, suggesting that hydrophilic bacteria could be transported further before being removed by attachment to soil. Once attached, however, the bacteria would be resuspended at a slower rate (McCaulou et al., 1994).

Growth and death of bacteria also contribute significantly to biofilm accumulation. Death of the bacteria causes losses from the biofilm. As indicated by Characklis et al. (1990), prior to death and subsequent lysis (destruction), starved cells may shrink in size but still remain viable. These cells begin to grow and reproduce again when a nutrient becomes available. Dennis et al (1998) determined that some bacteria can survive for prolonged periods with minimal nutrient supply.

Growth depends on the availability of the nutrient. Bacteria can starve and remain in a stable population even when nutrient is lacking. Richter et al. (1999) observed that surface roughness is very important in growth. They found that bacteria do not start to grow along scratches and edges on the surface but prefer flatter areas to settle. The growth pattern also depends on the type of bacteria.

Decay of bacteria may result from substrate depletion, toxic metabolite production, introduction of toxic material such as biocides in the cell environment. Cell decay is a first order process with respect to cell concentration.

Hermanowicz (1999) found that only a single soluble nutrient concentration is required to control cell division according to Monod kinetics. Thus the growth of the bacteria is dependent on nutrient concentration. Hermanowicz (1999) also adds that in a biofilm, growing cells must

displace other components to increase biofilm thickness. This displacement concept was implicitly formulated by Wanner et al., (1996) who used one dimensional conservation laws of mass, volume, momentum and energy to describe the process. (Sommer et al., 1995, Morshed et al., 1995, Rashid et al., 1999, Corapcioglu et al., 1997)

Wilderer et al. (2000) studied the competition of biomass in a biofilm. They concluded that an assumption of constant biofilm thickness could cause errors when predicting the performance of systems with large fluctuations of the biofilm thickness over time. The thickness of the biofilm effects both the process rates and the biofilm density. According to Beyenal et al. (2000), biofilm density is also dependent on fluid velocity and when velocity increases, biofilm density increases. In the literature, many studies have been conducted assuming constant biofilm density, independent of biofilm thickness (Grady et al., 1983, Park et al., 1984, Converti et al., 1994). However it was determined that biofilm density is dependent on biofilm thickness. It was also observed that biofilm density reduces as the biofilm thickness increased (Tanyolac et al., 1998).

Bishop et al. (1995) determined that biofilm thickness affects both biofilm structure and its performance. The average biofilm density is strongly affected by the biofilm thickness, resulting in a non-uniform relationship between the average density and the biofilm thickness. Through various chemical and microbiological tests, Bishop et al. (1995) determined that biofilm structure is highly stratified which can be characterized by biofilm density, a decrease of metabolically active biomass and a decrease in porosity with biofilm depth. They explained the reason for this stratification as competition for space and nutrient in the biofilm.

Peyton (1996) found that steady-state biofilm thickness is dependent on the substrate-loading rate. Increase in substrate loading rate significantly increases steady state biofilm

thickness. Thicker biofilms will undergo a higher shear as found by vanLoosdrecht et al. (1995). A higher loading rate will result in higher linear biofilm growth rate.

The processes described above are the mechanisms that are involved in accumulation of bacteria. The transport of bacteria occurs by advective flow and hydrodynamic dispersion. The advection-dispersion equation, that is used to describe the transport of bacteria is based on the premise that the center of mass of the bacteria is moving at the same rate as the average linear ground-water velocity. Hydrodynamic dispersion causes the bacteria to spread out both forward and backward in a pattern that follows a normal distribution. The bacterial front moves at a rate that is greater than the average linear ground water velocity. Dispersion is caused by the heterogeneities in the aquifer. Because of dispersion, the concentration of the bacteria will decrease with distance from the source. The bacteria will spread in the direction of flow (Freeze et al, 1979, Fetter, 1980). A bacterial cell is a passive unit compared to the advective forces of the water carrying the cell at an average linear velocity (Lindqvist et al, 1991). Entire population of cells move from high-density areas to low density areas and also spread out due to mechanical mixing. The resulting hydrodynamic dispersion causes some bacteria to move faster than others relative to the average water velocity. During field-scale tracer tests at the Chalk River Nuclear Laboratories, Champ et al. (1998) observed that bacteria can be very rapidly transported in fracture systems.

Many studies are focused on bacterial addition for the development of a biobarrier via the biostimulation of a microbial population and exopolysaccharides production (Ross et al., 1998). Biostimulation of indigenous bacteria is a concept that has yet to be investigated thoroughly. Biobarriers are used to control the groundwater movement for containment of contamination or biotreatment. When accumulated in a fracture, biofilm can reduce flow significantly.

The presence of biofilms in a medium and the consequential reduction in permeability and porosity has been the focus of many studies in the past (e.g. Dennis et al., 1998, Baveye et al., 1998). Dennis et al. (1998) performed a laboratory study to evaluate the feasibility of creating low-permeability waste containment barriers using soil treated with bacteria to produce a plugging biofilm and at the end they concluded that such plugging may be feasible. The reduction in permeability and or porosity, which can be referred to as plugging, clogging or fouling, suggests a wide range of applications in the control of groundwater contaminant transport (Suchomel et al., 1998). A biofilm accumulation can be a beneficial or an unwanted factor since it can plug pore spaces via the presence of bacterial cells and by the products of bacterial metabolism. The resulting reduction in hydraulic conductivity can have serious unwanted effects on the yield of wells and the efficiency of recharge facilities (Warner et al., 1994). Biofilm plugging has also been implicated in the closure of nutrient injection wells for in-situ bioremediation (Bishop, 1996).

In porous media, reduction of hydraulic conductivity up to three orders of magnitude has been reported by Dennis et al (1998). Shaw et al (1985) concluded that even when bacteria were killed after formation of a biofilm barrier, the biofilm matrix persisted and maintained a reduced hydraulic conductivity.

The reduction of permeability is attributed to the accumulation of biofilm, and also low solubility gases produced by bacteria, precipitation of metals by the activity of sulfate reducing bacteria, deposition of hydroxides produced by bacteria, filtration of suspended particles in groundwater and soil swelling (Vandevivere et al., 1992).

Vandevivere et al. (1992), performed percolation experiments using sand columns and aerobic bacteria and found that bacteria can quickly reduce the saturated hydraulic conductivity

by up to four orders of magnitude. They associated these rapid reductions with the formation of a bacterial mat at the inlet boundary of the sand columns. They concluded that coverage of solid surfaces by bacterial cells is heterogeneous.

Cunningham et al (1991) investigated biofilm accumulation in porous media using biofilm reactors and measured average thickness along a 50mm flow path, porosity and permeability reduction and friction factor increase. They used *pseudomonas aeruginosa* and operated their reactors under constant piezometric head. They observed a decrease in flow rate as biofilm accumulated. The biofilm thickness increased following a sigmoidal curve, reaching values around 60μm. The porosity of the porous media decreased between 50 to 96% as biofilm accumulation increased and permeability decreased around by 92 to 98%. Minimum permeability persisted after the biofilm thickness reached a maximum value.

Ross et al. (2001) developed a device that can measure the changes in hydraulic conductivity of a single fracture after the groundwater in the fracture is microbially stimulated. Their results showed that the limestone fracture became significantly clogged, where hydraulic conductivity reached 0.8% of its initial value of 340cm/min after 22 days. Ketcheson et al. (1997) determined that bioclogging of a fracture network could limit the delivery of nutrients and that would effect all of the nutrient dependent biofilm processes. The presence of biomass in a fracture network effects the groundwater flow by diverting and altering pathways

Thickness is also an important biofilm characteristic because it influences many of the accumulation processes and plays a major role in permeability reduction in porous fractured and fractured media. Detachment and attachment rates change due to increases and decreases in thickness as indicated above. Thickness also influences the diffusion process; changes fluid friction and influences heat transfer. As reported by Characklis et al (1990), biofilm thickness

can range between 10 to 1000μm whereas the cell size may only vary from 1 to 10μm. During the initial stages of accumulation, biofilm thickness does not vary significantly. Bacteria are usually spherical (*cocci*), rod like (*bacilli*) or helical, and the cells width, or diameter, varies from 0.2 to 2 micrometers. *Echericia coli* is reported to have a length of 1 to 7 μm and a width of 800nm. *Bac.pabuli* has a similar shape to *e.coli* and has a length up to 12μm, width up to 1μm. B. *subtilis sporum* have a length of about 2-3μm and a width of about 0.7 to 1μm. (Richter et al., 1999). In this study, for coding purposes, the dimensions of bacteria are taken as 1 micrometers width, 1 micrometers length and 1 micrometers thickness as an average.

To assist in understanding the process of biofilm development and to provide a tool for predicting the behavior of biofilms, analytical and numerical models of the bacterial transport processes have been developed. Noguera et al. (1999) explain biofilm models as simulation tools for use in engineering applications and as research tools for the study of biofilm processes. Studies by Taylor et al (1990b) suggest that models accounting for changes in permeability and porosity can be used to make estimates of these parameters where their main aim is to relate permeability to biofilm thickness.

Early modeling studies neglected the effect of biomass growth by assuming a specified microbial distribution and biofilm thickness. (Rauch et al., 1999). After the mid 1980s, more accurate descriptions of the biofilm system were introduced (Kissel et al., 1984, Wanner et al., 1986), both in time and space, thus making it possible to predict microbial species development over the depth of biofilm as a function of substrate flux.

Bishop et al. (1995) suggest that in order to be correct, biofilm models must account for both microbial kinetics in the biofilm and the transport kinetics of nutrients. Recently most

biofilm models take Monod growth kinetics into account (e.g. Hermanowicz, 1999, Richter et al. 1999, Dennis et al. 1998, Corapcioglu et al. 1997, Kreikenbohm et al. 1985)

Corapcioglu et al. (1997) studied bacterial transport in porous media by using a numerical model, which accounted for the transport of resident bacteria and nutrient support. Several column experiments conducted with indigenous bacteria by Taylor et al. (1990a) were numerically simulated to investigate the role of the contaminant adsorption on biofilm and mobile bacteria. Taylor et al. (1990a) used methanol as substrate. Corapcioglu et al. (1997)'s hypothesis is that because of their colloidal size and favorable surface conditions, bacteria can be efficient contaminant carriers. Results showed that biofilms grow rapidly around the top of the column where bacteria and nutrient are injected and are subsequently detached by increasing fluid shear stress. The adsorption of contaminants on bacterial surfaces reduces the mobility of contaminants in the presence of a biofilm. The contaminant concentration decreases significantly along the biofilm when contaminants partition into bacteria. They also determined that, as the amount of contaminant attached to bacteria increases, biofilm growth increases.

The one dimensional model by Wanner et al. (1986), consists of a set of mass balance equations to describe the spatial distribution and development in time of components in biofilm, considers biofilm growth and allows for processes such as attachment and detachment of cells at the biofilm surface. In other words, what Wanner et al (1986) presented was a biofilm mixed culture model that was based on transport and transformation processes. Wanner et al. (1996) improved this model by incorporating new properties such as heterogeneity and the attachment and detachment of particles. These models are based on the continuum approach. Most recent studies take into account the heterogeneity of the biofilm (Bishop et al., 1997, Lewandowski et al., 1994, Zhang et al., 1994). Bishop et al. (1995) indicates that shortcoming of most models is

that they assume the biofilm is homogeneous and don't take the heterogeneity into account. Bishop et al. (1997) investigate biofilm heterogeneity in a more detailed way and point out that biofilms accumulate in a heterogeneous format with a highly channelized structure.

In studies of transport in porous media, the main assumption is that bacterial cells form impermeable biofilms uniformly covering pore walls. Vandevivere et al. (1995), studied two porous media models and their comparisons suggest that existing models can not predict the saturated hydraulic conductivity reductions in fine sands, satisfactorily where as, in coarser material predictions are much better. Vandevivere et al. (1995) argue whether this is because of the main assumption of a continuous biofilm. A simpler model they studied assumes the biomass distribution as plugs instead of a continuous film, resulting in more accurate predictions of the saturated hydraulic conductivity reductions.

In the literature, rather than adding more phenomena into the model, simpler models were presented for fast and sufficiently accurate simulation of biofilm dynamics (e.g. Rauch et al., 1999). Rauch et al. (1999), modeled the removal of substrates by different bacterial species growing in a biofilm reactor using the biokinetic reactions, via a two step analytical procedure, assuming only two major processes in the biofilm: substrate diffusion and biochemical conversion. Richter et al. (1999) modeled the growth process using Monte Carlo simulations and compared the modeling results with laboratory results, in which the biofilm growth was investigated by light and scanning electron microscopy (SEM). Picioreanu et al. (1999), developed a model based on a discrete algorithm, describing the biofilm equations in unsteady-state. The equation was solved by assuming a biofilm characteristic thickness, and the final model includes fluid flow over an irregular biofilm surface, substrate transport and consumption, and growth. The results show that a heterogeneous biofilm with a rough surface and high

porosity occurs in the slow substrate transfer regime; whereas the biofilm develops as a compact structure in a substrate limited case generated by fast flow and fast internal diffusion.

In most previous modeling studies (e.g. Kissel et al., 1984, Wanner et al., 1986), the most common features include simultaneous substrate utilization and diffusion within the biofilm, external mass-transport resistance from the bulk liquid to the biofilm surface, growth of new biomass proportional to substrate utilization, biomass loss from endogenous respiration and detachment and formation of inert biomass (Rittmann et al., 1992). This study is focused on modeling the development of biofilms in fractured media. On the basis of the present scientific understanding, biofilms are complex systems and their properties are characterized by many different variables. This leads to difficulties in modeling the behavior of biofilm systems.

The objectives of this study are to develop an analytical model that accounts for the major processes of bacterial transport and accumulation including growth, decay, rate-limited sorption, desorption, detachment and attachment. A simple analytical model is undertaken in order to define the transport of bacteria in fractured media and define the separation between sorption dominated phase and attachment-detachment dominated phase. The model is derived for the case of a discrete fracture and several input functions are used. A sensitivity analysis is also conducted to determine the parameters that most significantly influence the accumulation of bacteria in discrete fractures.

2.0 MATHEMATICAL DEVELOPMENT

In this section, the governing equations describing the processes involved in the accumulation and transport of bacteria in a discrete fracture that leads to formation of a biofilm system are developed. First the advection-dispersion equation, which describes the transport process, is introduced. Then the advection-dispersion equation is modified to account for processes such as growth and decay of bacteria and rate-limited sorption-desorption, as well as attachment and detachment.

2.1 DEVELOPMENT OF THE GOVERNING EQUATION

The accumulation model for biofilm development in a discrete fracture is based on several parameters. In order to explain these terms, one can start by defining the transport of bacteria in porous media, considering the input and output of a fluid into a known volume. The two physical processes that control the input and output flux are advection and hydrodynamic dispersion. Advection is the component of solute movement attributed to transport by the flowing groundwater. The process of hydrodynamic dispersion occurs as a result of mechanical mixing and molecular diffusion as indicated by Freeze et al. (1979).

2.1.1 ADVECTION–DISPERSION EQUATION

The movement of solute and fluid in a porous medium can be defined simply as:

$$\frac{\partial c(x,t)}{\partial t} = v\frac{\partial c}{\partial x} \tag{2.1}$$

where v (L/T) is advective fluid velocity (average linear flow velocity), c (M/L^3) is concentration of bacteria in the fluid, x is the coordinate direction taken along the direction of flow and t is time (Figure 2.1).

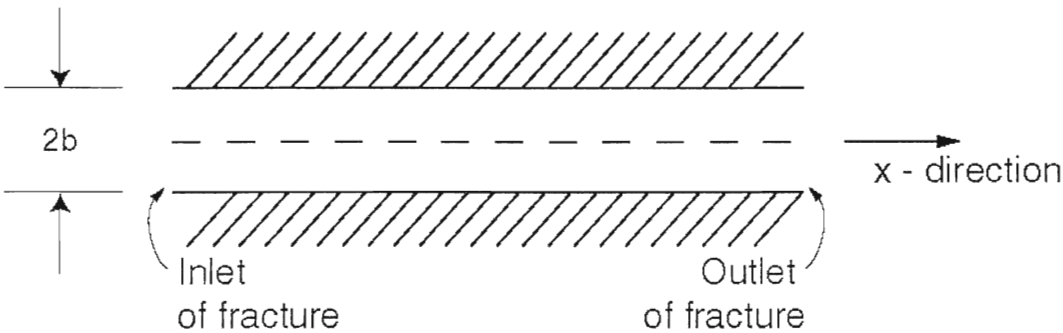

Figure 2.1 Side view of a fracture

Adding the effect of hydrodynamic dispersion and a source and sink term results in:

$$\frac{\partial c}{\partial t} + v\frac{\partial c}{\partial x} - D\frac{\partial^2 c}{\partial x^2} + \frac{G}{\theta} = 0 \tag{2.2}$$

where:

$$D = \alpha v + D^* \tag{2.3}$$

and D (L^2/T) is the coefficient of hydrodynamic dispersion, α (L) is longitudinal dispersivity and D* (L^2/T)is coefficient of molecular diffusion. Since molecular diffusion is not taken into consideration, D* is zero. The term G/θ represents the gain or loss of bacteria to the flowing groundwater where G equals to mass adsorbed over unit volume of media times time and θ is porosity.

Equation 2.2 is known as the Advection–Dispersion equation that describes advective and dispersive transport in porous media (Freeze and Cherry, 1978). The advection–dispersion equation has been the starting point of many biofilm modeling studies (e.g. Characklis et. al., 1990, Harvey et al., 1991). Although transport in fractured media is governed by the same processes as in porous media, the effects in fractured media can be different (Freeze et al., 1979). Hydrodynamic dispersion in discrete fractures arises due to local differences in aperture widths and roughness of the fracture walls (Novakowski and Lapcevic, 1992; Lapcevic et.al., 1999). The cubic law and not Darcy's law as in porous media govern the velocity in fractures. A modification is necessary for the sorption coefficients, which is explained in section 2.1.3.3.

2.1.2 ASSUMPTIONS

To account for the transport of bacteria in a discrete fracture using equation 2.2, several assumptions are required. These include:

- Molecular diffusion is neglected.

- Surface roughness of the fracture wall is not taken into consideration. The fracture walls are assumed to have smooth parallel walls and uniform separation with constant fracture aperture.
- The bulk fluid is incompressible and a gas phase does not exist in the bulk liquid.
- Flow of bulk fluid is assumed to be steady state and laminar.
- Sorption, advection, dispersion, growth and decay are the primary transport and accumulation processes during the early stages of biofilm accumulation. Attachment, detachment, advection, dispersion, growth and decay are dominant during the later stages of biofilm accumulation.
- The diffusion of bacteria from the fracture into the unfractured rock is not considered. For rock of large matrix porosity (i.e. >10%) and bacteria of small size , this assumption may lead to significant error in the prediction of migration at least during the adsorption-desorption phase. Because, however, the depositional surface is covered rapidly and attachment/detachment may dominate the transport and accumulation, the cumulative error is likely to be small.
- Sorption processes are rate limited during the biofilm accumulation.
- Although biofilm first accumulates in the forms of patches, it is assumed that biofilm accumulation is uniform, for modeling purposes. Biofilm thickness is assumed to be constant throughout the fracture plane. It is assumed that the growth rate of bacteria in the solution and in the sorbed phase is equal, the decay rate of bacteria in the solution and in the sorbed phase is equal, and that the bacteria shape is of a box (Figure 2.2).

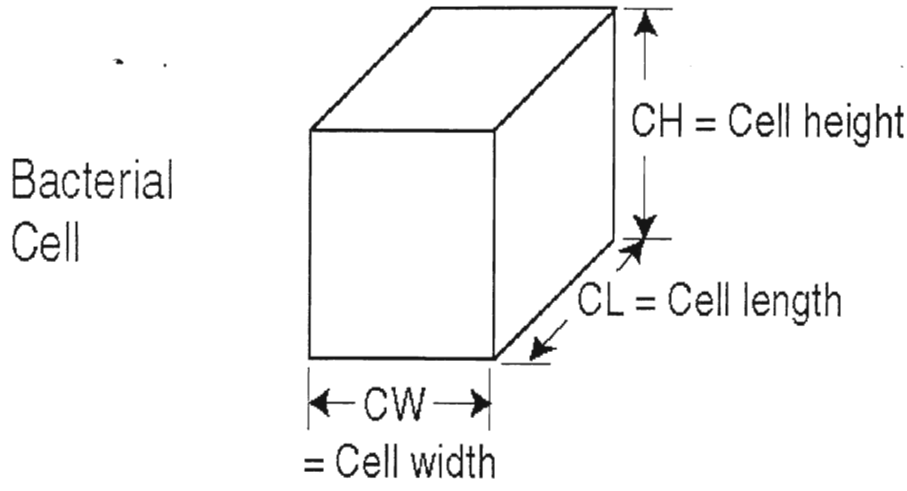

Figure 2.2 Bacterial cell dimensions

2.1.3 BACTERIAL ACCUMULATION EQUATIONS

The processes during the early stages of bacteria accumulation involve sorption processes including irreversible adsorption, decay and growth, and during the later stages of accumulation, these are replaced by attachment and detachment processes. The switch between dominant processes occurs when the substratum is covered by at least a monolayer of cells. At this time attachment and detachment of groups of cells begin to dominate the exchange between the fluid and the biofilm. The model developed herein is based on separation between these processes. Thus we will develop two separate equations, one for the early stages and one for the later stages of biofilm accumulation. The time at which these two stages are linked is calculated based on cell dimensions and fracture area. When there exists enough cells to cover the walls of the fracture, we assume that the substratum–bulk fluid interface does not exist anymore and the dominant processes will involve attachment-detachment.

2.1.3.1 ADSORPTION – DESORPTION DOMINATED PHASE (PHASE I)

The sorption term includes both desorption and adsorption processes. In order to explain sorption, Harvey et al. (1991) substituted the following expression for the source/sink term:

$$G = \frac{\rho_b}{\theta}\frac{\partial s}{\partial t} \tag{2.4}$$

where ρ_b (M/L^3) is the dry bulk density of solids, θ is porosity, s is the concentration of adsorbed bacteria and $\partial s/\partial t$ is rate at which bacteria is sorbed. Freeze et al. (1979) states that adsorption reactions for bacteria in groundwater are normally viewed as being very rapid relative to the flow velocity.

Substituting G into the advection-dispersion equation, the resulting equation for porous media is (Harvey et al, 1991, Characklis et al., 1990, Freeze et al., 1979):

$$\frac{\partial c}{\partial t} + v\frac{\partial c}{\partial x} - D\frac{\partial^2 c}{\partial x^2} + \frac{\rho_b}{\theta}\frac{\partial s}{\partial t} = 0 \tag{2.5}$$

Since growth and decay are important processes influencing the accumulation, decay and growth in the aqueous phase are represented by (Fry et al., 1993):

$$\frac{dc}{dt} = \lambda c + \mu c \tag{2.6}$$

where λ (1/T) is the decay constant and μ (1/T) is the specific growth rate for bacteria in the fluid. The growth and decay rates in the aqueous phase and sorbed phases are taken as the same. Because of the nutrient transport in aqueous phase and in the biofilm, the growth and decay rates in the aqueous and sorbed phases may differ from each other. This requires the modeling of nutrient transport. However at low thickness values, the biofilm will not play a restricting role in the nutrient transport. Thus the growth and decay equation for sorbed phase is very similar to the equation for aqueous phase:

$$\frac{ds}{dt} = \lambda s + \mu s \tag{2.7}$$

The value of μ can be calculated by using Monod kinetics. Monod kinetics has been a standard in defining the growth of bacterial cultures since publication in 1949 (Monod, 1949). This model is based on the idea that a limited number of growth constants define the behavior of bacterial cultures (Ferenci, 1999). The relationship between the concentration of a limiting nutrient and the growth rate of bacteria is defined by Monod's growth equation as follows (Corapcioglu et al., 1997, Monod,J., 1949, Rashid et al., 1999, Morshed et al., 1995, Henshaw et a., 1999, Vandevivere et al., 1992, Kreikenbohm et al., 1985, Horn et al., 1997, Charpentier, 1999, Ferenci, 1999, Schirmer et al., 1999, Mitchell et al., 2001, Guha et al., 1996):

$$\mu = \frac{\mu_{max} S}{K_S + S} \tag{2.8}$$

where μ_{max} (1/T) is the maximum specific growth rate of bacteria, S (M/L^3) is the substrate concentration , K_s (M/L^3) is the saturation coefficient or half velocity coefficient as referred by Krekienbohm et al. (1985) and Clement et al. (1997). Corapcioglu et al.(1997) refers to K_s as the Monod half saturation constant. It is the value of substrate concentration when the maximum growth rate is half. The K_s value can be found by plotting growth rate(μ) versus substrate concentration from laboratory data. Then K_s is the value corresponding to $\mu/2$. When the aqueous phase bacteria concentration is much less than the Monod half saturation constant, the kinetics are first order, and as the bacterial concentration increases, the kinetics become saturated (Mitchell et al., 2001, Tchobanoglous, 1991).

Irreversible adsorption is accounted for by the expression:

$$\frac{dc}{dt} = vk_p c \tag{2.9}$$

where k_p (1/L) is the irreversible adsorption constant (Harvey et al., 1991).

After substitution of the terms, the equation for aqueous phase in porous media is:

$$\frac{\partial c}{\partial t} + \frac{\rho_b}{\theta}\frac{\partial s}{\partial t} = D\frac{\partial^2 c}{\partial x^2} - v\frac{\partial c}{\partial x} - vk_p c - \lambda c + \mu c \tag{2.10}$$

The equation for the sorbed phase is:

$$\frac{\partial s}{\partial t} = k_1 c - k_2 s + \mu s - \lambda s \tag{2.11}$$

where k_1 is the rate-limited adsorption coefficient and k_2 is the rate-limited desorption coefficient (Lapidus et al., 1952).

2.1.3.2 ATTACHMENT–DETACHMENT DOMINATED PHASE (PHASE II)

In this phase, there is no irreversible sorption. The substratum is covered with biofilm, thus sorption processes do not occur anymore.

Attachment, which accounts loss from the flowing bulk fluid concentration, is described by:

$$\frac{dc}{dt} = k_{at} c \tag{2.12}$$

where k_{at} is the attachment coefficient (1/T) (Characklis et al., 1990, Characklis et al., 1973, Characklis et al., 1989, Clement et al., 1997, Kreikenbohm et al, 1985)

Detachment, which is the loss from the sorbed concentration in the biofilm, is:

$$\frac{dc}{dt} = k_{\text{det}} s \tag{2.13}$$

where k_{det} is the detachment concentration (1/T) (Characklis et al., 1990, Characklis et al., 1973, Characklis et al., 1989, Peyton et al., 1995, Peyton et al., 1993, Dukan et al., 1996, Arcangeli et al., 1995, Kreikenbohm et al, 1985, Wilderer et al., 2000).

The equation for the bacterial concentration in the fluid during the attachment–detachment phase is given by:

$$\frac{\partial c}{\partial t} + \frac{\rho_b}{\theta}\frac{\partial s}{\partial t} = D\frac{\partial^2 c}{\partial x^2} - v\frac{\partial c}{\partial x} + \mu c - \lambda c \tag{2.14}$$

The governing equation for the sorbed phase is:

$$\frac{\partial s}{\partial t} = k_{at} c + \mu s - \lambda s - k_{\det} s \tag{2.15}$$

2.1.3.3 MODIFICATION FOR FRACTURE PROPERTIES

In order to obtain a governing equation for transport in a discrete fracture, the equations must be re-written to account for sorption to and desorption from the fracture walls. This is done by substitution of 2/2b for ρ_b/θ, where 2b (L) is the fracture aperture. The substitution accounts for the difference between sorption on to a specific surface (fracture wall) versus sorption onto bulk media (porous media). For porous media,

$$A = \frac{\rho_b}{\theta} \tag{2.16}$$

where A is the surface area to void space volume ratio. Solute is transported through the fracture aperture in the case of fractured media. If the fracture surface is assumed to be planar then:

$$SA = 2 \times W \times L$$
$$V = 2b \times W \times L \tag{2.17}$$

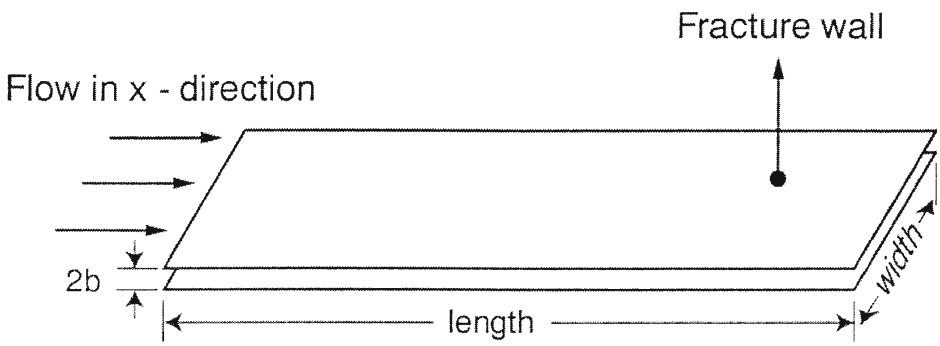

Figure 2.3 Fracture dimensions and fluid flow direction

where SA (L^2) is the total surface area of two fracture walls, W (L) is the fracture width, L (L) is the fracture length, V is the void space volume (L^3), and 2b (L) is the fracture aperture (Figure 2.3). Thus,

$$A = \frac{SA}{V} = \frac{2}{2b} \tag{2.18}$$

After substituting equation 2.18, the governing equation for Phase I and Phase II in fractured media becomes, respectively:

$$\frac{\partial c}{\partial t}+\frac{2}{2b}\frac{\partial s}{\partial t}=D\frac{\partial^2 c}{\partial x^2}-v\frac{\partial c}{\partial x}-vk_p c-\lambda c+\mu c \tag{2.19}$$

$$\frac{\partial c}{\partial t}+\frac{2}{2b}\frac{\partial s}{\partial t}=D\frac{\partial^2 c}{\partial x^2}-v\frac{\partial c}{\partial x}+\mu c-\lambda c \tag{2.20}$$

2.1.4 INITIAL AND BOUNDARY CONDITIONS

For the solution to Phase I of the biofilm accumulation problem, the initial condition at time equal to zero is:

$$c(x,0)=0 \tag{2.21}$$

$$s(x,0)=0 \tag{2.22}$$

The inner boundary condition for the solution is:

$$c(0,t)=f(t) \tag{2.23}$$

where f(t) is an arbitrary function of some concentration.

The outer boundary condition for the solution is:

$$c(\infty,t)=0 \tag{2.24}$$

The boundary conditions for Phase II are similar with the exception that:

$$c(x,0) = c(x,\tau) = c_\tau \tag{2.25}$$

where c_τ (M/L^3) is the aqueous phase concentration, calculated using the Phase I equations, at time equal to τ which is the time at which Phase I equations are switched to Phase II. The sorbed phase concentration is found by solving equation 2.11 and substituting c_τ.

$$s(x,0) = s(x,\tau) = \frac{k_1 c_\tau}{k_2 - \mu + \lambda}\left[1 - \exp\left(-(k_2 - \mu + \lambda)\tau\right)\right] \tag{2.26}$$

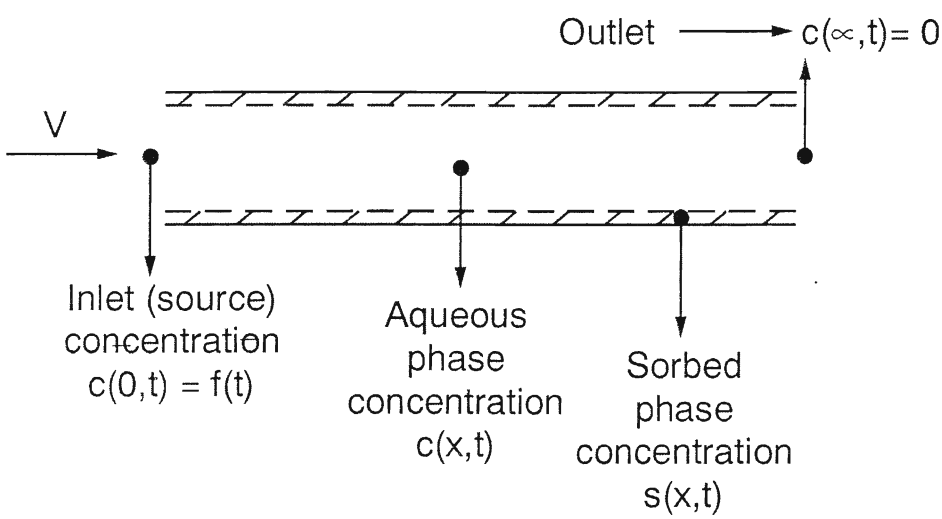

Figure 2.4 Boundary Conditions

As stated above, we use f(t) as an arbitrary function for the inner boundary condition. Different equations for different types of source concentration can be substituted into equation

2.23 for f(t). In the following, four different types of source concentrations were considered including constant initial concentration, the Heaviside step function, exponentially decaying concentration and exponentially rising concentration. These are:

Constant source concentration:

$$c(0,t) = c_0 \tag{2.27}$$

where c0 is a constant concentration.

Heaviside step function concentration:

$$c(0,t) = c_0 H(t - t') \tag{2.28}$$

where H(t-t′) is the Heaviside step function.

Exponential decaying concentration:

$$c(0,t) = c_0 \exp(-Bt) \tag{2.29}$$

where B is the decay constant.

Exponential rising concentration:

$$c(0,t) = c_0 [1 - \exp(-Bt)] \tag{2.30}$$

2.2 ANALYTICAL SOLUTION

The analytical solution to the governing equation derived above is presented in this section. The solution method is based on the use of Laplace transforms.

2.2.1 THE LAPLACE TRANSFORM

Once the linear partial differential equation is derived, it is necessary to find the solution to this equation subject to the given initial and boundary conditions. For partial differential equations such as equations 2.19 and 2.11 where there are only two independent variables, the Laplace transform can be applied to one variable as a means of reducing the equation to an ordinary differential equation. In this case, the Laplace transform can be used to eliminate the time derivative from this transient problem, and reduce the derivative terms to dependency on the x-coordinate only (Savant et al, 1962, Spiegel, 1965). The forward Laplace transform is defined by the improper integral:

$$L\{f(t)\} = \bar{f}(p) = \int_0^\infty e^{-pt} f(t) dt \tag{2.31}$$

where L is the Laplace transform operator, f(t) is the time dependent function in real time t, and p is the Laplace transform variable.

When the transform above is applied to the derivative of the function, f(t), the Laplace transform of the first order differential term is:

$$L\left\{\frac{df(t)}{dt}\right\} = pL\{f(t)\} - f(0) \tag{2.32}$$

where f(0) is the initial condition. Thus, the first order differential term is eliminated and the initial condition is incorporated.

After the application of the Laplace transform, the solution is obtained in Laplace space using standard methods for ordinary differential equations. In order to utilize the solution, an inverse operation to the Laplace transform must be performed. The inverse Laplace transform is given by:

$$f(t) = \frac{1}{2\pi i^*}\int_{p_0-i^*\infty}^{p_0+i^*\infty} e^{pt}\bar{f}(p)dp \tag{2.33}$$

where $\bar{f}(p)$ is the Laplace transform of the function f(t), p is a value such that the contour integration is to the right of any singularities of $\bar{f}(p)$ and i^* is the imaginary number.

Application of the Laplace transform to equation 2.19 and 2.11 results in:

$$\left(p\bar{c} - c(x,0)\right) + \frac{2}{2b}\left(p\bar{s} - s(x,0)\right) = D\frac{\partial^2 \bar{c}}{\partial x^2} - v\frac{\partial \bar{c}}{\partial x} - vk_p\bar{c} - \lambda\bar{c} + \mu\bar{c} \tag{2.34}$$

$$\left(p\bar{s} - s(x,0)\right) = k_1\bar{c} - k_2\bar{s} + \mu\bar{s} - \lambda\bar{s} \tag{2.35}$$

Application to the boundary conditions gives:

$$L\{c(0,t)\} = L\{f(t)\} = \bar{f}(p) \tag{2.36}$$

for the general case and for the constant source concentration:

$$L\{c(0,t) = c_0\} = \bar{c}(0,p) = \frac{\bar{c}_0}{p} \tag{2.37}$$

and for Heaviside step source:

$$L\{c(0,t) = c_0 H(t-t')\} = \bar{c}(0,p) = \bar{c}_0\left[\frac{\exp(-t'p)}{p}\right] \tag{2.38}$$

and for an exponential decaying source:

$$L\{c(0,t) = c_0 \exp(-Bt)\} = \bar{c}(0,p) = \frac{\bar{c}_0}{p+B} \tag{2.39}$$

and for an exponential rising source:

$$L\{c(0,t) = c_0[1-\exp(-Bt)]\} = \bar{c}(0,p) = \bar{c}_0 - \frac{\bar{c}_0}{p+B} \tag{2.40}$$

Application to the outer boundary condition gives:

$$L\{c(\infty,t)\} = L\{0\} \Rightarrow \bar{c}(\infty, p) = 0 \tag{2.41}$$

2.2.2 THE SOLUTION IN LAPLACE SPACE

The governing equations for Phase I are set equal zero to write the equations in standard form:

$$(p\bar{c} - c(x,0)) + \frac{2}{2b}(p\bar{s} - s(x,0)) - D\frac{\partial^2 \bar{c}}{\partial x^2} + v\frac{\partial \bar{c}}{\partial x} + vk_p\bar{c} + \lambda\bar{c} - \mu\bar{c} = 0 \tag{2.42}$$

$$(p\bar{s} - s(x,0)) - k_1\bar{c} + k_2\bar{s} - \mu\bar{s} + \lambda\bar{s} = 0 \tag{2.43}$$

The solution of equation 2.43 is found algebraically as:

$$\bar{s} = \frac{k_1\bar{c}}{p - \mu + k_2 + \lambda} \tag{2.44}$$

Equation 2.44 is substituted into equation 2.42, and the result is a homogeneous equation having constant coefficients. Thus:

$$p\bar{c} + \frac{2}{2b}\left(p\frac{k_1\bar{c}}{p-\mu+k_2+\lambda}\right) - D\frac{\partial^2\bar{c}}{\partial x^2} + v\frac{\partial\bar{c}}{\partial x} + vk_p\bar{c} + \lambda\bar{c} - \mu\bar{c} = 0 \tag{2.45}$$

Equation 2.45 is re-arranged to:

$$\frac{\partial^2\bar{c}}{\partial x^2} - \frac{v}{D}\frac{\partial\bar{c}}{\partial x} - \frac{\bar{c}}{D}\left(vk_p + \lambda - \mu + p + \frac{2}{2b}\left(p\frac{k_1}{p-\mu+k_2+\lambda}\right)\right) = 0 \tag{2.46}$$

For simplicity we set:

$$\alpha = vk_p + \lambda - \mu + p + \frac{2}{2b}\left(p\frac{k_1}{p-\mu+k_2+\lambda}\right) \tag{2.47}$$

so that equation 2.46 is reduced to:

$$\frac{\partial^2\bar{c}}{\partial x^2} - \frac{v}{D}\frac{\partial\bar{c}}{\partial x} - \frac{\alpha}{D}\bar{c} = 0 \tag{2.48}$$

For an nth order homogeneous linear differential equation, of the form:

$$a_o\frac{\partial^n y}{\partial x^n} + a_1\frac{\partial^{n-1} y}{\partial x^{n-1}} + \ldots + a_{n-1}\frac{\partial y}{\partial x} + a_n y = 0 \tag{2.49}$$

where a_n are all real constants. If the characteristic equation which is:

$$a_0 r^n + a_1 r^{n-1} + \ldots + a_{n-1} r + a_n = 0 \tag{2.50}$$

and has n distinct real roots r_1, r_2, ..., r_n, then the general solution of the equation is:

$$y = c_1 e^{r_1 x} + c_2 e^{r_2 x} + \ldots + c_n e^{r_n x} \tag{2.51}$$

where c_n are arbitrary constants. For the present equation n=2 and the roots are found from the solution of a quadratic equation.

Thus the solution is:

$$\bar{c}(x, p) = \gamma \exp\left(x \frac{v + \sqrt{v^2 + 4D\alpha}}{2D} \right) + \beta \exp\left(x \frac{v - \sqrt{v^2 + 4D\alpha}}{2D} \right) \tag{2.52}$$

where γ and β are constants to be determined from the boundary conditions. Substituting equation 2.41 into 2.52 results in:

$$\gamma = 0 \tag{2.53}$$

Then equation 2.37 is substituted into the following equation

$$\bar{c}(x,p) = \beta \exp\left(x \frac{v - \sqrt{v^2 + 4D\alpha}}{2D} \right) \tag{2.54}$$

which results in:

$$\beta = \bar{f}(p) \tag{2.55}$$

Thus the final solution is:

$$\bar{c}(x,p) = \bar{f}(p) \exp\left(x \frac{v - \sqrt{v^2 + 4D\alpha}}{2D} \right) \tag{2.56}$$

and equations 2.37, 2.38, 2.39, 2.40 can be substituted for $\bar{f}(p)$.

This is the solution for the earliest stages of biofilm accumulation (Phase I). As previously indicated, after a certain concentration of sorbed bacteria is accumulated on both fracture walls, the sorption processes are replaced by attachment and detachment processes (in Phase II). This requires a solution to be derived for the later stages of biofilm accumulation. The Phase II equations are solved in the same manner as Phase I equations. Note that the source concentration is modified according to the time that the link occurs. For example, with exponential decay or rise, the new starting point will occur where the source concentration for the previous equation stopped.

Application of the forward Laplace Transform equations 2.20 and 2.15, results in:

$$\left(p\bar{c}-c(x,\tau)\right)+\frac{2}{2b}\left(p\bar{s}-s(x,\tau)\right)=D\frac{\partial^2\bar{c}}{\partial x^2}-v\frac{\partial\bar{c}}{\partial x}+\mu\bar{c}-\lambda\bar{c} \tag{2.57}$$

$$\left(p\bar{s}-s(x,\tau)\right)=k_{at}\bar{c}+\mu\bar{s}-\lambda\bar{s}-k_{\det}\bar{s} \tag{2.58}$$

Equation 2.58 is re-arranged:

$$\bar{s}=\frac{k_{at}\bar{c}+s(x,\tau)}{p-\mu+\lambda+k_{\det}} \tag{2.59}$$

and then substituted into equation 2.57, resulting in:

$$\left(p\bar{c}-c(x,\tau)\right)+\frac{2}{2b}\left(p\frac{k_{at}\bar{c}+s(x,\tau)}{p-\mu+\lambda+k_{\det}}-s(x,\tau)\right)=D\frac{\partial^2\bar{c}}{\partial x^2}-v\frac{\partial\bar{c}}{\partial x}+\mu\bar{c}-\lambda\bar{c} \tag{2.60}$$

Note that equation 2.60 includes real values of s(x,τ) and c(x,τ), that must be calculated separately via inversion of the Phase I equations and equation 2.26. In order to write equation 2.60 in a simpler form the following definitions are used:

$$\theta=\mu-\lambda-p-\frac{2}{2b}\frac{pk_{at}}{p-\mu+\lambda+k_{\det}} \tag{2.61}$$

$$\phi=-c_{\tau}+\frac{2}{2b}\left(\frac{p}{p+k_{\det}-\mu+\lambda}-1\right)\left(\frac{k_1c_{\tau}}{k_2-\mu+\lambda}\left[1-\exp\left(-\left(k_2-\mu+\lambda\right)\tau\right)\right]\right) \tag{2.62}$$

Thus, by substitution, equation 2.60 is reduced to:

$$\frac{\partial^2 \bar{c}}{\partial x^2} - \frac{v}{D}\frac{\partial \bar{c}}{\partial x} + \frac{\theta}{D}\bar{c} = \frac{\phi}{D} \tag{2.63}$$

Equation 2.63 is a non-homogenous partial differential equation, which is solved directly using the method of Variation of Parameters. The solution is given by:

$$\bar{c}(x,p) = \frac{\phi}{\theta} + \frac{-\phi + \bar{f}(p)\theta}{\theta}\exp\left\{\frac{1}{2}\frac{\left(v - \sqrt{v^2 - 4D\theta}\right)}{D}x\right\} \tag{2.64}$$

where the parameters are as previously defined.

2.2.3 NUMERICAL INVERSION OF THE LAPLACE TRANSFORM

Once the solution is obtained in Laplace space, it is transformed back into the real domain. This is done via numerical inversion. There are several well-known inversion algorithms such as the Stehfest Method, the Talbot Method, the Crump Method, and the De Hoog Method (Stehfest, 1979, Crump, 1976, Talbot, 1979, DeHoog et al., 1982).

The numerical inversion method presented by DeHoog et al. (1982) is an improved version of Crump method and is based on expressing the inverse of solution in Laplace space as a Fourier series.

The DeHoog Numerical Method is coded as a subroutine called Hoog2 by Neville et al. (1988) and the solutions in Laplace space are inverted by simply calling Hoog2 subroutine in the main code. (Neville et al., 1988) Numerical inversion is used in this case because the complexity of the solution, (i.e. equation 2.67), render analytical inversion impossible.

3.0 IMPLEMENTATION AND SENSITIVITY ANALYSIS

In this section, the model developed previously will be coded and a sensitivity analysis will be applied.

3.1 IMPLEMENTATION

The solution developed in the previous chapter is coded in Fortran99 and implemented as a code named BIOFRAC. The code, sample input and sample output files can be found in Appendix A. The code calculates bacterial concentrations versus time for a specific location along a discrete fracture. The parameters describing the fracture properties and the properties of bacteria are read from a separate input file. The main program loops through time calling the numerical inversion routine. The solution is coded as a function, which is called directly from the inversion routine.

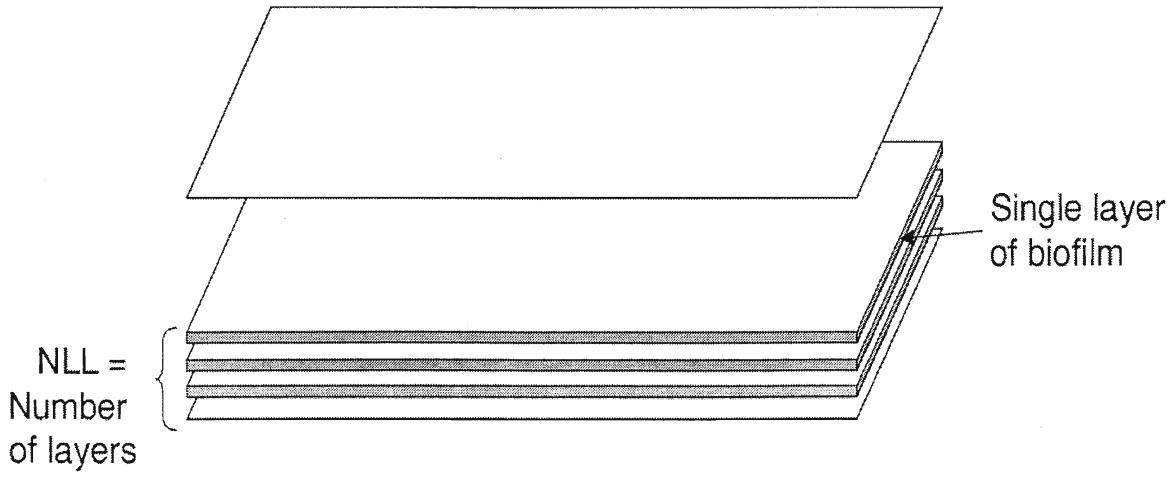

Figure 3.1 Biofilm layers in discrete fracture

To determine the time at which the Phase I processes end, the thickness and spread of bacteria is calculated using:

$$XCHECK = \frac{2 * NLL * NFL * XFW}{XCL * XCW} \tag{3.1}$$

where 2*NLL is the number of layers of biofilm on both fracture walls (can be more than one if required, as can be observed in Figure 3.1), NFL is the fracture length (L), XFW is the fracture width (L), XCL is the bacterial cell length (L) and XCW is the bacterial cell width (L). Thus, XCHECK is the number of bacterial cells that are necessary to cover both fracture walls and the XCHECK formula is based on the equation:

$$XCHECK \times \text{Area of a bacteria} = 2 \times NLL \times \text{Area of single fracture wall} \tag{3.2}$$

which is then compared to:

$$ROWTOT = \frac{AVSORB \times XCH \times NFL \times XFW}{XCMASS} \tag{3.3}$$

where

$$ROWAV = \frac{\sum_{1}^{j=\text{number of columns}} C_{ij}}{NFL} \tag{3.4}$$

$$AVSORB = \frac{k_1 \times ROWAV}{k_2 - \mu + \lambda}\left[1 - \exp\left(-\left(k_2 - \mu + \lambda\right)\tau\right)\right] \tag{3.5}$$

and where i is time (T) for the i^{th} time and j is the location along the fracture (L) where the concentration is calculated. Along the fracture length, the concentration is calculated every one meter. ROWAV is the average concentration at a certain time in the fracture (M/L^3) between the source and location, j. XCMASS is the mass of one bacterial cell (M). Average concentration in the fracture at a certain time (ROWAV) is found simply by taking the arithmetic mean of the concentrations at different fracture locations at that time and then converting to number of cells per volume, from mass per volume. AVSORB is the sorbed phase concentration calculated via equation 2.26 and ROWAV is equal to c_τ. ROWTOT is average concentration in the fracture at a certain time, in terms of number of cells per unit volume of aqueous phase.

ROWTOT and AVSORB are calculated for each time step and if ROWTOT is greater than or equal to XCHECK, the number of layers of bacteria (NLL) are accumulated on the fracture walls (i.e. the substratum is fully covered and adsorption–desorption is dominated by attachment–detachment). The time when ROWTOT is greater than or equal to XCHECK, corresponds to τ in equation 2.26. Prior to XGAP, the concentration at any point in the fracture is calculated by equations 2.19 and 2.11. Following XGAP, the concentration is calculated by equations 2.15 and 2.20.

The functions corresponding to equations 2.37, 2.38, 2.39, 2.40 are coded separately. When a call to the subroutine Hoog2 is made by the main program, Hoog2 inverts the functions into real space and calculates the array C_{ij} corresponding the time array T_i.

The output is in files BIOFRAC.out and BIOFRAC.plt. The output is in the form of C_{ij} vs. T_i. C_{ij} is a two dimensional array where columns are calculated using equations 2.11, 2.19 or 2.15, 2.20 depending on τ for each location along the fracture and rows are for each time step. At the moment when XCHECK is greater than or equal to zero, time τ is assigned as XGAP. Before τ, XGAP is equal to zero. After τ is assigned to XGAP, the value of XGAP is fixed and any time after that is calculated by:

$$T_i = T_i - XGAP \tag{3.6}$$

Double precision arithmetic is used in the functions, subroutines and the main code, which aids in reducing the round off error caused by the numerical inversion.

In real fractures, as indicated previously, biofilms form in patches at various locations on the fracture walls. At those locations the biofilm is accumulated, sorption processes stop and attachment-detachment processes start, whereas at locations where no accumulation has occurred yet, sorption processes continue. Since this is an analytical model, the uniform thickness assumption is necessary, which requires that sorption processes stop at once and are followed by attachment-detachment.

3.2 VERIFICATION OF THE SOLUTION AND THE CODE

The Phase I and Phase II solutions were verified by comparing the present result to the Ogata-Banks solution. Although Ogata-Banks is the solution to the advection-dispersion equation in porous media, it can be used for fractured media by modifying the source and sink

term to account for fractured media properties. Both solutions can be reduced to the Ogata–Banks solution algebraically, when the sorption, attachment-detachment, growth and decay constants are set to zero. The codes are verified in the same manner as are the solutions. First each equation was coded separately, then the constants were set to zero. Both codes followed exactly the same behavior as the Ogata–Banks solution.

The Ogata-Banks solution in Laplace space is:

$$\bar{c}(x,p)=\frac{C_0}{p}\exp\left(x\frac{v-\sqrt{v^2+4Dp}}{2D}\right) \tag{3.7}$$

and the Non-Homogenous Ogata–Banks Solution in Laplace Space is:

$$\bar{c}(x,p)=\frac{Z}{p}+\frac{(-p+C_0)}{p}\exp\left\{\frac{1}{2}\frac{\left(v-\sqrt{v^2+4Dp}\right)}{D}x\right\} \tag{3.8}$$

where Z is the non-homogenous function.

The Phase II solution reduces to the Non-Homogenous Ogata-Banks Solution if the non-homogenous parts are the same. In Appendix B, an example comparison is plotted in order to compare Ogata-Banks to the Phase I solution and Non-Homogenous Ogata-Banks to the Phase II solution in Figure 3.2, using the parameters that are shown in Table 3.1.

Constant source concentration	50 gr m^{-3}
Groundwater velocity	5.0 m day^{-1}
Dispersivity	0.5 m
Duration	6.5 days
Non-Homogenous Function Value	10

Table 3.1 Parameters for Ogata-Banks and Non-Homogenous Ogata-Banks Solutions

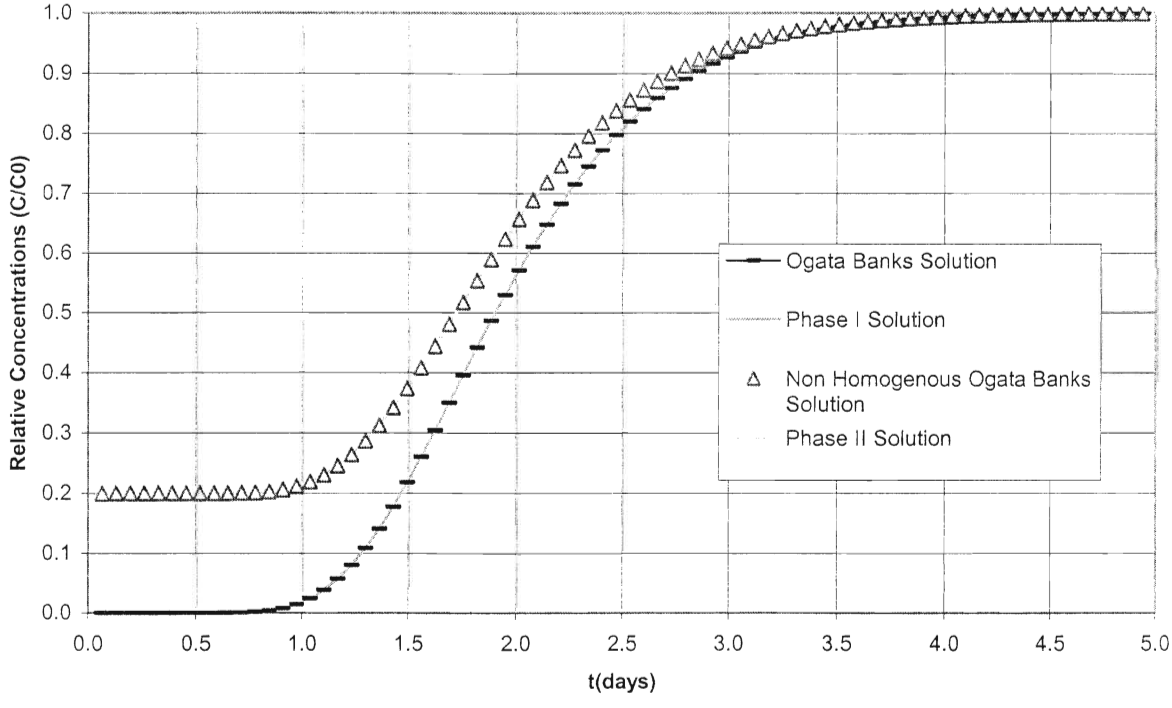

Figure 3.2.1 Comparison of solutions

Another method of verification is comparing the solution presented here to the solution to advection-dispersion equation as presented by Harvey et al. (1991) which describes transport

of bacteria in porous media with retardation, first order decay and pulse input concentration. Since the input and boundary conditions are not explicitly presented in the paper by Harvey et al. (1991), a satisfactory comparison was not possible. The solution presented herein was modified for porous media again and data from Harvey et al. (1991) was simulated. However, the two simulations did not show agreement as can be seen in Figure 3.2.2

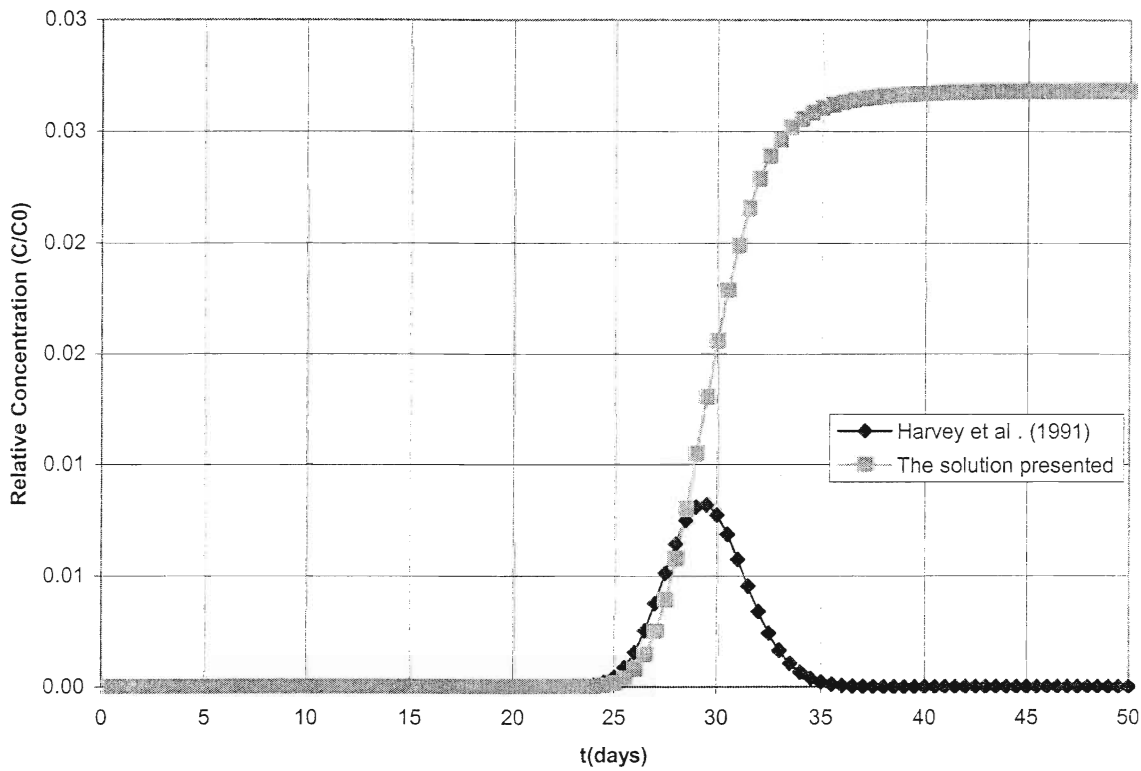

Figure 3.2.2 Harvey et al. (1991) vs. the solution presented

3.3 SENSITIVITY ANALYSIS

The code is used to generate data for relative concentration (C/C_0) versus time plots. For comparison, a base case was established having best estimates of each parameter as determined from the literature. Although a formal sensitivity analysis was not conducted, the influence of individual parameters was estimated by varying each parameter, keeping all others fixed. All the graphs presented are for an observation point at 10m and the numbers in parenthesis are the duration of Phase I.

3.3.1 BASE CASE

The base case for the sensitivity analysis is chosen using the code BIOFRAC that involves Phase I and Phase II solutions linked together. The input parameters for the base case are shown in Table 3.2:

Constant source concentration	10.0 gr m^{-3}
Groundwater velocity	5.0 m day^{-1}
Dispersivity	0.5 m
Fracture aperture	0.0005 m
Fracture length	10 m
Fracture width	2.0 m
Bacterial cell width	5.0×10^{-6} m

Bacterial cell length	5.0×10^{-6} m
Bacterial cell height	5.0×10^{-6} m
Mass of one bacterial cell	1.0×10^{-13} gr
Number of layers of biofilm on a single	2
Rate-limited adsorption constant	3.0 day^{-1}
Rate-limited desorption constant	6.0 day^{-1}
Detachment constant	4.0 day^{-1}
Attachment constant	1.0 day^{-1}
Irreversible adsorption constant	1.0×10^{-5} m^{-1}
Duration	5000 days
Number of time points	100

Table 3.2 Input for base case

The parameters used for the base case are gathered from the literature. Constant source concentration, velocity, fracture length, dispersivity and fracture width are arbitrary numbers chosen within the range of values that can occur in fractured media (Lapcevic et al., 1999)

Bacterial dimensions are averaged from various literature data. Smets et al. (1999) determined cell length between 2.2μm and 1.4μm, cell width as 0.9μm, and radius as 0.56m to 0.92μm for *pseudomonas fluorescens*. Chapelle (1993) gives a range of 0.1μm to 10μm for bacteria diameter. According to Characklis et al. (1990), the bacteria size is between 1μm to 10μm. Harvey et al. (1991) used numbers as low as 0.2μm, just like Cusak et al. (1992) whom used 0.3μm. Clement et al. (1997) gave cell dimensions as 2μm. Considering these values, an average size of 5μm is taken for all sides assuming a rectangular prism geometry.

One bacterial cell is composed of 20% dry material and 80%water. Balkwill et al. (1988) analyzed aquifer microorganisms and derived the value 1.72×10^{-10} mg/cell. Chapelle (1993) used cellular mass of 1.0×10^{-13} gr/cell which was adopted for this study.

The assumption of uniform biofilm thickness suggests that when a single layer of biofilm is accumulated, the entire substratum surface is covered. However, it is known that, biofilms form in patches during the early stages. In order to minimize the errors that may occur from the uniform thickness assumption, the number of layers of biofilm can be increased in the simulation process. Setting the number of layers to greater than one, will increase the likelihood that a natural case is simulated.

Adsorption-desorption and attachment-detachment rates in porous media fall in a very wide range between values as low as 0.01 to as high as 200 day^{-1} (Cunningham et al., 1991, Corapcioglu et al., 1997, Kreikenbohm et al, 1985, Clement et al., 1997, Arcangeli et al, 1995 and 1997, Zhang et al., 1995, Hu et al., 1996, Peyton et al., 1996). The values chosen for the base case are similar to the values from Peyton et al, 1996. Because such a wide range is suggested by the literature, the sensitivity analysis is also performed over a wide range.

The results of the base case simulation does not appear as a smooth breakthrough curve. In order to predict the trends of breakthrough curves, two simulations are run. First a base case simulation according to Table 3.2 was run, then a second simulation with rate-limiting process rates are set to equal as in:

$$k_1 = k_{at} = 3\,\text{day}^{-1}$$
$$k_2 = k_{\text{det}} = 6\,\text{day}^{-1} \qquad (3.8)$$

The growth and decay rate, because they can be very dominant, are initially set to zero in order to keep the base case as simple as possible. Similarly the irreversible adsorption constant is taken as low as possible initially. The results for the base case give by Table 3.2 are plotted in Figure 3.3, and the results for the case when process rates are set equal (in equation 3.8) are given in Figure 3.4.

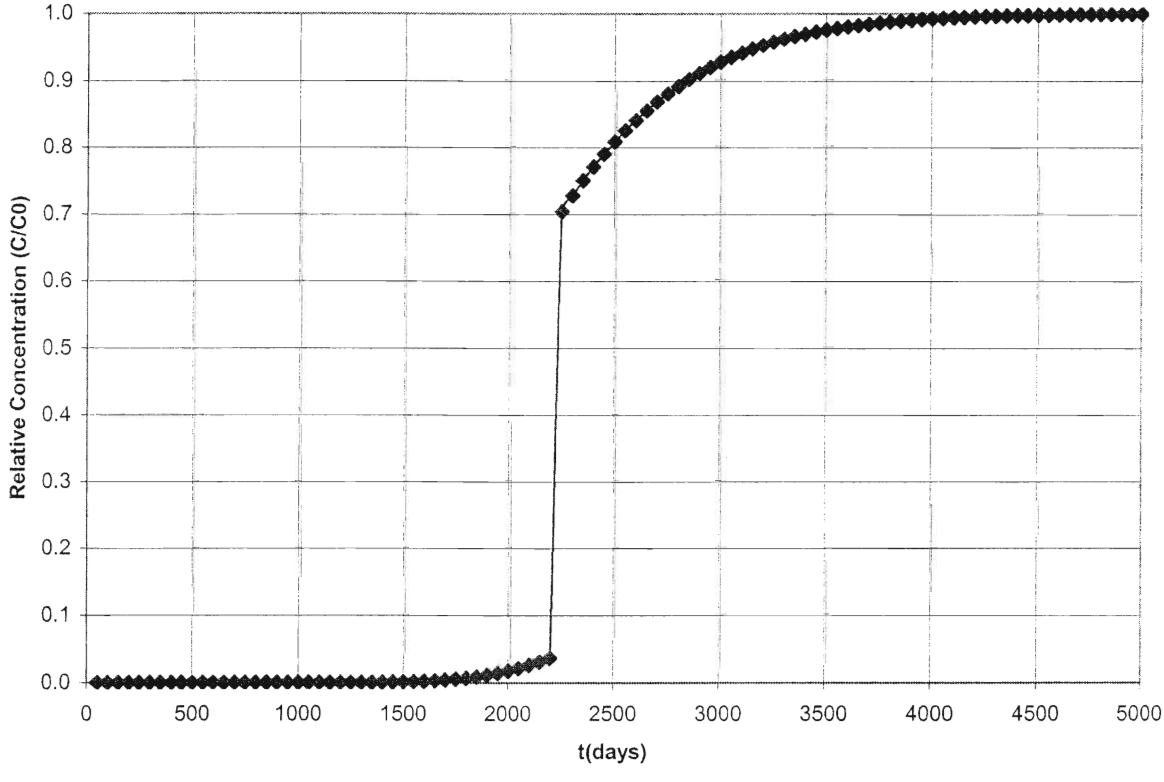

Figure 3.3 Base case plot for Table 3.2

3.3.2 ADDITION OF GROWTH AND DECAY RATES

After the simulations are completed for the values in Table 3.2, growth and decay are added in order to illustrate the effects. The new values are as seen in Table 3.3:

Constant source concentration	10 gr m^{-3}
Groundwater velocity	5.0 m day^{-1}
Dispersivity	0.5 m
Fracture aperture	0.0005 m
Fracture length	10 m
Fracture width	2.0 m
Bacterial cell width	5.0×10^{-6} m
Bacterial cell length	5.0×10^{-6} m
Bacterial cell height	5.0×10^{-6} m
Mass of one bacterial cell	1.0×10^{-13} gr
Number of layers of biofilm on a single fracture wall	2
Rate-limited adsorption constant	3.0 day^{-1}
Rate-limited desorption constant	6.0 day^{-1}
Detachment constant	4.0 day^{-1}
Attachment constant	1.0 day^{-1}
Irreversible adsorption constant	1.0×10^{-5} m^{-1}
Duration	15000 day

Number of time points	100
Maximum specific growth rate	9.0 day^{-1}
Decay rate	3.0 day^{-1}
Monod half saturation constant	5.0 gr m^{-3}
Substrate concentration	3.0 gr m^{-3}

Table 3.3 Input for Simulation with Growth and Decay

The growth and saturation coefficient rates are taken from Characklis et al, 1990 for *pseudomonas aeruginosa*. Substrate concentration is chosen arbitrarily. The decay rate is taken from Desouky et al. (1996). The breakthrough curve for the values in Table 3.3 can be seen in Figure 3.5. The substrate concentration and Monod half saturation constant effect the resulting growth rate, μ in equation 2.8. Thus a separate sensitivity analysis for these two parameters is not performed.

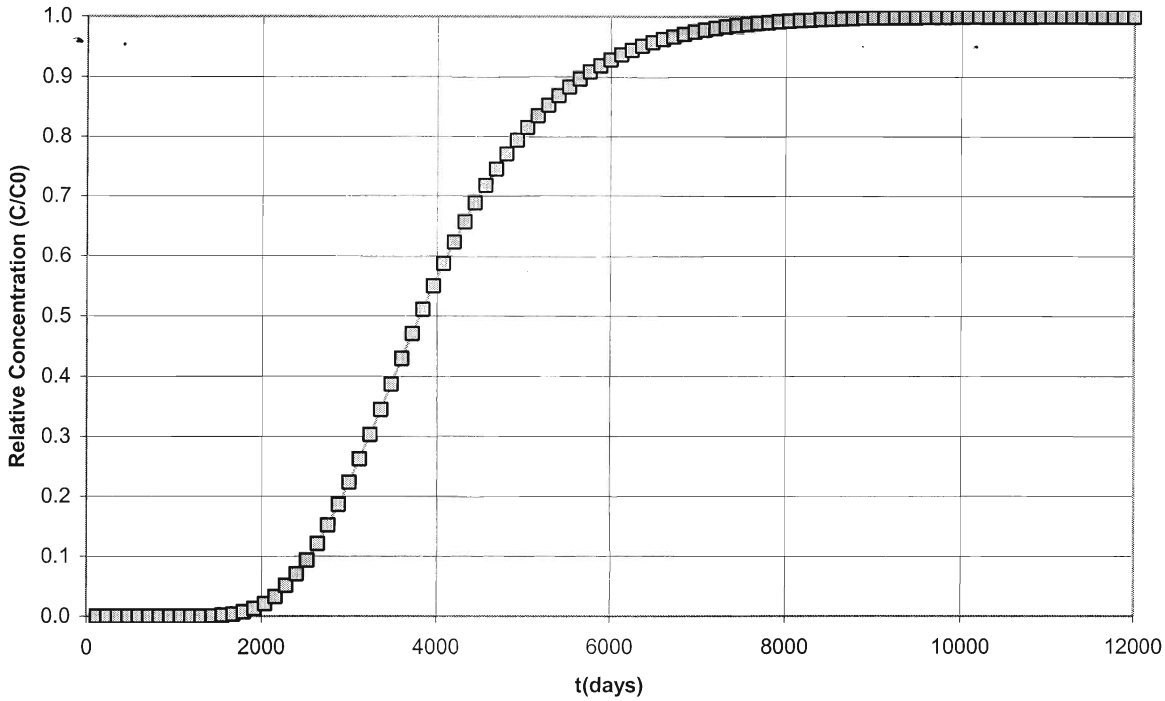

Figure 3.4 Base case input with rate-limiting process rates are set equal.

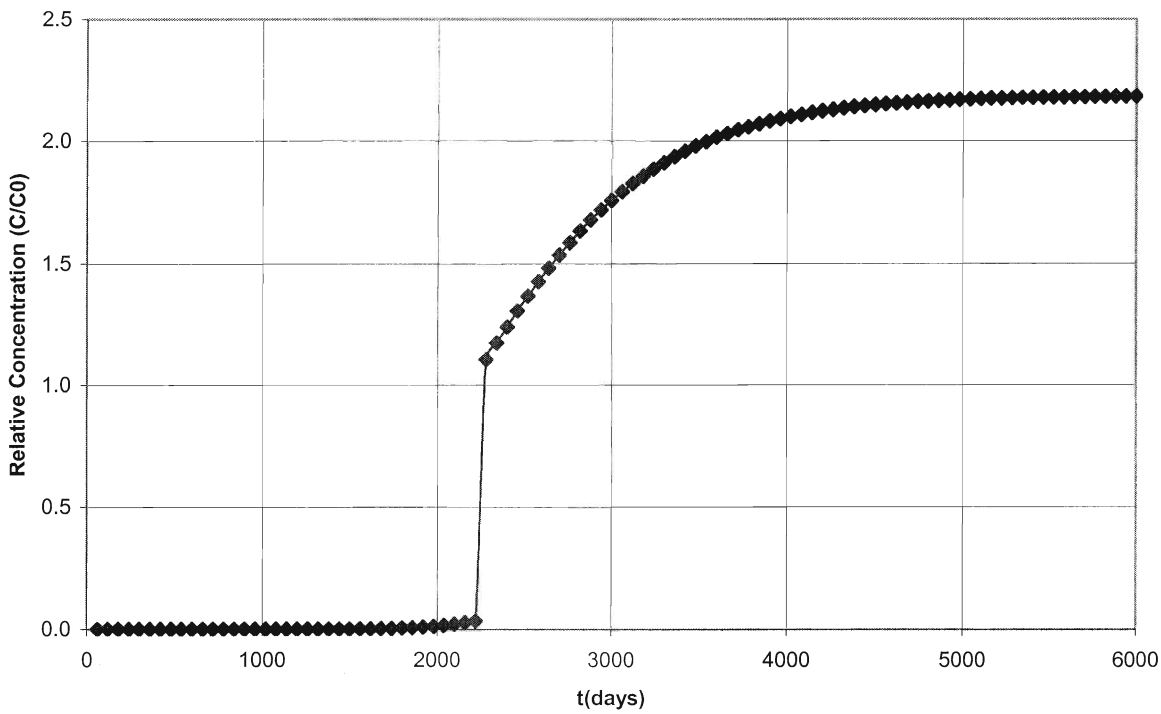

Figure 3.5 Growth and decay plot for Table 3.3

3.3.3 BASE CASE RESULTS

The aqueous phase bacteria concentrations are simulated at an observation point located 10m form the source. The constant concentration of 10 gr/m^3 bacteria is provided as source throughout the 5000 day duration of the base case simulation. The breakthrough curve for the base case is plotted in Figure 3.3. The first appearance of bacteria at the observation location is around 1500 days, which is referred to as the induction period (Characklis, 1990, Kornegay, 1968). The curve becomes constant around 4000 days where the concentration in the fracture is almost equal to the source concentration. Between 1500 to 4000 days biofilm accumulation occurs actively. After 4000 days, the accumulation significantly declines and eventually stops. Thus the biofilm accumulation stops without the addition of further layers, at that plateau stage. The adsorption and desorption are dominated by attachment and detachment at 2200 days. The 2200^{th} day is the end of the period needed for accumulation of 2 layers of biofilm. At the end of this period, the substratum is covered with biofilm, thus the bulk fluid-substratum interface no longer exists. After 2200 days, attachment and detachment begins. If the overall breakthrough curve is considered, attachment-detachment dominates the majority of the accumulation period, which indicates adsorption-desorption is significant only in the early time. Also it should be noted that, in this simulation, the attachment rate is lower than adsorption rate, similarly, the detachment rate is lower than the desorption rate. Such a difference results in a rapid rise in the aqueous concentration at the time following the 2200days mainly because irreversible adsorption is eliminated and the major rate-limiting process rates are changed. If detachment is kept equal to the desorption rate, and attachment equal to the adsorption rate, at low irreversible

adsorption of 1.0×10^{-5} day^{-1}, the switch between the curves is much smoother as can be seen in Figure 3.4.

In order to eliminate the rise in the relative concentration at time equal to τ, reducing the time steps was tried by increasing the number of time points. Unfortunately this did not help the curve become smoother.

In Figure 3.4, the attachment rate is equal to adsorption rate of 3 day^{-1}, and the detachment rate is equal to desorption rate of 6 day^{-1}. The constant concentration of 10 gr/m^3 bacteria is provided as source through out the 12000 day duration of the simulation. In this case, since the adsorption and attachment rates are higher, the three stages of accumulation last longer, and it takes the aqueous concentration longer to reach the source concentration at the observation point. The first appearance of bacteria at the observation location is around 1500 days, almost the same time as base case. The curve becomes constant around 8500 days where the concentration in the fracture is almost equal to the source concentration. Beginning at 1500 days biofilm accumulation occurs actively. The accumulation period is longer than the base case. After 8500 days, the rate of accumulation declines and relative concentration reaches the value 1.0. The adsorption and desorption are dominated by attachment and detachment at 2160 days. This value is very close to the that of the base case. Similar to the base case, attachment-detachment dominates the majority of the accumulation period. The major difference between the two simulations are the duration of the log accumulation period and the starting of the plateau stage.

The addition of growth and decay processes does not influence the time at which Phase I is complete (Figure 3.5). In this case, adsorption-desorption becomes dominated by attachment-detachment at 2200 days, similar to the base case. The simulation for the base case

was run for 5000 days, whereas the case with growth and decay was run for 6000 days. The durations of the induction and accumulation periods remain similar as for the initial base case. The relative concentration increases to 2.18 during the plateau period, which is an expected result due to the addition of the growth rate.

When rate-limiting process rates are set to be equal, the addition of growth and decay does not influence the breakthrough curve in a significant manner (Figure 3.6). Adsorption-desorption becomes dominated by attachment-detachment at 2150 days. The simulation when k_1 equals to k_{at} and k_2 equals to k_{det} without growth and decay was run for 12000 days, whereas the case with growth and decay was run for 15000 days. The relative concentration increases to 2.18 during the plateau period similar to the simulation plotted in Figure 3.5. The main difference other than the durations is that the switch between two curves is much smoother with no sudden rises.

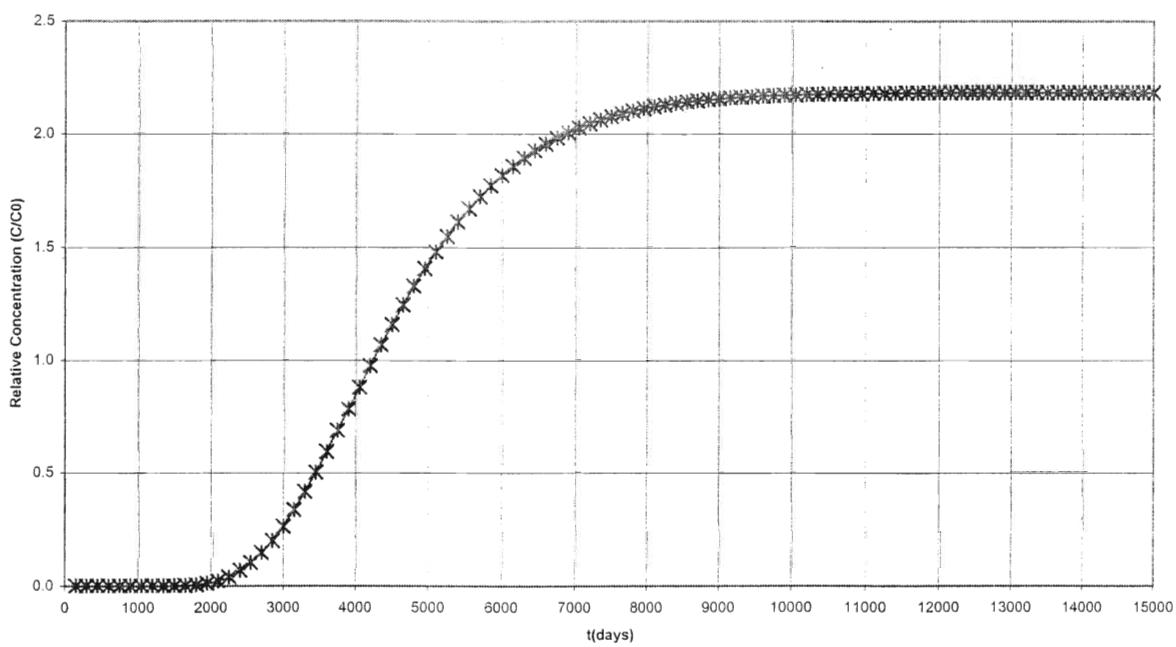

Figure 3.6 Growth and decay are added to base case rate-limiting process rates are set equal.

3.4 SENSITIVITY ANALYSIS AND DISCUSSION

The first parameter investigated is the constant source condition. The code BIOFRAC is run for C_0 values starting from 0.00001 gr m^{-3} to 1000 gr m^{-3}. First the base case is simulated with different source concentration (Figure 3.7) and then the rate-limiting process rates are set equal and simulations are repeated to receive a smooth curve (Figure 3.8). The increase in the concentration of bacteria input to the system does not influence the base case curve in the form of a shift or a drop or rise in case of Figure 3.8. If Figure 3.7 is considered, a sudden rise at the switch point is observed for each simulation, which is a result of the difference between adsorption-desorption and attachment-detachment rates. The results indicate that the accumulation of two layers of biofilm does not occur until the source concentration is as high as 1 gr m^{-3} for both cases. This is an expected result since as the source concentration increases, the amount of bacterial input increases, providing more opportunity for bacteria to reversibly and irreversibly sorb to the substratum. The first appearance of bacteria at the observation location remains at 1500 days regardless of the source concentration and regardless of sorption or attachment-detachment rates. Similarly the ratios of periods of induction, log accumulation and plateau stages do not differ from the base case. In Figure 3.7, as source concentration increases, the amount of sudden rise decreases, as the accumulation of two layers occur faster.

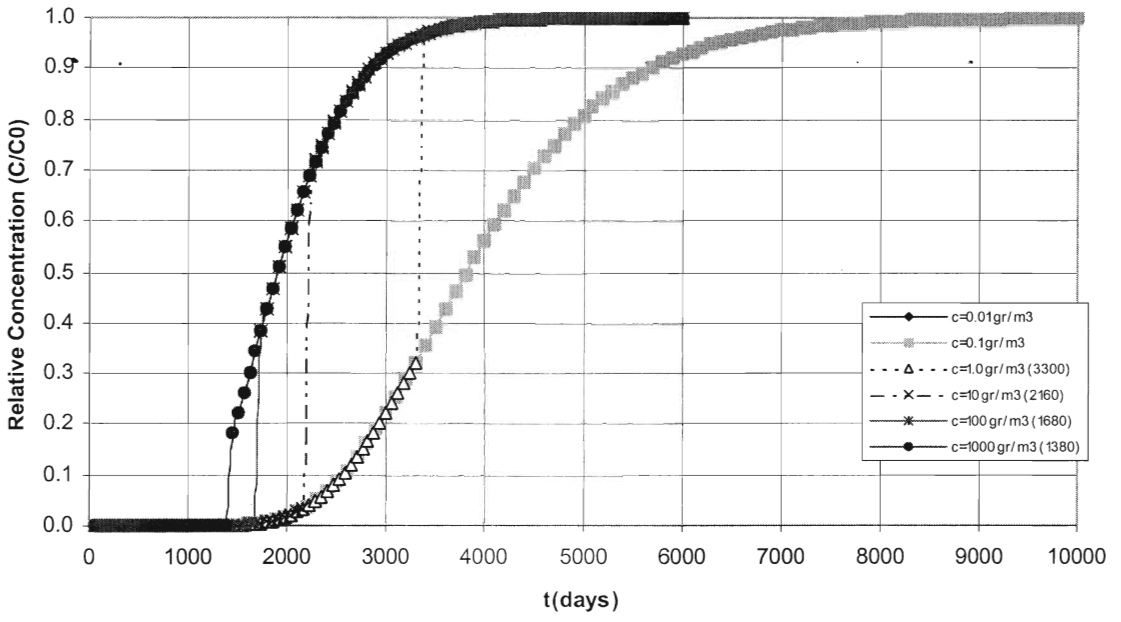

Figure 3.7 Sensitivity analysis for source concentration

The effect of increase in source concentration is observed as a change of the periods for Phase I and Phase II. When the amount of constant source concentration is equal to 1 gr m^{-3}, Phase I lasts for 3360 days in Figure 3.8 and 3300 days in Figure 3.7. As the source concentration increases, τ decreases. the larger quantities of bacteria are supplied. Results are presented in Table 3.4.

Source Concentration (C0) (gr m^{-3})	Duration of Phase I (τ) (day)
Between 0.0001 and 0.1	10000, Phase II does not occur
1.0	3360
10	2160
50	1800
100	1680
1000	1440

Table 3.4 Sensitivity analysis results for source concentration

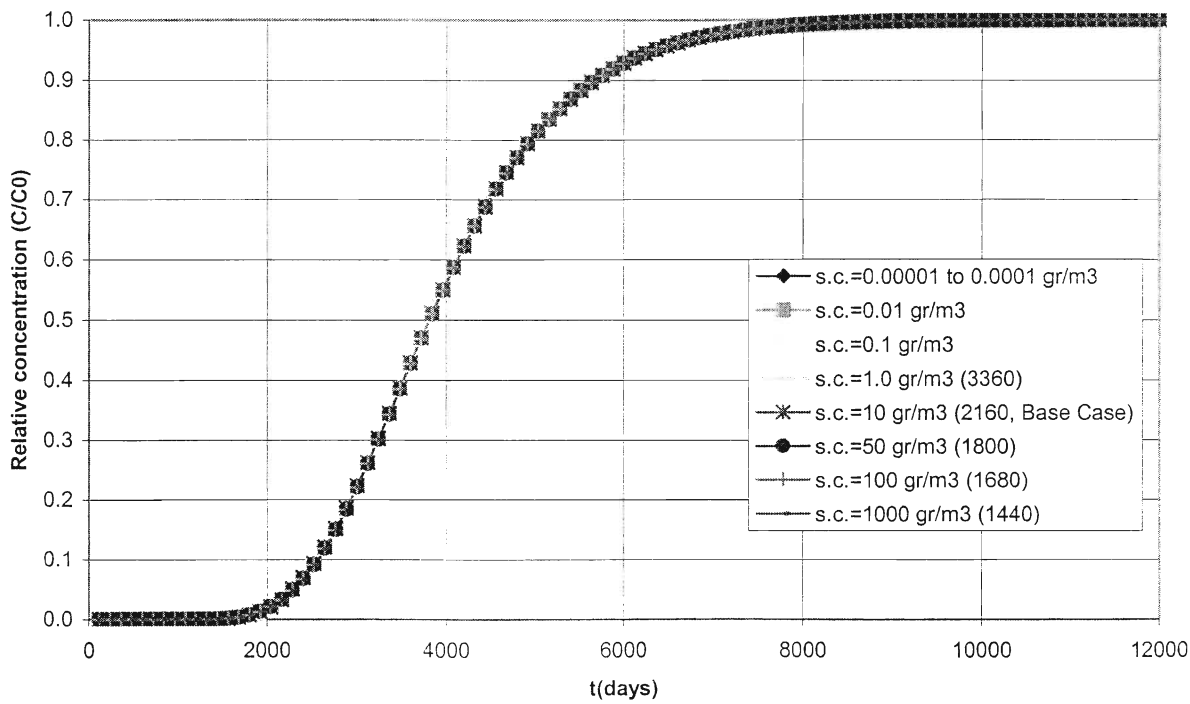

Figure 3.8 Sensitivity analysis for source concentration with rate-limiting process rates are set equal

Sensitivity analyses to velocity, and dispersivity are observed to be same as the behavior inferred from the Ogata-Banks code. An increase in velocity results in curves that achieve stabilization at a faster rate and the aqueous bacteria front arrives at the outlet, sooner (Figure 3.9, Figure 3.10 and Figure 3.11).

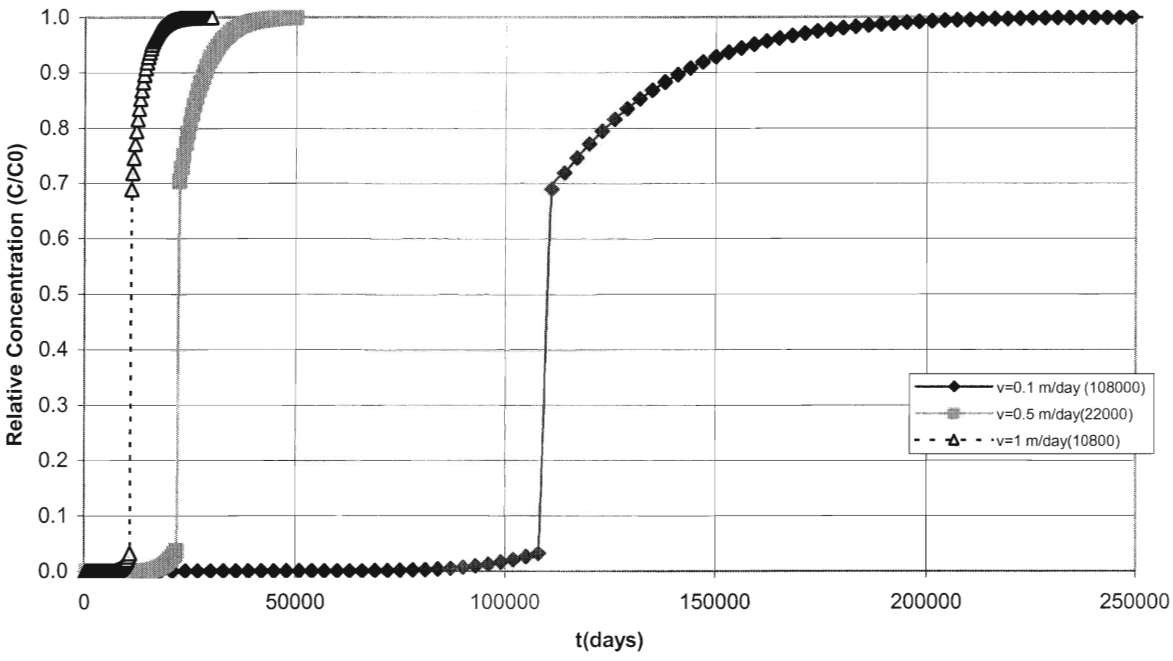

Figure 3.9 Sensitivity analysis for velocity

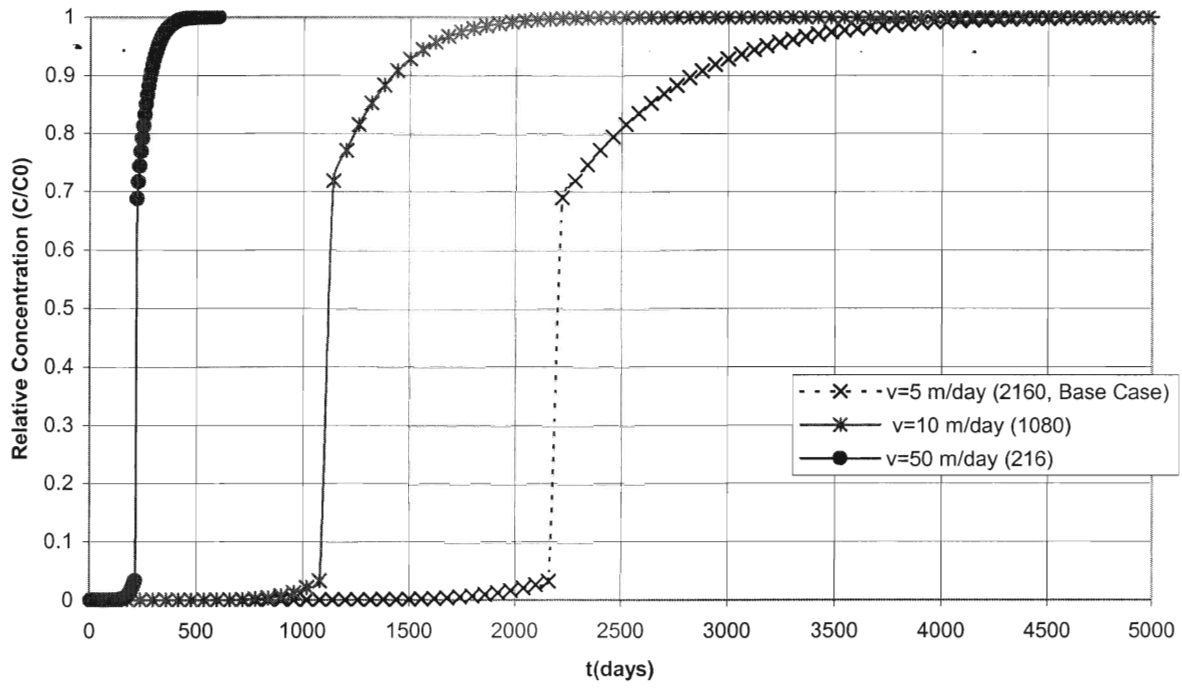

Figure 3.10 Sensitivity analysis for velocity Plot 2

As the velocity increases, the transport of bacteria occurs at a faster rate, however accumulation is not as significantly influenced by velocity as much as is transport. However, regardless of the increase or decrease in the value of velocity, the duration of Phase I does not exceed the first quarter of the duration of all three stages of accumulation as can be seen from the results given in Table 3.5 and Table 3.6. The simulations were run until the end of the plateau stage for each velocity thus end at various times. Thus, the appearance times of bacteria, durations of log accumulation and time to plateau phase differs in each simulation. However, the proportion between the Phase I duration and Phase II duration are similar. In the case where the rate-limiting process rates are set equal, the switch between phases occur as a smooth curve (Figure 3.11, Table 3.5), whereas when the base case is simulated (Figures 3.9 and 3.10, Table 3.6), a sudden rise occur at the switch points. As opposed to the source concentration

simulations, the change in relative concentration from τ to $\tau+1$ is constant for each curve. The increase or decrease in velocity does not effect the amount of rise. When Figures 3.9 and 3.10 are compared to Figure 3.11, it is observed that, in the case when rate-limited process rates are set equal, the log accumulation and plateau stages are longer, hence the Phase II lasts longer. The base case has the same Phase I durations as Figure 3.11, however the plateau stages are reached more rapidly.

Velocity (m day^{-1})	Duration of Phase I (τ) (day)	Duration of Simulation (TSTOP) (day)
1.0	10800	30000
5.0	2160	5000
10	1080	5000
50	216	600

Table 3.5 Sensitivity analysis results for velocity

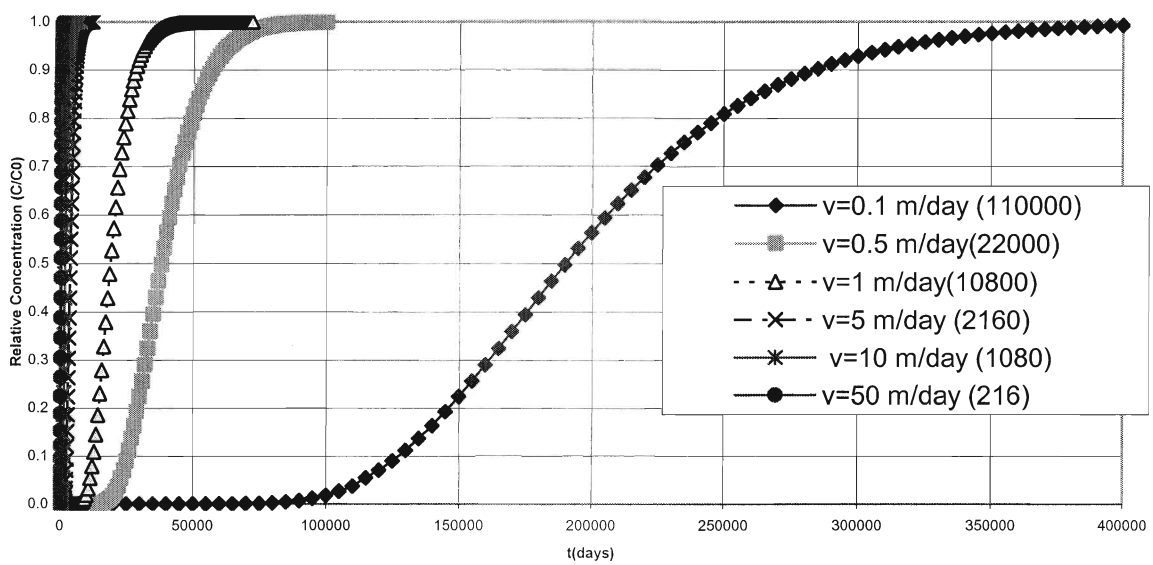

Figure 3.11 Sensitivity Analysis for velocity with rate-limiting process rates are set equal

The sensitivity analysis for dispersivity is conducted for values between 0.01 and 5m. The effect of dispersivity is easily observed in that as dispersivity increases, the time required to reach the outlet increases and the slope of the breakthrough curve becomes less steep (Figures 3.12 and 3.13). The simulations were conducted for base case over 5000 to 10000 days. When dispersivity was as high as 5m, the log accumulation period exceeded the simulation period and the plateau was reached slightly over 10000 days in case of Figure 3.12, and over 12000 days in case of Figure 3.13. As dispersivity increases, the two layers of biofilm covers the substratum much faster, hence Phase I is shorter and attachment-detachment are the most dominant processes during the log accumulation period. The duration of the log accumulation period is significantly influenced by changes in dispersivity. The Phase I duration does not change significantly between the base case and the simulation done with equalized rate-limiting process rates. However, the duration of the processes decrease in case of base case. As discussed previously this is mainly due to reduction in attachment and detachment rate between two simulations. The results of the sensitivity analysis for dispersivity are given in Table 3.6.

Dispersivity (m)	Duration of Phase I (τ) (day)
0.01	3700
0.05	3350
0.1	3100
0.5	2160
1.0	1700
5.0	700

Table 3.6 Sensitivity analysis results for dispersivity

The sensitivity analysis for fracture aperture is run for 5 different values. The simulations last until the end of the plateau stage for each value, and thus end at various times. In case of fracture aperture (Figures 3.14 and 3.15), as the aperture decreases, the time required for the plateau stage increases drastically. This could be because lower the fracture aperture, the slower the transport is expected.

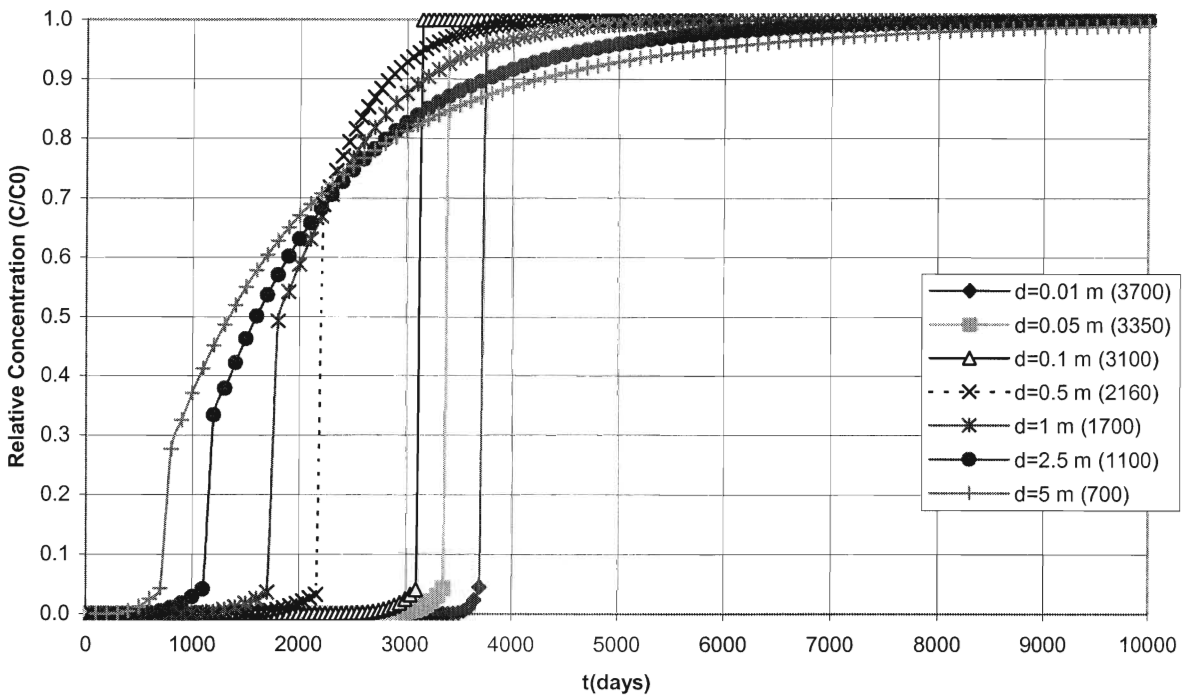

Figure 3.12: Sensitivity analysis for dispersivity

The change in fracture aperture does not effect the ratio of the duration of Phase I to Phase II. Phase I still lasts through the first quarter of the simulation. However the total duration of accumulation increases as fracture aperture decreases. The rise in the relative concentration, in the base case simulation, does not change with increasing fracture aperture. There occurs a slight

difference between the switch points in Figure 3.14 and Figure 3.15, which indicates the duration of Phase I is very similar. The results for aperture simulations are in Table 3.7.

Fracture Aperture (2b) (m)	Duration of Phase I (τ) (day)
2.5×10^{-5}	44000
5.0×10^{-5}	22000
0.0001	10800
0.0005	2200
0.001	1080

Table 3.7 Sensitivity analysis results for fracture aperture

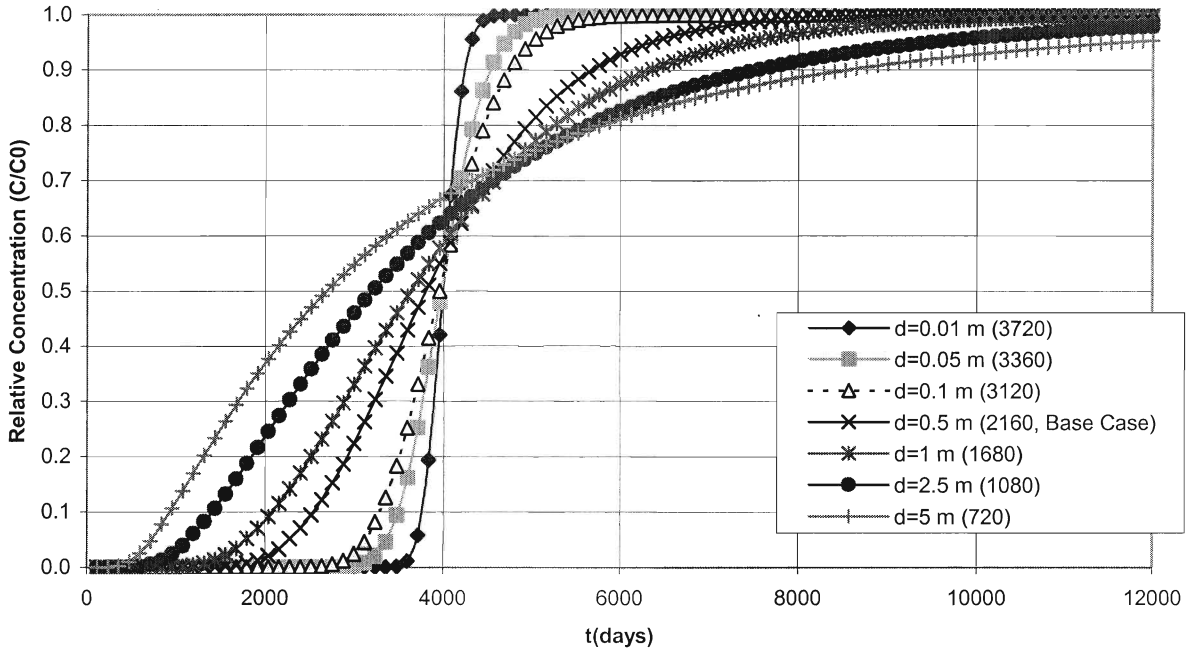

Figure 3.13 Dispersivity with rate-limiting process rates are set equal

the base case simulation, does not change with increasing fracture aperture. There occurs a slight difference between the switch points in Figure 3.14 and Figure 3.15, which indicates the duration of Phase I is very similar. The results for aperture simulations are in Table 3.7.

Fracture Aperture (2b) (m)	Duration of Phase I (τ) (day)
2.5×10^{-5}	44000
5.0×10^{-5}	22000
0.0001	10800
0.0005	2200
0.001	1080

Table 3.7 Sensitivity analysis results for fracture aperture

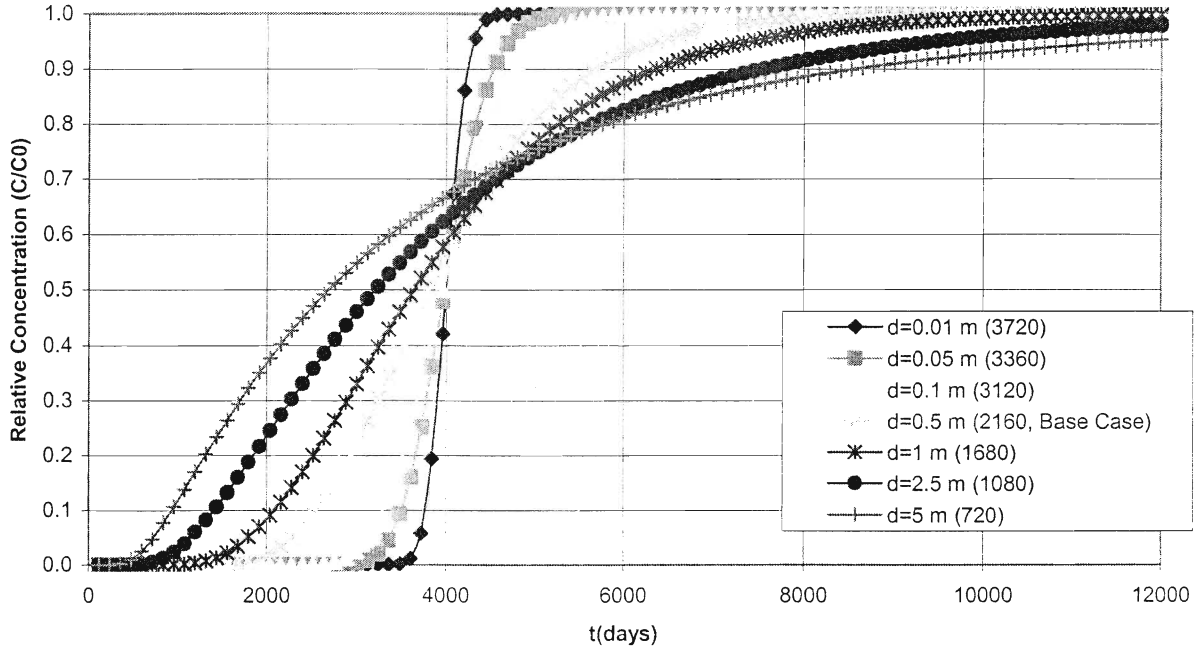

Figure 3.13 Dispersivity with rate-limiting process rates are set equal

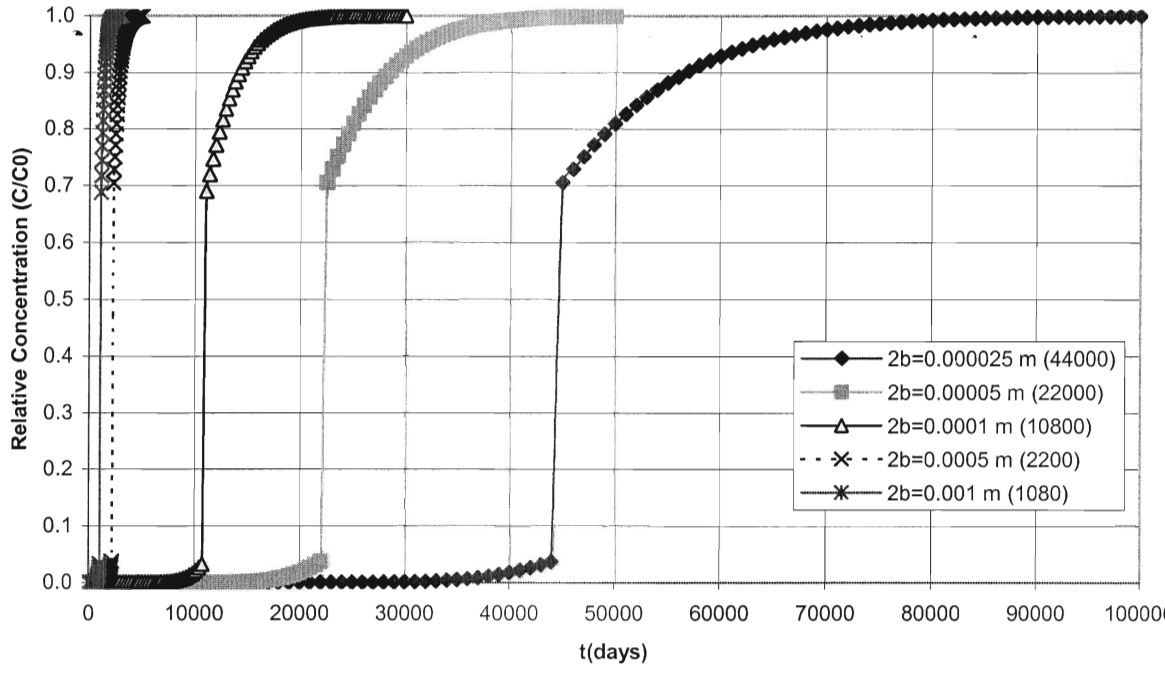

Figure 3.14 Sensitivity analysis for fracture aperture

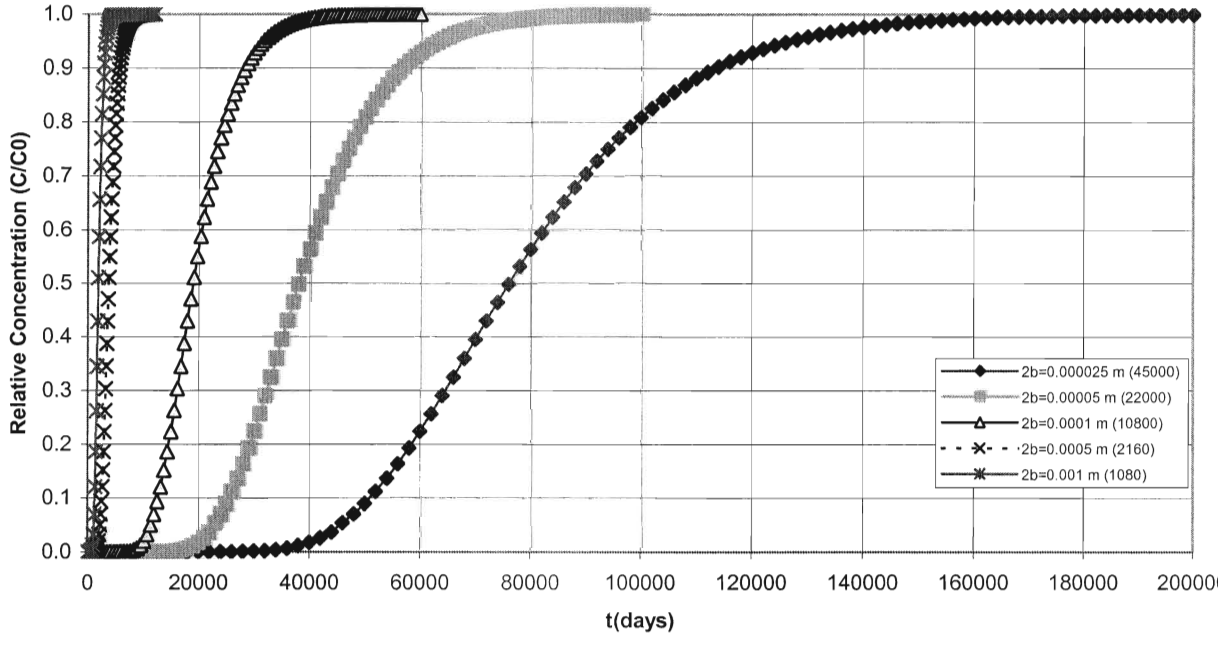

Figure 3.15 Sensitivity analysis for fracture aperture with rate-limiting process rates are equal

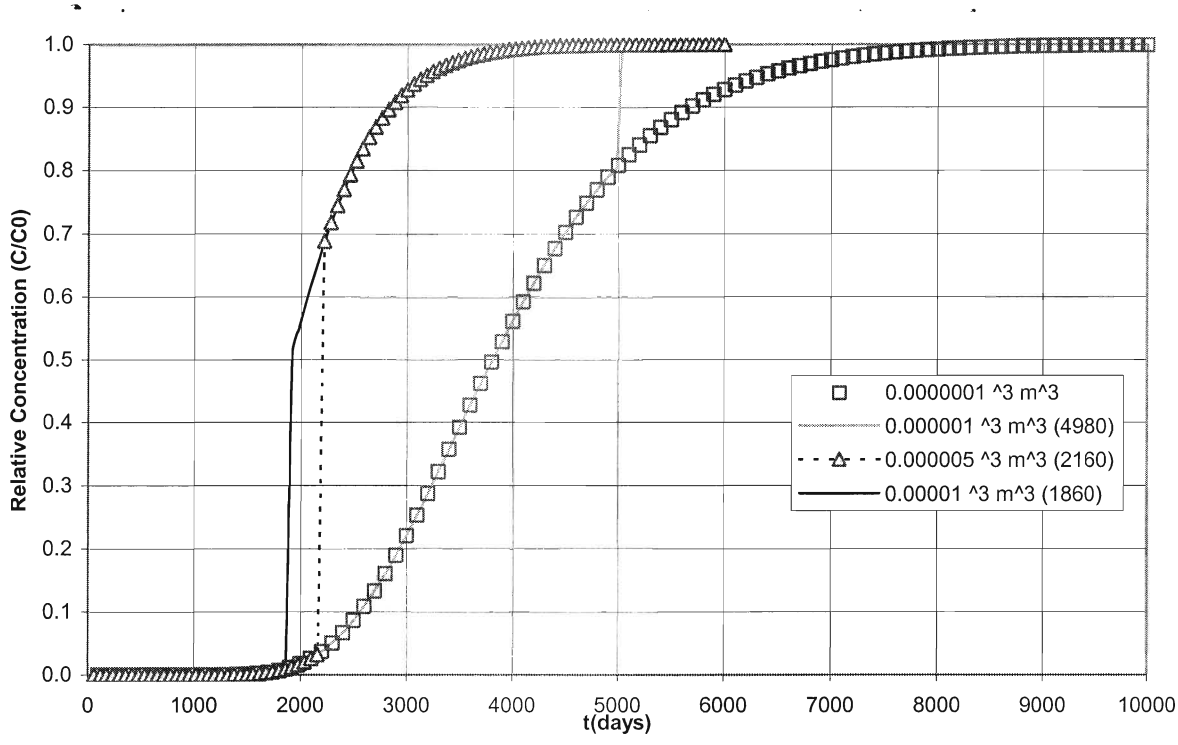

Figure 3.16 Sensitivity analysis for bacteria cell size

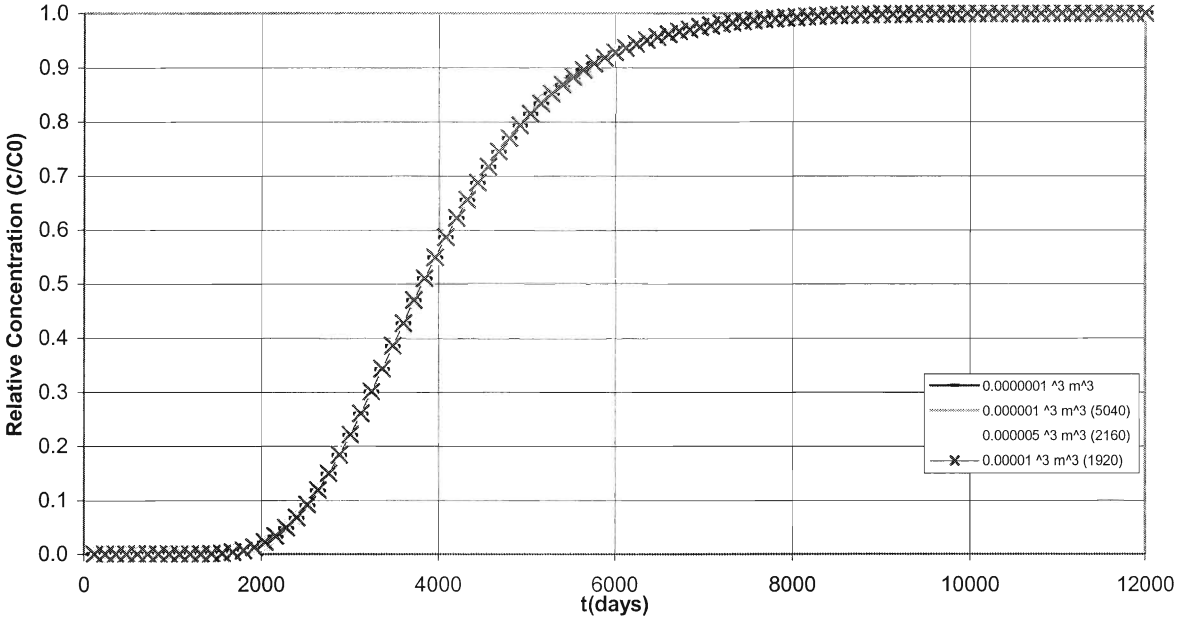

Figure 3.17 Sensitivity analysis for bacteria cell size with rate-limiting process rates are equal

Cell size influences the duration of Phase I. The determination of the point at which Phase I is completed, is based on the bacterial cell size and mass. The larger the bacteria, the faster the substratum will be covered. The concentration of bacterial cells is represented as mass per volume of aqueous phase. Thus, if the mass of one bacterial cell is higher, then when the concentration is divided by mass of one bacterial cell, the number of cells will be lower. When the number of cells are less, then the accumulation will occur at a slower rate. In the simulation for base case, because Phase I process rates are different than Phase II process rates, a rise occur at the switch point. Also, the duration of log accumulation stage is shorter , Phase I lasts shorter as cell size increases (Figure 3.16). Since Phase II dominates the over all accumulation and rates in Phase II are faster, the log accumulation period occurs faster. In case where Phase I process rates are equal to Phase II process rates, the durations of the 3 accumulation stages remain the same for different values of bacteria size (Figure 3.17). Such behavior suggests that, bacteria size, coupled with rate-limiting processes can effect the duration of the accumulation period.

In order to predict the rate of biofilm accumulation, a sensitivity analysis on the number of layers is also performed. When the number of layers is equal to two, the switch between phases occurs as in the base case. It is assumed that the substratum is fully covered, thus no substratum–bulk fluid interface occurs, and adsorption-desorption is dominated by attachment-detachment. The results of the sensitivity analysis to the number of biofilm layers indicate that the first layer of biofilm occurs at 2000 days, and then another layer is accumulated every 100days. In the case where Phase I process rates are equal to Phase II process rates, it was found for the base case that a single layer of biofilm is formed in 2040 days, and the second layer is accumulated only 120 days after that (Figure 3.19). For three and four layers of biofilm, the

Phase I duration is 2400 days. It is observed that the initial accumulation of biofilm layers fall into the log accumulation stage.

Number of Layers	Duration of Accumulation (days)
1	2000
2	2200
3	2300
4	2400
5	2500

Table 3.8 Accumulation of layers

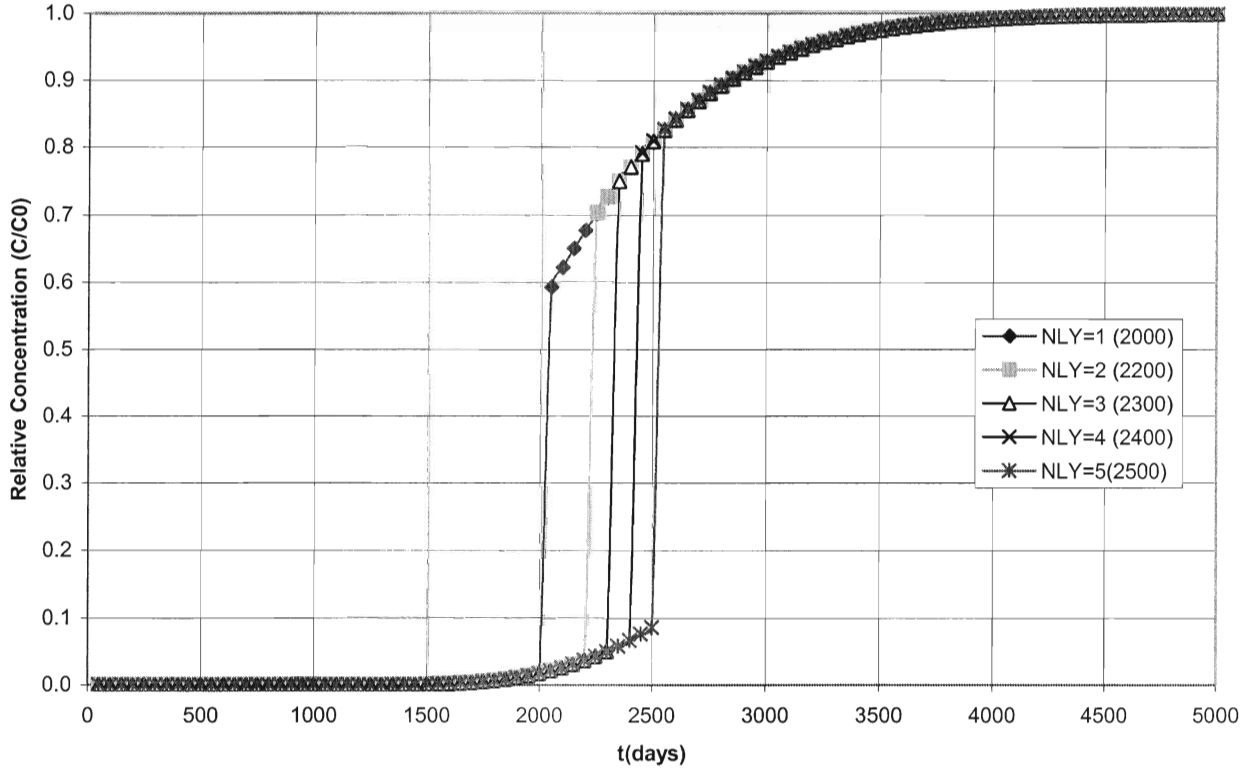

Figure 3.18 Sensitivity analysis for number of layers

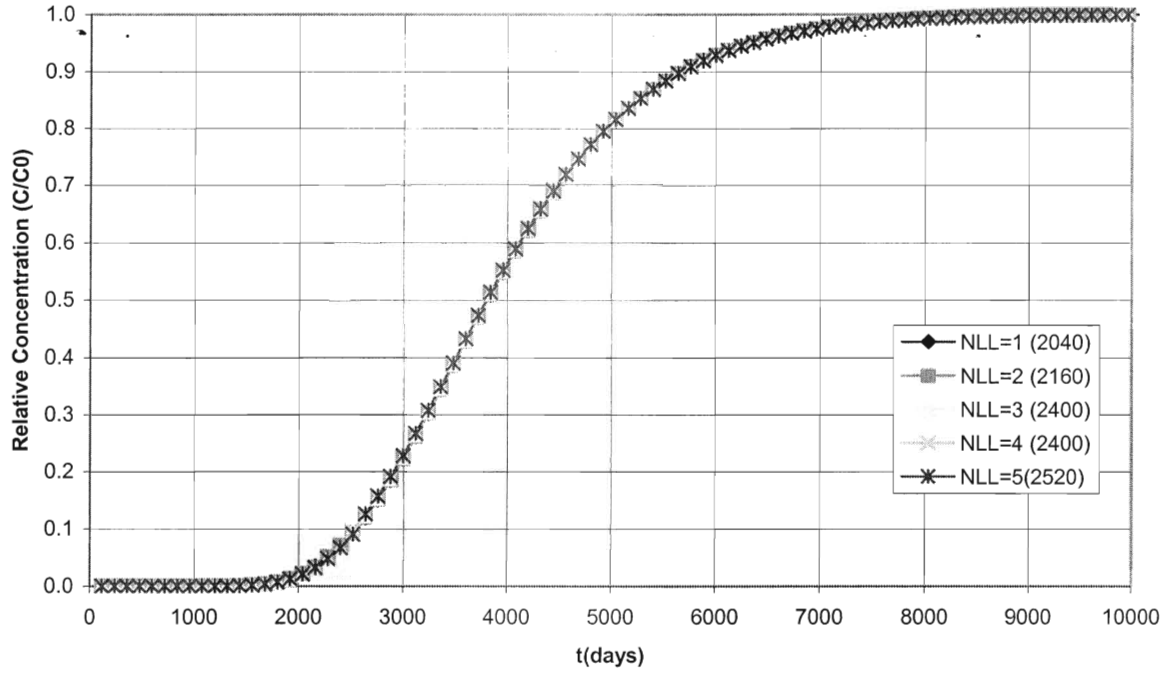

Figure 3.19 Number of biofilm layers with rate limiting process rates are set equal

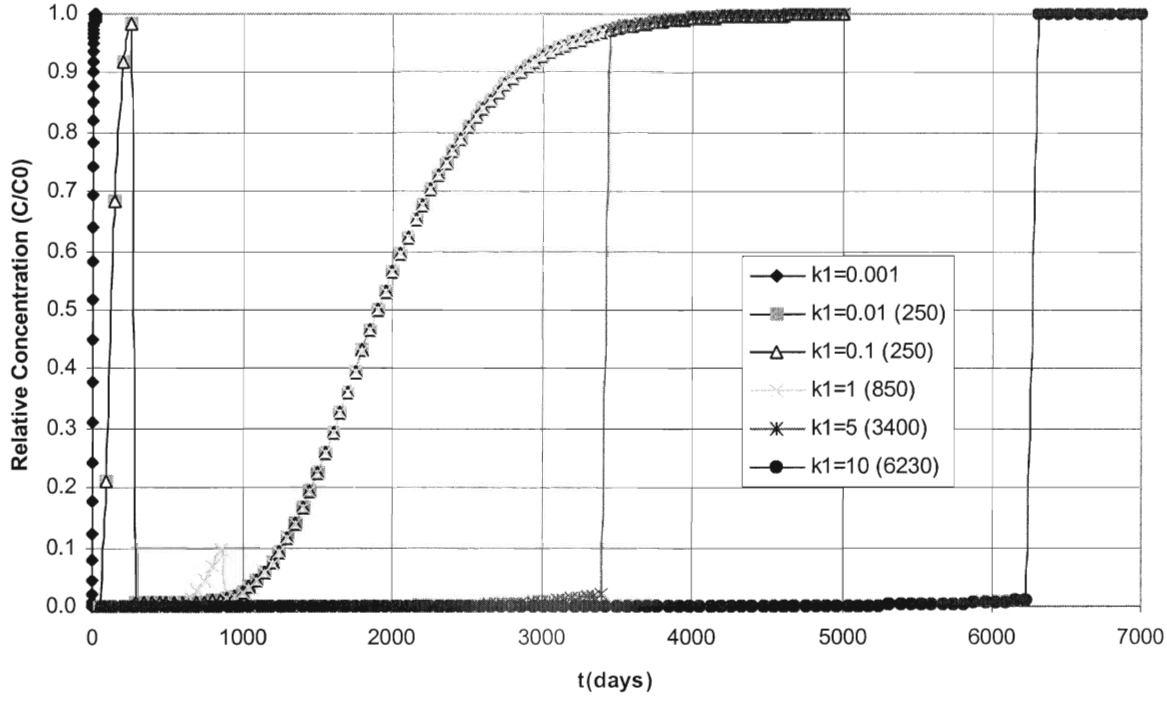

Figure 3.20 Sensitivity analysis for rate-limited adsorption

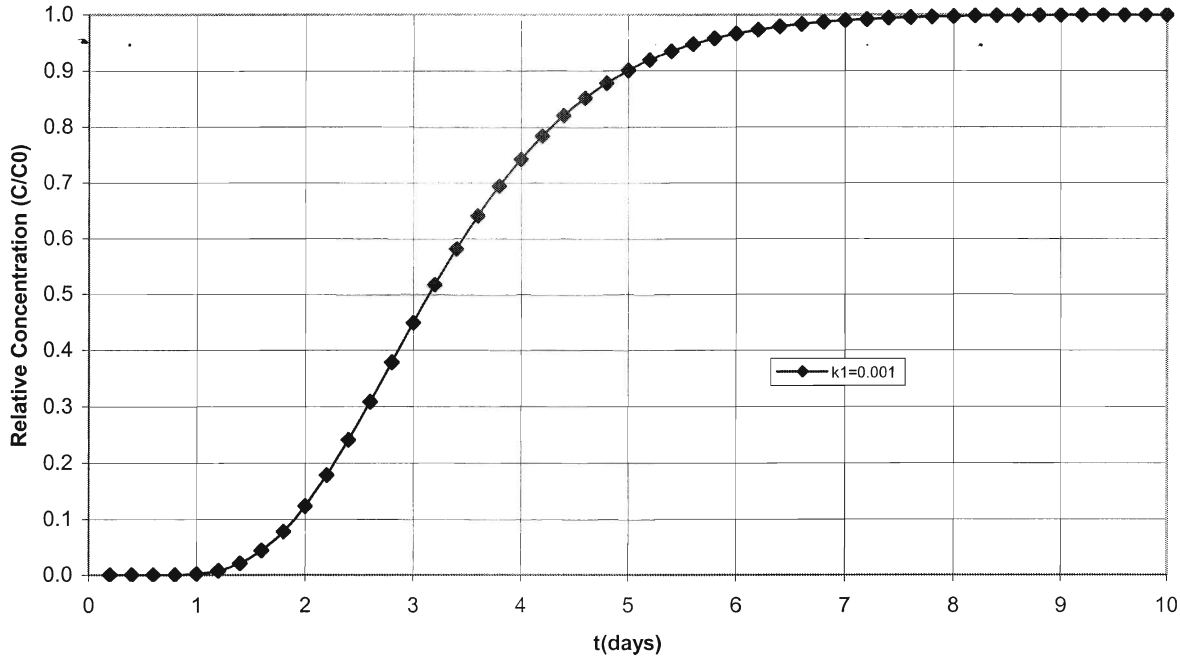

Figure 3.21 Sensitivity analysis for rate-limited adsorption Plot 2

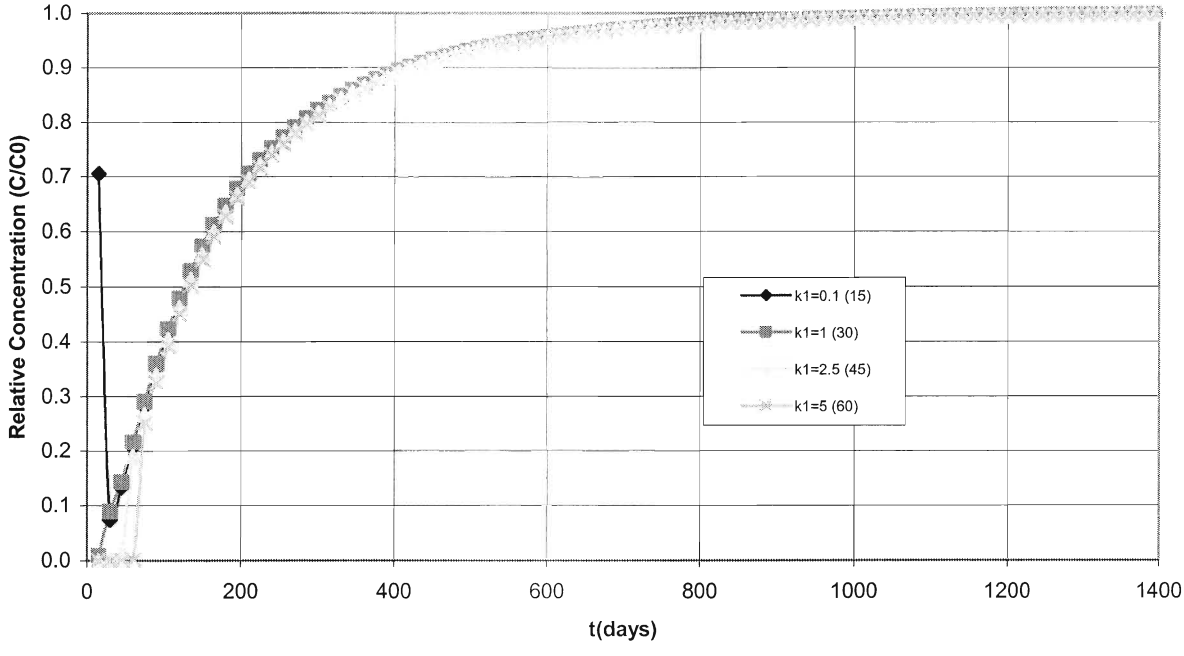

Figure 3.22 Sensitivity analysis for rate-limited adsorption at observation point x=1m

The sensitivity analysis for rate-limited process rates are only conducted for the base case, as it is the effects of changes in those rates are that being sought. The results for rate-limited adsorption indicate that when the rate is lower than 0.01 day^{-1}, Phase I dominates the whole accumulation period and two layers of biofilm do not occur. Thus we see a smooth Phase I curve (Figure 3.21). For the base case, when the rate equals to 0.01 day^{-1}, two layers accumulate in 250 days. It is observed that as adsorption rate increases, the duration of Phase I increases (Figure 3.20, Table 3.9). When the adsorption rate is high, the bacteria entering the fracture from the inlet adsorbs to the substratum faster, leaving the aqueous phase moving towards outlet with less concentration of bacteria. Thus when the same volume of aqueous phase reaches the outlet, the concentration is significantly less. With lesser concentration at the outlet accumulation takes longer. So, despite the expectation of a drop in the duration of Phase I with increasing adsorption, the accumulation slows down at "the outlet". For rate-limited adsorption values less than and equal to 1.0 day^{-1}, the switch point occurs in the form of a rise. Before the vale of τ, the adsorption rate is so low, that desorption dominates the processes and increases the aqueous phase concentration, but after the switch point, the attachment rate is higher than the adsorption rate, thus the aqueous concentration declines and diminishes the log accumulation process. For values higher than 1, because of the difference between Phase I and Phase II rates, a sudden rise occurs. Inspecting the adsorption pattern towards the inlet (at 1m) it is observed that the accumulation occurs much faster, in 15 to 60 days (Figure 3.22). The inverter, calculates very little data before τ, thus the values are relatively high, and a drop occurs at τ. This indicates that during the period before τ, accumulation occurs very rapidly, and then Phase II takes over and occurs slower than Phase I.

Rate-Limited Adsorption Coefficient (k_1) (day^{-1})	Duration of Phase I (τ) (day)
1.0×10^{-5}	(no Phase II)
0.0001	(no Phase II)
0.001	(no Phase II)
0.01	250
1.0	850
5.0	3400
10.0	6230

Table 3.9 Sensitivity analysis results for rate-limited adsorption

A sensitivity analysis on rate-limited desorption is applied for values between 0.5 and 20.0 day^{-1}. When the desorption rate is less than 0.001 $days^{-1}$, the accumulation is slow at the outlet, up to 1.5×10^7 days. In the case where the desorption rate is 0.1 $days^{-1}$, at the time of switch the rise in relative concentration is from 6.0×10^{-4} to 1.0 all of a sudden. At 0.5 $days^{-1}$, the switch occur at 19750 days. Thus Phase I is completed in 19750 days and the accumulation of two layers is completed. There exists a significant difference between Phase I mass transfer rates and Phase II mass transfer rates, depending on the amount of this difference, there exists a sudden rise in the concentration in τ. Higher the difference between the mass transfer rates, higher the rise occurs. As the desorption rate increases, the duration of Phase I decreases. Since the adsorption and desorption are reverse processes, the effect of desorption is the opposite of adsorption. When the bacteria entering the fracture desorb rapidly at the inlet, the concentration in aqueous phase moving towards outlet is higher, thus allowing more bacteria to reach the outlet in a shorter period of time. A change in the desorption also influences the ratio of Phase I and

Phase II periods. As the desorption decreases, the log accumulation period is shorter and more rapid. Also, the lower the desorption rate, the longer the Phase I (Figures 3.23 and 3.24, Table 3.10). As the desorption rate increases, the curve reaches the plateau stage sooner, since more bacteria is desorbed backed into the aqueous phase. In case of low desorption rates, the aqueous phase, transported to the outlet carries less bacteria, but eventually, the adsorbed bacteria towards the inlet desorbs back into the aqueous phase, and transported to the outlet, hence all the breakthrough curves slowly or rapidly, depending on the rates, reach the plateau stage where the relative concentration is 1.0. Similarly at 1m, as the desorption rate increases, the duration of the accumulation decreases since more and more bacteria is carried to 1m with increasing desorption.

Rate-Limited Desorption Coefficient (k_2) (day^{-1})	Duration of Phase I (τ) (day)
0.5	19750
1.0	10750
3.0	4680
6.0	2580
10	1440
15	1020
20	780

Table 3.10 Sensitivity analysis results for rate-limited desorption

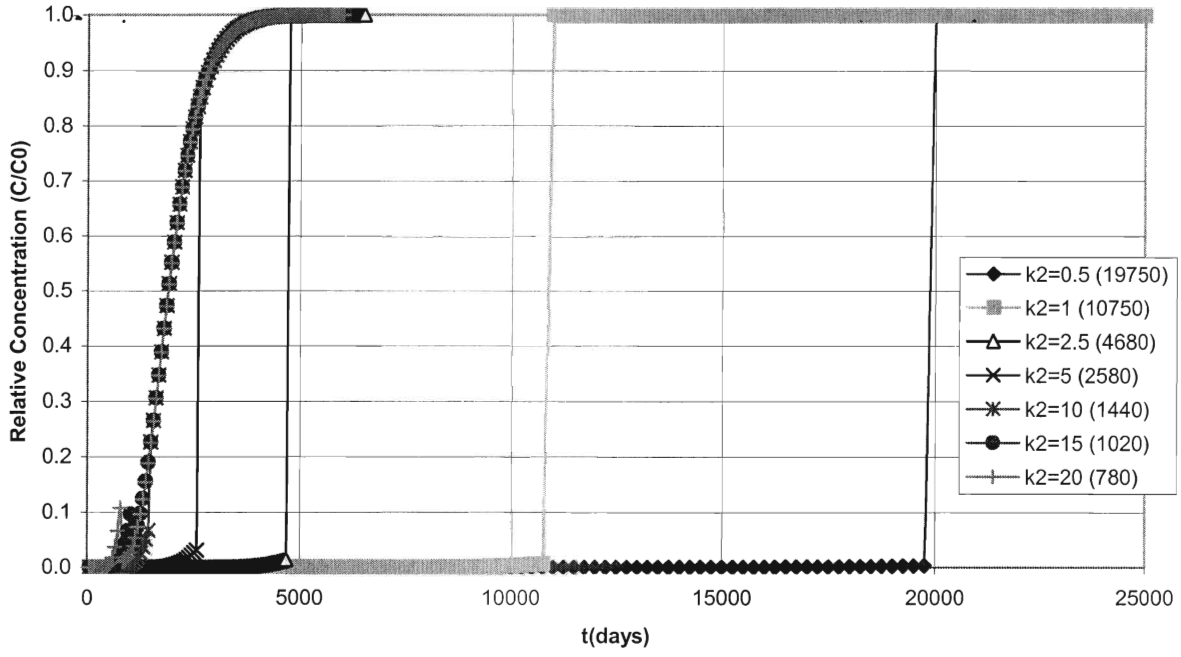

Figure 3.23 Sensitivity analysis for rate-limited desorption

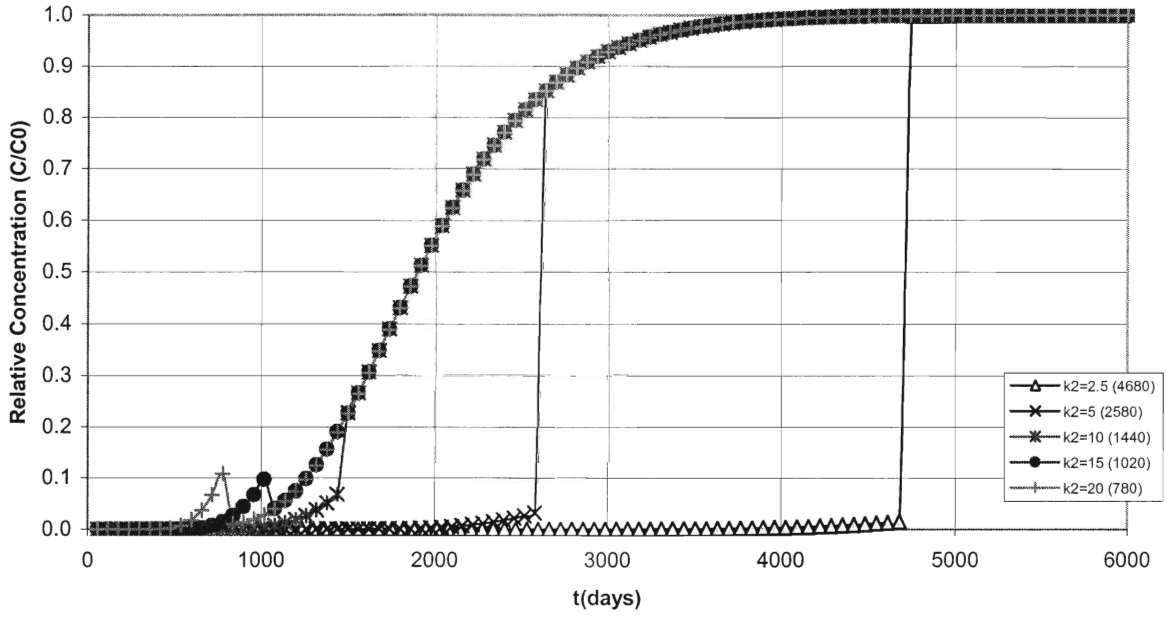

Figure 3.24 Sensitivity analysis for rate-limited desorption plot 2

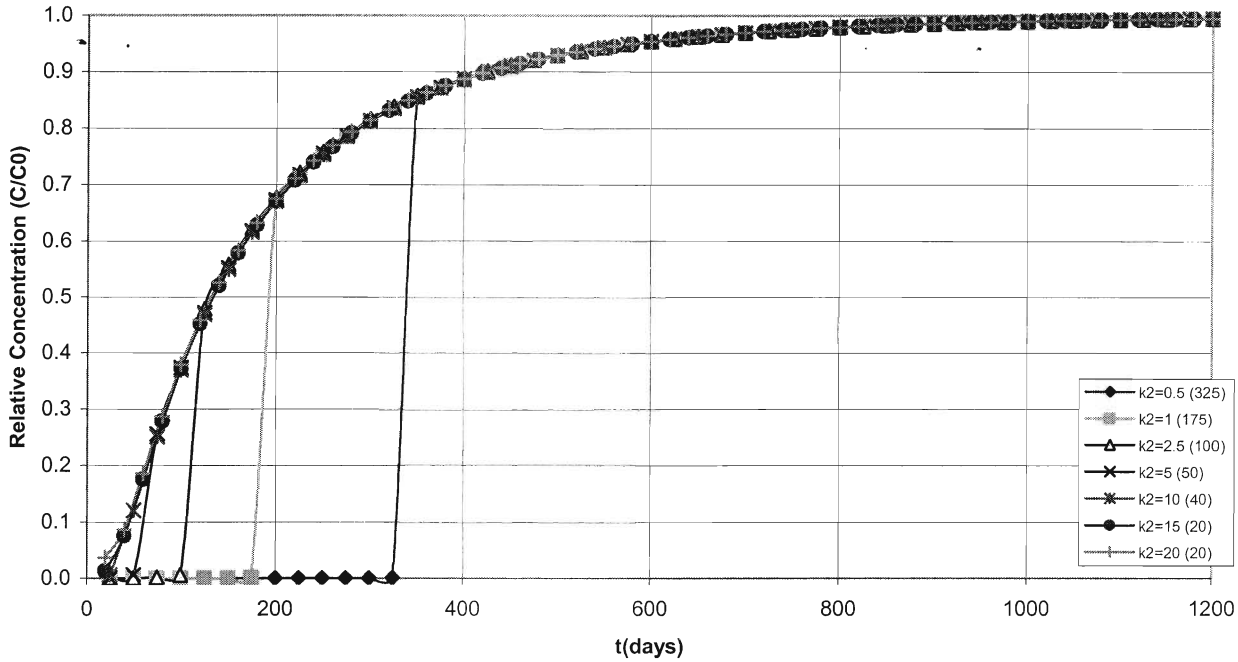

Figure 3.25 Sensitivity analysis for rate-limited desorption at observation point x=1m

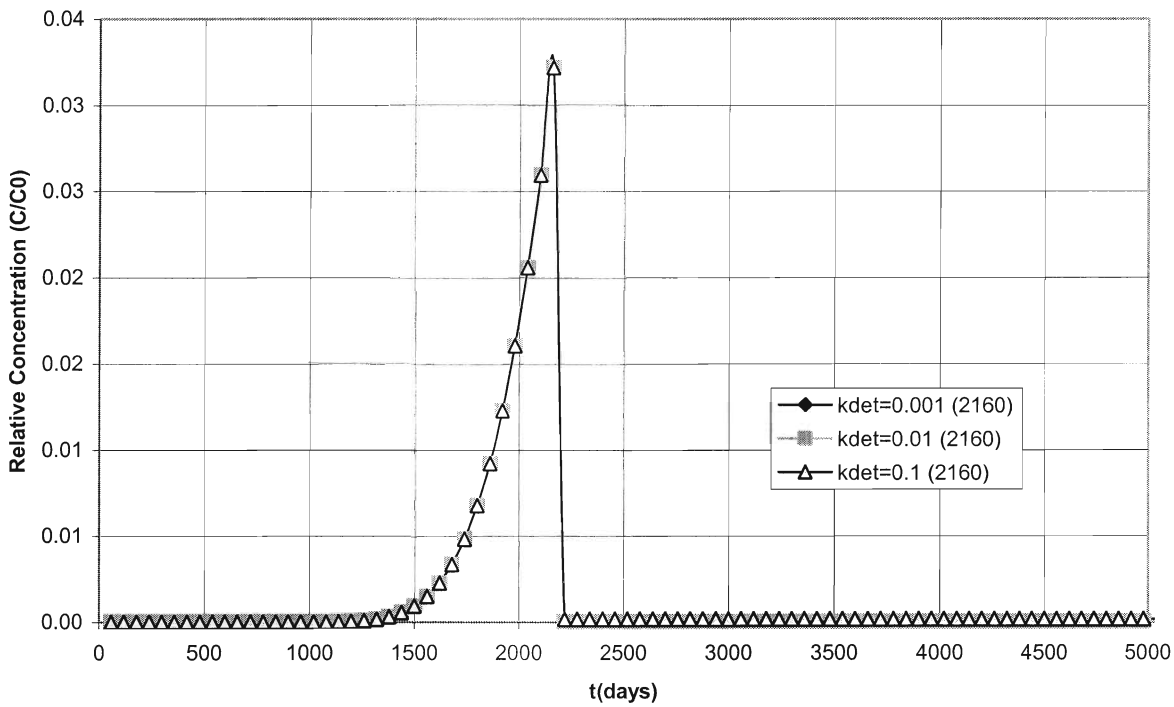

Figure 3.26 Sensitivity analysis for detachment

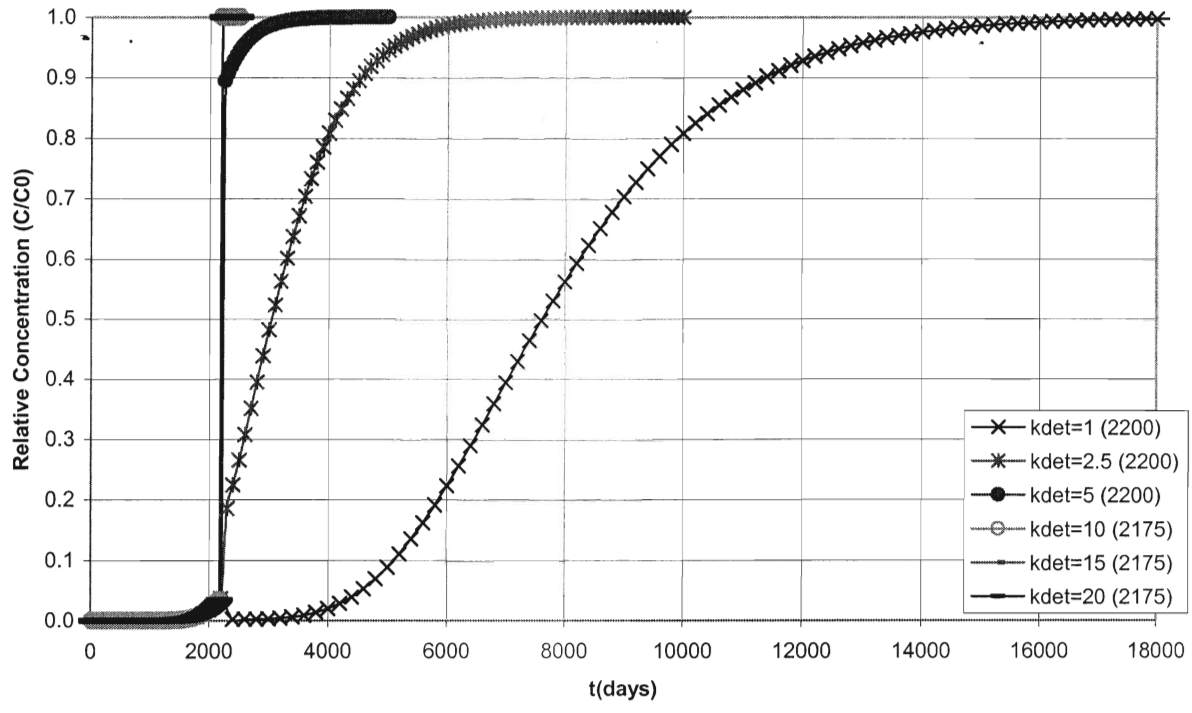

Figure 3.27 Sensitivity analysis for detachment Plot 2

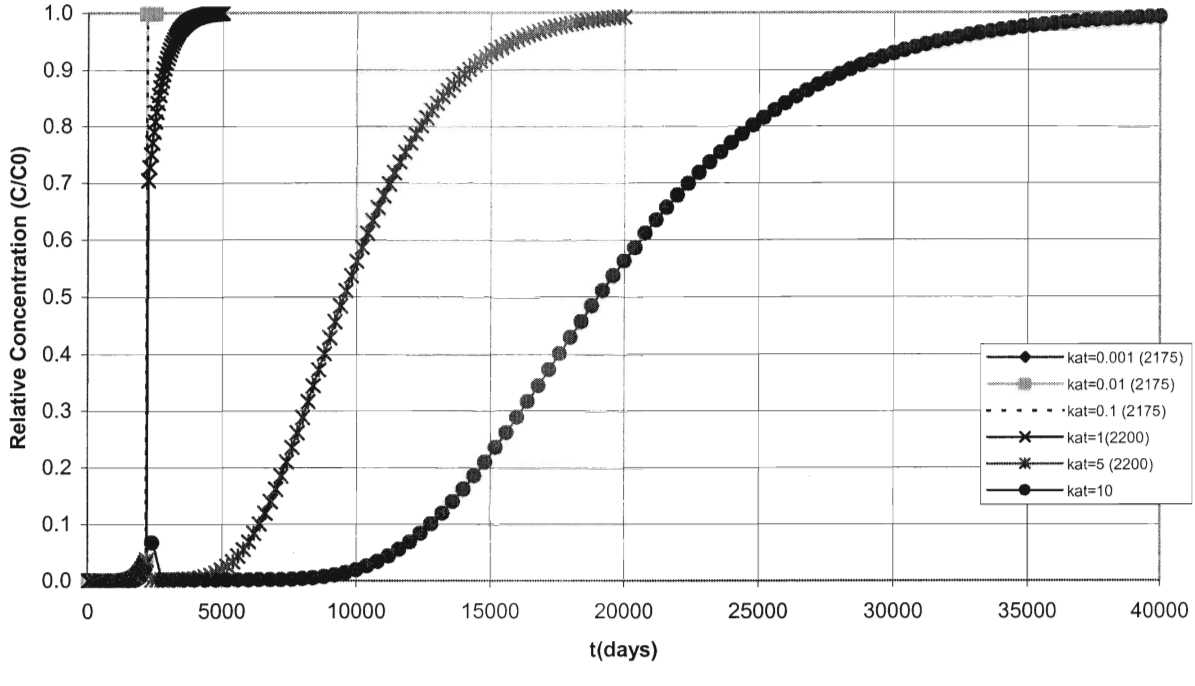

Figure 3.28 Sensitivity analysis for attachment

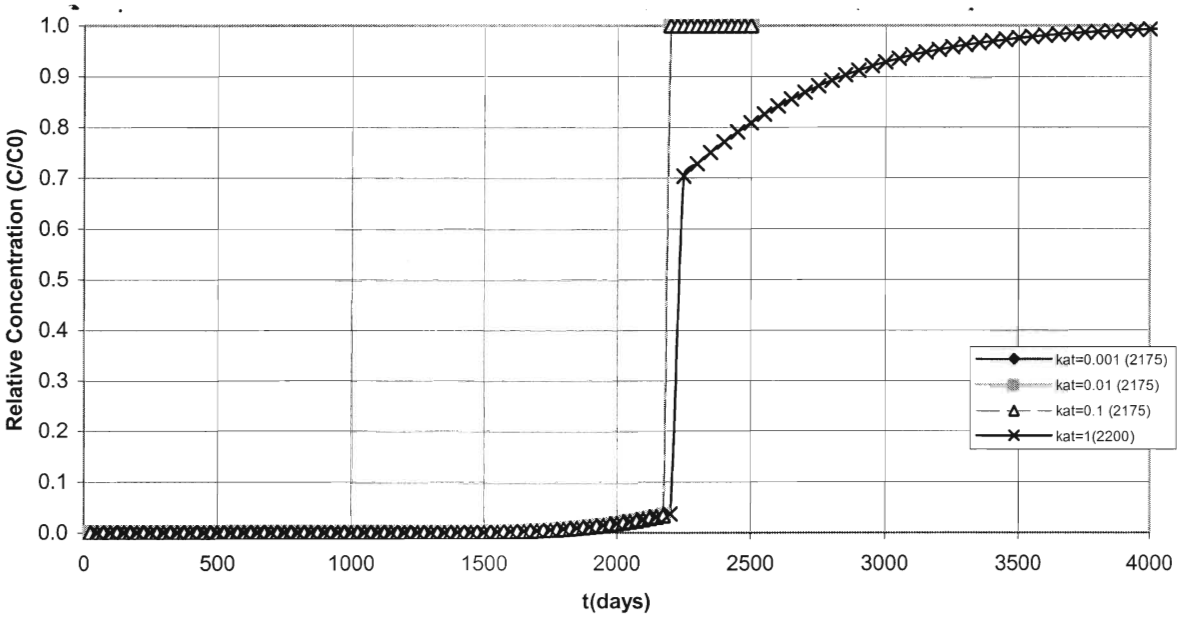

Figure 3.29 Sensitivity analysis to attachment Plot 2

Both in the attachment and detachment sensitivity analyses it is observed that Phase I occurs rapidly, and Phase II dominates the majority of accumulation period. If detachment rate is less than or equal to 0.01, Phase I lasts till 2160 days, however after τ, the aqueous phase concentration drops drastically, mainly due to the attachment rate being much higher than the detachment rate and dominating the accumulation process (Figure 3.26). When the detachment rate starts to increase, the duration of Phase II decreases. Duration of Phase I is independent of Phase II rates as expected. For the detachment rates between 1 and 5 day^{-1}, Phase II dominates the majority of the accumulation and is very slow. The switch point is at 2200 days. After 5 day^{-1}, the switch point drops to 2160 due to the time set up, since TSTOP is reduced too (Figure 3.27). The rise or drop is seen at the switch point as previously, due to the effect of different mass transfer rates in two phases. Simulations show that Phase II duration speeds up after 5 day^{-1}. The effect of the detachment in Phase II is very similar to the effect of the desorption in

Phase I. It should not be forgotten that the detachment occurs in larger masses of cells stuck together where the desorption occurs at single cellular scale. Thus in real life, same rate of the detachment would increase the aqueous phase solution concentration more than the desorption. When the detachment rate is higher than or equal to 10 day^{-1}, the difference between Phase I mass transfer rates and the detachment rate increases, thus a sudden rise in the aqueous phase concentration is seen, due to the increasing detachment rate. Also it is observed that the Phase II aqueous concentration is quite high, which indicates the ineffectiveness of the attachment.

As the attachment rate increases the log accumulation period lasts longer. Since the attachment is much more rapid, the aqueous phase concentration decreases, thus it takes more source concentration to carry the relative concentration to 1.0 (Figures 3.28 and 3.29). Attachment rate has no effect on Phase I duration, however the differences in τ occur due to the changing simulation period. When the attachment rate is lower than 1.0, Phase I period lasts longer and immediately after Phase I stops, the concentration increases very rapidly due to the differences in the mass transfer rates in two phases. When the attachment is so low, that it is very insignificant, the detachment dominates the Phase II and increases the aqueous phase concentration very fast. The log accumulation period is very fast, and since Phase II is short, the plateau phase is reached quickly. As the attachment rate increases, the log accumulation and the plateau stages and Phase II in overall slow down and relative concentration of 1.0 is reached in the late time. The increase in the attachment rate will aid in chunks of bacteria sticking the surface thus lowering the aqueous phase concentration.

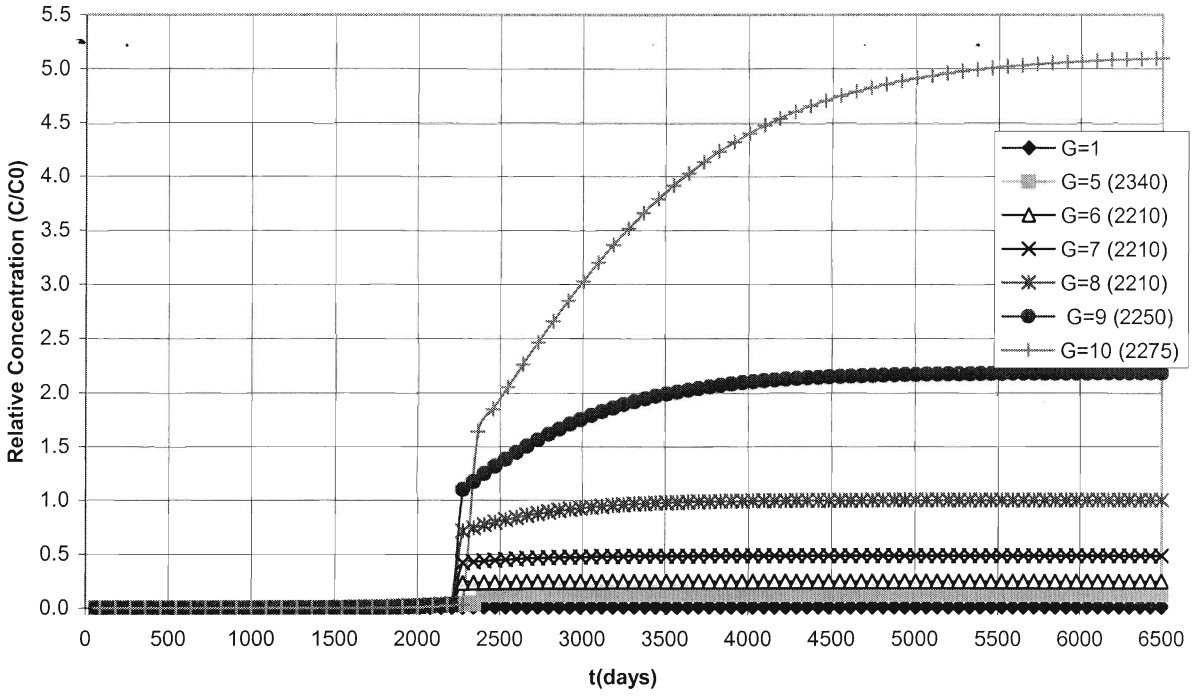

Figure 3.30 Sensitivity analysis for growth

The growth rate neither effects the duration of Phase I, nor the Phase II (Figures 3.30 and 3.31). For various growth rates, duration of Phase I and Phase II are the same. Increasing the growth rate, slightly speeds up the log accumulation stage. However, the relative concentration is influenced by the growth rate. As the growth rate increases, the relative concentration increases which indicates that the aqueous concentration at the observation point is much higher than the source concentration, which can be explained by the growth rate. The nutrient and the decay rates act as limiting processes, thus the growth does not continue to increase the aqueous phase concentration, and eventually a plateau is reached. The addition of the growth and the decay does not effect the durations of accumulation stages or the accumulation phases. When the mass transfer rates in two phases are equal to each other, the switch between two phases occur as a smooth curve. Duration of Phase I is between 2250 and

2400 days. When the sensitivity analysis is applied to the base case, the duration of Phase I is between 2210 and 2340 days. If the growth rate is less than or equal to 1.0 day^{-1}, with the presence of decay rate, decay rate dominates and there is not enough bacteria to create two layers of biofilm. Also, if growth rate is much higher than the decay rate, then growth dominates all processes and accumulation of layers may block the fracture. In case when the mass transfer rates are different, a sudden rise in aqueous phase concentration is seen, as in previous sensitivity analyses.

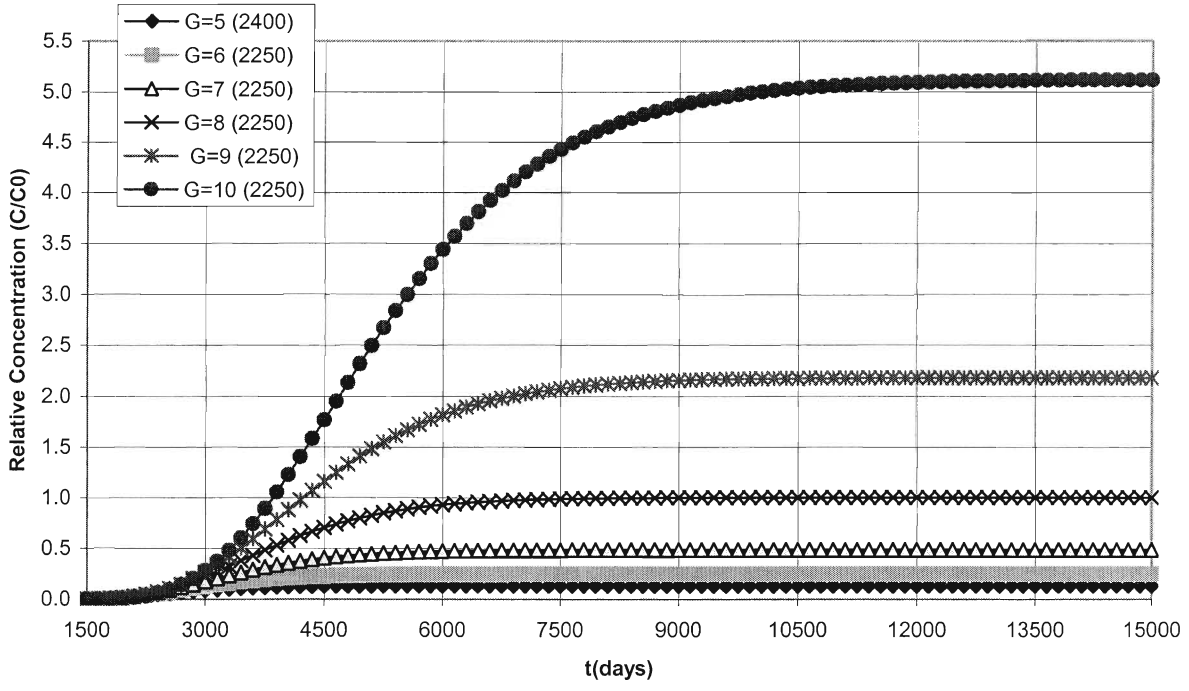

Figure 3.31 Sensitivity analysis for growth with rate-limiting process rates are set equal

The decay rate (Figures 3.32 and 3.33) does not influence the duration of the Phase I or Phase II periods the same as the growth rate. Also, similar to the growth rate, the decay rate has an influence only on the relative concentration and slightly on the log accumulation period. As

the decay rate decreases, the log accumulation period is shorter, the relative concentration decreases and plateaus at lower relative concentrations than 1.0. If the decay rate is as high as 6.0 day^{-1} then there exists a lack of bacteria to form 2 layers of biofilm, thus Phase I dominates and the relative concentration plateaus at a very low value, less than 0.05. As experienced before, with the two phases' mass transfer rates equal, a smooth curve is received, whereas in simulations done with the base case data, there exists a sudden rise at the switch point. As the decay rate decreases, the rise increases. With high decay rates, since no switch occur, a smooth breakthrough curve plateau at low relative concentration is observed.

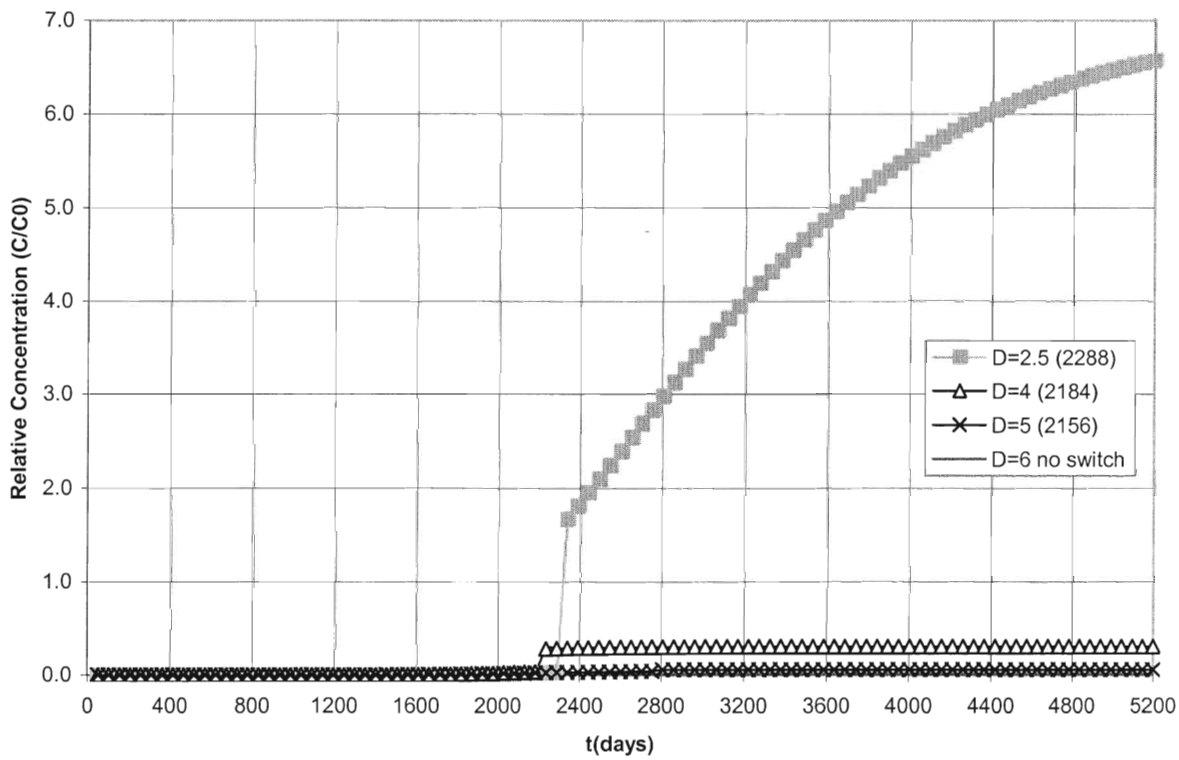

Figure 3.32 Sensitivity analysis for decay

Irreversible adsorption is one of the Phase I processes and has a relatively important effect on the accumulation period. Even with low values, the bacteria irreversibly adsorb to the substratum, thus fewer bacteria are carried to the outlet. As irreversible adsorption increases, the duration of Phase I increases, which indicates the accumulation is slowing down. This effect is similar to rate-limited adsorption but in this case the breakthrough curve may not reach the relative concentration of 1.0, instead depending on the value of the irreversible adsorption rate, may plateau at a lower relative concentration. When the irreversible adsorption has a value of 1.0, the inflowing bacteria are sorbed at the inlet so that less are carried to the outlet, however that amount carried to the outlet is not enough to create two layers of biofilm (Table 3.11), thus Phase I dominates the process with very low relative concentration value (Figures 3.35 and 3.36). The rates of 0.5 and 1.0 are high enough to prevent the accumulation, thus without reaching two layers, the relative concentration reaches a constant value less than 0.015. Values between 0 and 0.5 allow the accumulation. At the switch point, τ, the sudden rise is observed again. An increase in the irreversible adsorption, causes the Phase I to last longer and the rise at τ is slightly increased. Those values let the relative concentration eventually reach 1.0, due to the constant source concentration. When the mass transfer values of two phases are set to equal, all the curves exhibit exactly the same behavior, except the duration of Phase I changes (Figure 3.36).

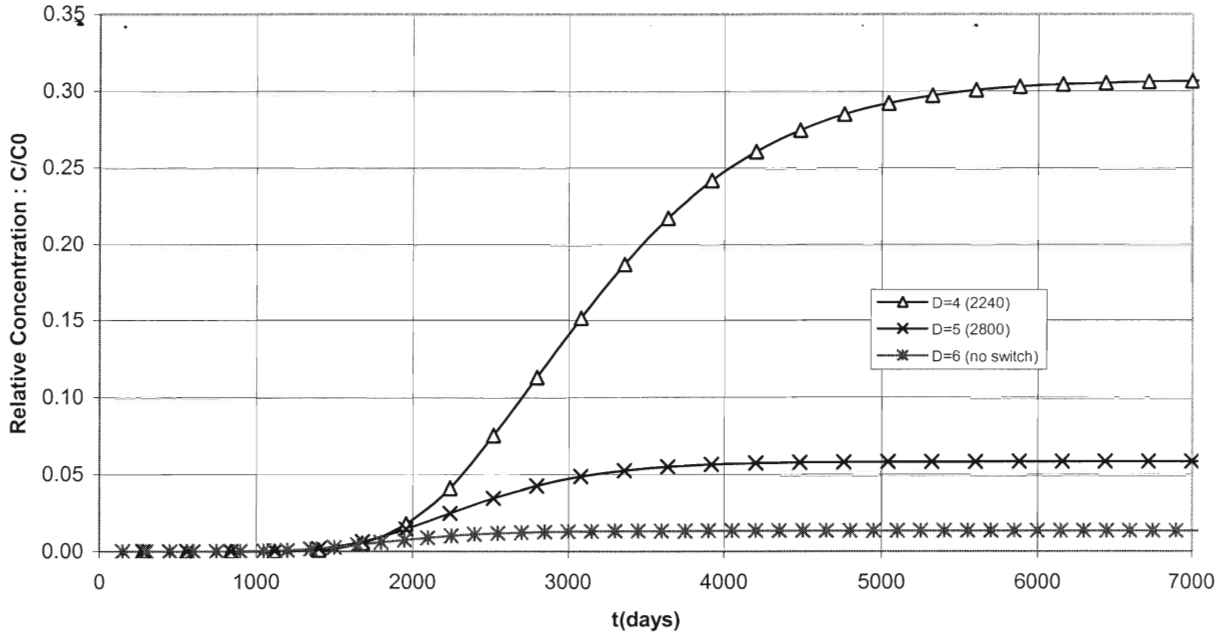

Figure 3.33 Sensitivity analysis for decay rate with rate-limiting process rates are set equal

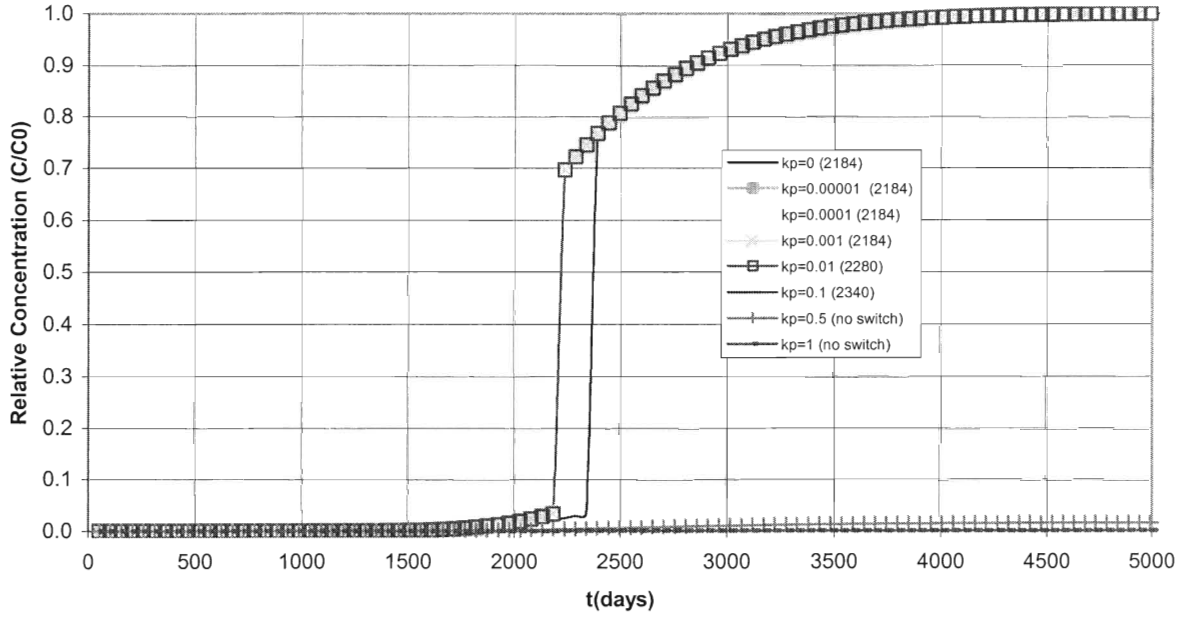

Figure 3.34 Sensitivity analysis for irreversible adsorption

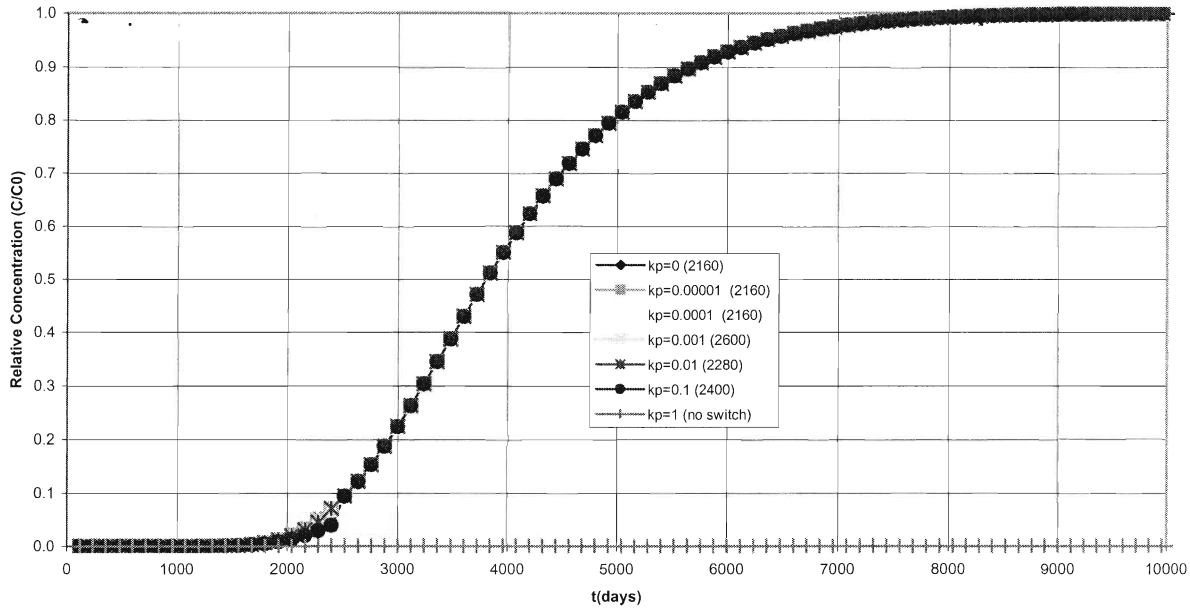

Figure 3.35 Sensitivity analysis for irreversible adsorption with rate-limiting process rates are set equal

Irreversible Adsorption Coefficient (kp) (day^{-1})	Duration of Phase I (τ) (day)
0	2184
1.0×10^{-5}	2184
0.0001	2184
0.001	2184
0.01	2280
0.1	2340
0.15	No switch
1.0	No switch

Table 3.11 Sensitivity analysis for irreversible adsorption coefficient

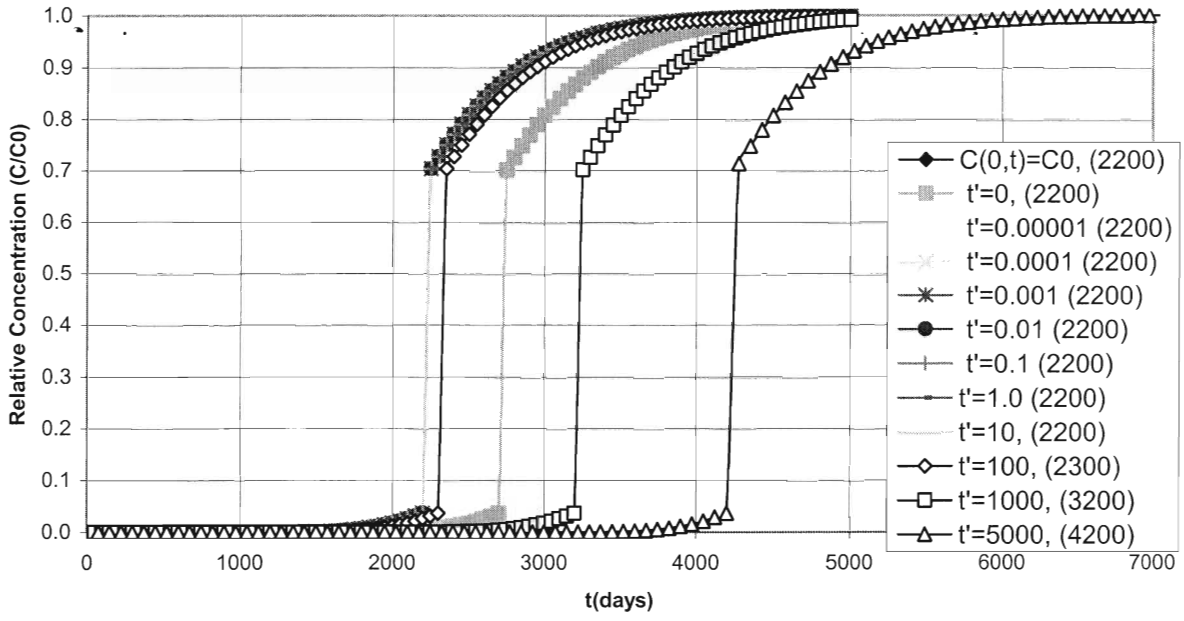

Figure 3.36 Base case versus Heaviside Step Function

The code BIOFRAC can simulate four different types of source concentrations. The base case and all the sensitivity analysis are simulated with the first source concentration where a constant bacterial concentration is supplied into the fracture all through the simulation period.

The next source concentration that is simulated is the Heaviside Step Function, a function that increases discontinuously from zero to one at the origin being constant, as represented by Equation 2.28. In other words, it increases discontinuously from zero to one at t=t′. In this simulation, the usage of Heaviside is that, before t′, there is no source concentration influx and after t′ there exists a constant source concentration, which is equal to c_0. This enables us to control the arrival of the bacterial front. The duration of Phase I is not effected till t′ exceeds 10 days. After 10days as t′ increases, the duration of Phase I increases. This is due to the lagging effect of Heaviside Step Function. The rise at τ remain the same with changing t′.

Also, the log accumulation and the plateau durations are not effected from the lagging effect (Figure 3.36).

The third input function is the exponentially decaying function where the input bacteria concentration is decaying in time with a factor of B, as presented earlier in Equation 2.29. Even with very low values, exponential decay constant has a major effect on the accumulation. It does not allow the relative concentration to rise to 1 and plateau there. The breakthrough curve peaks at a low relative concentration and then decays (Figure 3.37). The higher the exponential decay constant B is, the more drastic the effect on accumulation is. When B is higher than or equal to 0.05, the accumulation of 2 layers of bacteria does not occur. Since source concentration is not enough, and what adsorbs, desorbs back into the aqueous phase. This is coupled with the very low value of irreversible adsorption. So, at the observation point, the outlet, the accumulation does not occur.

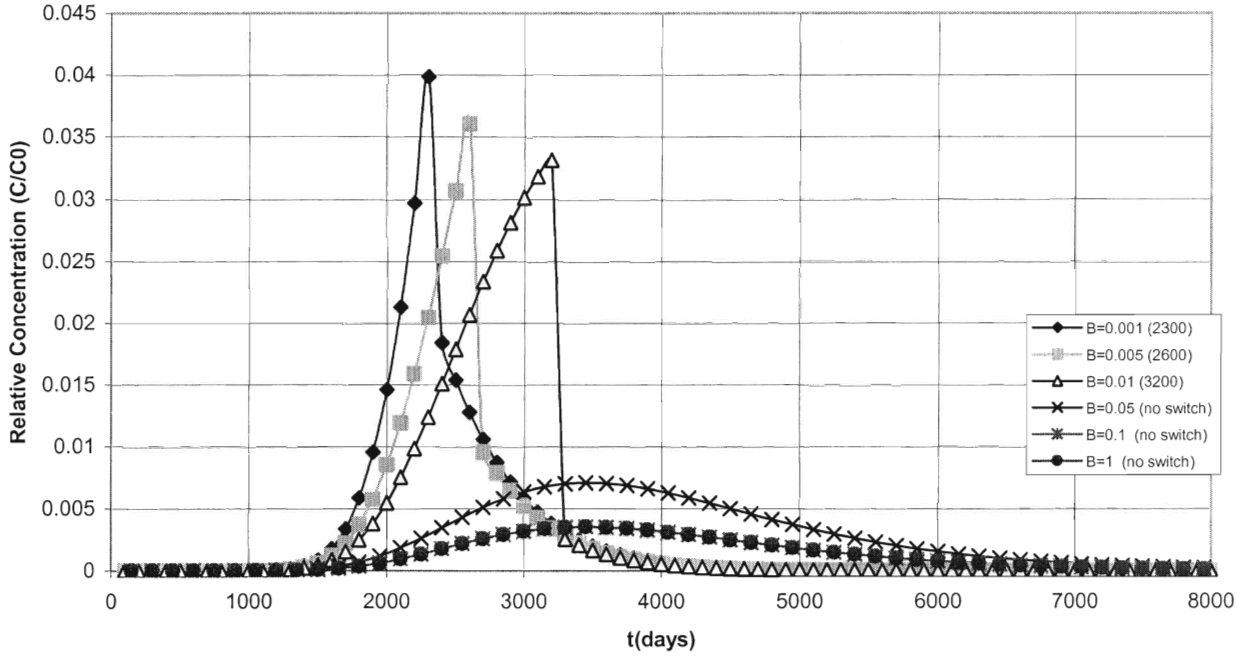

Figure 3.37 Exponentially decaying source function

Last function that controls the input source concentration is the exponentially rising function (Equation 2.30, Figure 3.38). This time the exponential rise constant is B. This input function does not allow the concentration to rise past the value of c_0.

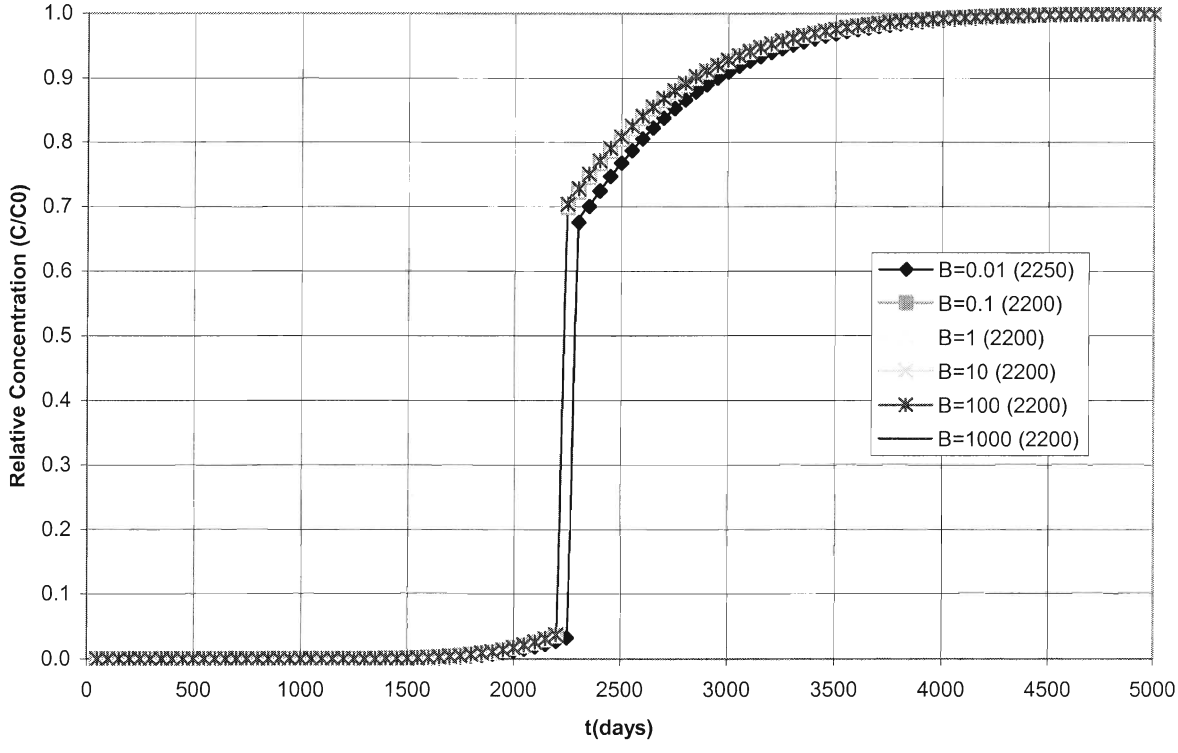

Figure 3.38 Exponentially rising source function

4. CONCLUSIONS

The purpose of this research was to develop an analytical model for bacterial accumulation in a discrete fracture. The first objective was to identify the processes involved in bacterial accumulation and transport, then develop a mathematical model describing the processes and solve this in the Laplace space. The second objective was to use the model to determine which of the identified processes are dominant in controlling the rate of bacterial transport and accumulation.

The understanding of basic processes that aid in accumulation, lead to organization of the solution of the problem in two phases. The first phase, called Phase I, is the adsorption-desorption dominated phase, which occurs at the bulk fluid-substratum interface and ends with the accumulation of two layers of biofilm, covering the entire of substratum. Adsorption-desorption stops at this point and the second phase, called Phase II, which is the attachment-detachment dominated phase, starts. Adsorption-desorption processes occur as single cells, whereas attachment-detachment processes occur as groups of cells. Those four processes are assumed to be rate limited.

A simple analytical model is undertaken in order to define the transport of bacteria in fractured media and define the separation between sorption dominated phase and attachment-detachment dominated phase.

The development of the model starts with the advection-dispersion equation. After advection-dispersion equation was joined with accumulation processes which include growth, decay, adsorption-desorption, attachment-detachment, irreversible adsorption, it was modified to account for fractured media. Four source functions were included to account for the input

source condition for bacterial transport. The solution method is based on the Laplace transform method, which was used to reduce the time differential term to an algebraic term. The final governing equation is simplified and solved as an ordinary differential equation.

A Fortran code BIOFRAC, was written to simulate the concentration versus time at an observation location. The code used based on inversion of the Laplace transform and the output was in real space. The model for Phase I was verified by comparing to the Ogata-Banks solution and the model for Phase II was verified by comparing to a Non-Homogenous version of the Ogata-Banks solution. The thorough verification process demonstrated clearly that the model developed, is capable of accurately describing the bacterial transport processes that occur in a discrete fracture. Once the implementation of the code was accomplished, a sensitivity analysis on the input parameters was performed.

Source concentration was observed to be an important parameter since it strongly influences the effect of transport on accumulation. The sensitivity analysis was run with a constant source concentration. It was observed that the accumulation of two layers of biofilm does not occur until the source concentration is as high as 1 gr m^{-3}. As more bacteria are supplied, the duration of Phase I decreases and the accumulation occurs at a faster rate.

An increase in velocity cause transport to occur at a faster rate, thus bacteria are accumulated sooner. Similarly, as dispersivity increases, the rate of which the two layers of biofilm cover the substratum is much faster. Increasing fracture aperture allows for more transport and thus more accumulation, resulting in a decrease in the duration of Phase I. Cell mass and size play a role at the switch between Phase I and Phase II. The larger the bacteria size, the faster the substratum will be covered, thus the faster the accumulation. The simulations conducted with changing number of layers indicate that the accumulation occurs

mainly during the log accumulation period and the duration of accumulation of layers have a constant time difference between each layer.

Increasing the adsorption rate also increases the duration of Phase I. In order to observe the behavior of sorption processes, two observation locations are used, one towards the inlet at 1m and one at the outlet at 10m. Contrary to the assumption of uniform biofilm thickness, the accumulation starts from the inlet and slowly moves towards the outlet. The effluent bacteria stars sorbing towards the inlet, thus the bacterial concentration in aqueous phase moving towards the outlet drops, slowing the accumulation at the outlet.

Increasing the desorption rate, reduces the duration of Phase I, speeding up the accumulation, The reasoning is exactly the same as the reasoning for the adsorption. The bacteria start to desorb and adsorb from the inlet, thus when desorption rate is high, more adsorbed bacteria desorb back to the aqueous phase, thus more bacteria are carried towards the outlet, making it possible to accumulate faster at the farther distances from the outlet.

It was also observed that Phase I occurs more rapidly than Phase II. The effect of increasing attachment rate is longer log accumulation period. The increase in attachment causes larger groups of bacteria to stick the surface, thus lowering the aqueous phase concentration. Similar to desorption, higher rates of detachment speeds up the transport.

The effect of growth and decay rates are seen in the overall relative concentration. Both processes have no significant effect on transport, however increase the concentrations in both aqueous and sorbed phases.

Irreversible adsorption has a dominant effect on both transport and accumulation processes. If the rate of irreversible adsorption is high and more bacteria stick at the outlet, less bacteria are transported towards the outlet. Since it is an irreversible process, it can effect the

aqueous phase concentration, making it impossible for the relative concentration to reach a value of 1.0.

The simulations were also run for different input functions. Four source concentrations are simulated. The constant source concentration is used in sensitivity analysis. Heaviside Step Function, exponentially decaying and exponentially rising functions are simulated separately.

5. REFERENCES

Arcangeli,J.P., Arvin,E., 1995, Growth of an Aerobic and an Anoxic Toluene-Degrading Biofilm – A Comparative Study, Water Science and Technology, V32, No.8, pp125-132.

Arcangeli,J.P., Arvin,E., 1997,Modellin of the Growth of a Methanotropic Biofilm, Water Science and Technology, V36, No.1, pp199-204.

Balkwill,D.L., Leach,F.R., Wilson,J.T., McNabb,J.F., White,D.C., 1988, Equivalence of Microbial Biomass Measures Based on Membrane Lipid and Cell Wall Components, Adenosine Triposhpate, and Direct Counts in Subsurface Aquifer Sediments, Microbial Ecology, V16, pp73-84.

Baveye,P., Vandevivere,P., Hoyle,B.L., DeLeo,P.C., Sanchez de Lozada,D., 1998, Environmental Impact and Mechanisms of the Biological Clogging of Saturated Soils and Aquifer Materials, Crit.Rev.Environ.Sci.Technol., V.28, No.2, pp123-191.

Behrendt,J., 1999, Modeling of Aerated Upflow Fixed Bed Reactors For Nitrification, Water Science and Technology, V.39, No.4, pp85-92.

Beyenal,H., Lewandowski,Z., 2000, Combined Effect of Substrate Concentration and Flow Velocity On Effective Diffusivity In Biofilms, Water Research, V.34, No.2, p528-538.

Bishop,P.L., Zhang,T.C., Fu,Y.C., 1995, Effects of Biofilm Structure, Microbial Distributions and Mass Transport on Biodegradation Processes, Water Science and Technology, V.31, No.1, pp143-152.

Bishop,P., 1997, Biofilm Structure and Kinetics, Water Science and Technology, 36(1), p287-294.

Brusseau,M.L., Srivastava,R., 1997 (a), Nonideal transport of Reactive Solutes in heterogeneous Porous Media 2. Quantitative Analysis of the Borden Natural-gradient Field Experiment, Journal of Contaminant Hydrology, V28, pp115-155.

Brusseau,M.L., 1995, The Effect of Non-Linear Sorption on Transformation of Contaminants During Transport in Porous Media, Journal of Contaminant Hydrology, V17, pp277-291.

Brusseau,M.L., Hu,Q., Srivastava,R., 1997 (b), Using Flow Interruption to Identify Factors Causing Nonideal Contaminant Transport, Journal of Contaminant Hydrology, V24, pp205-219.

Carlson,G., Silverstein,J., 1998, Effect of Molecular Size and Charge on Biofilm Sorption of Organic Matter, Water Resources, V.32, No.5, pp1580-1592.

Champ,D.R., Schroeter,J., 1988, Bacterial Transport In Fractured Rock-A Field Scale Tracer Test At The Chalk River Nuclear Laboratories, Water Science and Technology, V.20, No.11/12, p81-87.

Chapelle,F.H., 1993, Groundwater Microbiology and Geochemistry, John Wiley & Sons, Inc.

Characklis,W.G., 1973, Review Paper, Attached Microbial Growths - I. Attachment and Growth, Water Research, V7, p1113-1127.

Characklis,W.G., Marshall,K.C., 1990, Biofilms, John Wiley and Sons Inc.

Characklis,W.G., Wilderer,P.A., 1989, Structure and Function of Biofilms, John Wiley and Sons Inc.

Charpentier,B.C., 1999, Numerical Simulation of Biofilm Growth in Porous Media, Journal of Computational and Applied Mathematics, V103, pp55-66.

Clement,T.P., Peyton,B.M., Skeen,R.S., Jennings,D.A., Petersen,J.N., 1997, Microbial Growth and Transport in Porous Media Under Denitrification Conditions: Experiments and Simulation, Journal of Contaminant Hydrology, V24, pp269-285.

Converti,A., Sommariva,C., Del Borghi,M., 1994, Transient Responses in Systems with Cells Immobilized Within Large-Pore Matrices, Chemical Engineering Science, 49(7), p937.

Corapcioglu,M.Y., Kim,S., 1997, The Role of Biofilm Growth in Bacteria-Facilitated Contaminant Transport in Porous Media, Transport in Porous Media, 26, p161-181.

Cunningham,A.B., Characklis,W.G., Abedeen,F., Crawford,D., 1991, Influence of Biofilm Accumulation on Porous Media Hydrodynamics, Environmental Science and Technology, V25, pp1305-1311.

Cusack,F.M., Singh,S., Novosad,J., Chmilar,M., Blenkinsopp,S.A., Costerton,J.W., 1992, The Use of Ultramicrobacteria for Selective Plugging In Oil Recovery by Waterflooding, Society of Petroleum Engineers, SPE 22365

Crump K.S., 1976, Numerical Inversion of Laplace Transforms Using a Fourier Series Approximation, J. Assoc. Comput. Machinery, V23, pp.89-96 .

deHoog,F.R., Knight,J.H., Stokes.,A.N., 1982, An Improved Method for Numerical Inversion of Laplace Transforms. ,SIAM J. Sci. Stat. Comput., V3, pp.357-366.

Lapcevic,P.A., Novakowski,K.S., Sudicky,E.A., 1999, The Handbook of Groundwater Engineering, Boca Raton, Fla., CRC Press.

Lapcevic, P.A., Novakowski, K.S., and Sudicky, E.A. 1999. The Interpretation of a Tracer Experiment Conducted in a Single Fracture under Conditions of Natural Groundwater flow. Water Resour. Res.,35(8), 2301-2312.

Dennis,M.L., Turner,J.P., 1998, Hydraulic Conductivity of Compacted Soil Treated with Biofilm, Journal of Geotechnical and Geoenvironmental Engineering, February 1998, pp120-126.

Desouky, S.M., Abdel-Daim,M.M., Sayyouh,M.H., Dahab,A.S., 1996, Modeling and Laboratory Investigation of Microbial Enhanced Oil Recovery, Journal of Petroleum Science and Engineering, V15, pp309-320.

Dukan,S., Levi,Y., Piriou,P., Guyon,F., Villon,P., 1996, Dynamic Modeling of Bacterial Growth in Drinking Water Networks, Water Research, V.30, No9, pp1991-2002.

Ferenci,T., 1999, 'Growth of Bacterial Cultures' 50 Years on: Towards an Uncertainty Principle Instead of Constants in Bacterial Growth Kinetics, Res.Microbiol, 150, pp.431-438.

Fortin,J., Flury,M., Jury,W.A., Streck,T., 1997, Rate-Limited Sorption of Simazine in Saturated Soil Columns, Journal of Contaminant Hydrology, V25, pp219-234.

Freeze,R.A., Cherry,J.A., 1979, Groundwater, Prentice Hall

Fetter,C.W., 1980, Applied Hydrogeology, Prentice-Hall Inc.

Fry,V.A., Istok,J.D., Guenther,R.B., 1993, An Analytical Solution to the Solute Transport Equation with Rate-Limited Desorption and Decay, Water Resources Research, V.29, No9, pp3201-3208.

Grady,C.P.L., 1983, Modeling of Biological Fixed Films – A State of the Art Review, in: Wu,Y.C., Smith,E.D., Fixed Film Biological Process for Wastewater Treatment, Noyes Data Corporation, p.75

Goltz,M.N., Roberts,P.V., 1986, Interpreting Organic Solute Transport Data from Field Experiment Using Physical Nonequilibrium, Journal of Contaminant Hydrology, V1, pp77-93.

Goltz,M.N., Oxley,M.E., 1991, Analytical Modeling of Aquifer Decontamination by Pumping When Transport is Affected by Rate-Limited Sorption, Water Resources Research, V27, No4, pp547-556.

Guha,S., Jaffe,P.R., 1996, Determination of Monod Kinetic Coefficients for Volatile Hydrophobic Organic Compounds, Biotechnology and Bioengineering, V50, pp693-699.

Harvey,R.W., Garabedian,S.P., 1991, Use of Colloid Filtration Theory in Modeling Movement of Bacteria through Contaminated Sandy Aquifer, Environmental Science and Technology, 25, pp.178-185.

Henshaw,P., Medlar,D., Mcewen,J., 1999, Selection of a Support Medium for a Fixed-Film Green Sulphur Bacteria Reactor, Water Research, V.33, No14, pp3107-3110.

Hermanowicz,S.W., 1999, Two-Dimensional Simulations of Biofilm Development: Effects Of External Environmental Conditions, Water Science and Technology, V.39, No.7, pp107-114.

Horn,H., Hempel,D.C., 1997, Growth and Decay in an Auto-/Heterotrophic Biofilm, Water Research, V31, No.9, pp2243-2252.

Hu,Q., Brusseau,M.L., 1996, Transport of Rate-Limiting Sorbing Solutes in an Aggregated Porous Medium: A Multiprocess Non-Ideality Approach, Journal of Contaminant Hydrology, V24, pp53-73.

Lindstrom,F.T., 1976, Pulsed Dispersion of Trace Chemical Concentrations in a Saturated Sorbing Porous Medium, Water Resources Research, V12,No.2, pp229-238.

Lindqvist,R., Bengtsson,G., 1991, Dispersal Dynamics of Groundwater Bacteria, Microbial Ecology, V21. pp49.72.

Lindqvist,R., Bengtsson,G., 1995, Diffusion-Limited and Chemical-Interaction-Dependent Sorption of Soil Bacteria and Microspheres, Soil Biol.Biochem., V27., No.7, pp941-9427

Logan,J.D., 1996, Solute Transport in Porous Media with Scale-Dependent Dispersion and Periodic Boundary Conditions, Journal of Hydrology, V184, pp261-276.

Maraqa,M.A., 2001, Prediction of Mass-Transfer Coefficient for Solute Transport in Porous Media, Journal of Contaminant Hydrology, V50, pp1-19.

McCaulou,D.R., Bales,R.C., McCarthy,J.F., 1994, Use of Short-Pulse Experiments to Study Bacteria Transport Through Porous Media, Journal of Contaminant Hydrology, V15, p1-14.

Miller,C.T., Weber,W.J.,Jr., 1984, Modeling Organic Contaminant Partitioning in Ground-Water Systems, Ground Water, V22, No.5, pp584-592.

Mitchell,C., McNevin,D., 2001, Alternative Analysis of Bod Removal In Subsurface Flow Constructed Wetlands Employing Monod Kinetics, V35, No5, pp1295-1303.

Monod,J., 1949, The Growth of Bacterial Cultures, Ann. Rev. Microbiol.3, p371-394.

Morshed,J., Kaluarachchi,J.J., 1995, Critical Assessment of the Operator-Splitting Technique in Solving the Advection-Dispersion-Reaction Equation: 2. Monod Kinetics and Coupled Transport, Advances in Water Resources, V.18, No.2, pp101-110

Murali,V., Aylmore,L.A.G., 1083, Competitive Adsorption During Solute Transport in Soils, 1.Mathematical Models, Soil Sciences, V135, pp143-150.

Neville,C., 1988, University of Waterloo, Unpublished notes.

Novakowski,K.S., 1985, A field example of measuring hydrodynamic dispersion in a single fracture, Water Resources Research, Vol. 21, Issue 8, pp.1165-1174.

Novakowski, K.S., and Lapcevic, P.A. 1994. Field measurement of radial solute transport in a discrete rock fracture. Water Resour. Res., 30(1): 37-44.

Noguera,D.R., Okabe,S., Picioreanu,C., 1999, Biofilm Modeling: Present Status and Future Directions, Water Science and Technology, V.39, No.7, pp273-278.

Park,Y., Davis,M.E., Wallis,D.A., 1984, Analysis of Continuous Aerobic, Fixed-Film Bioreactor: I-Steady-State Behavior, Biotechnology and Bioengineering 26, p457.

Peyton,B.M., Characklis,W.G., 1992, Kinetics of Biofilm Detachment, Water Science and Technology, V.26, No.9-11, p1995-1998.

Peyton,B.M., Characklis,W.G., 1993, A Statistical Analysis of the Effect of Substrate Utilization and Shear Stress on the Kinetics of Biofilm Detachment, Biotechnology and Bioengineering, V41, pp728-735.

Peyton,B.M., Skeen,R.S., Hooker,B.S., Lundman,R.W., Cunningham,A.B., 1995, Evaluation of Bacterial Detachment Rates in Porous Media, Applied Biochemistry and Biotechnology, V51/52, pp785-797.

Peyton,B.M., 1996, Effects of Shear Stress and Substrate Loading Rate on Pseudomonas Aeruginosa Biofilm Thickness and Density, Water Research, V.30, No.1, p29-36.

Picioreanu,C., vanLoosdrecht, M.C.M., Heijnen,J.J., 1999, Discrete-Differential Modeling of Biofilm Structure, Water Science and Technology, V.39, No.7, p115-122.

Rashid,M., Kaluarachchi,J.J., 1999, A Simplified Numerical Algorithm for Oxygen and Nitrate-Based Biodegradation of Hydrocarbons Using Monod Expressions, Journal of Contaminant Hydrology,V.40, pp53-77.

Rauch,W., Vanhooren,H., Vanrolleghem,P.A., 1999, A Simplified Mixed-Culture Biofilm Model, Water Research, V33, No.9, p2148-2162.

Richter,A., Smith,R., Ries,R., Lenz,H., 1999, Growth of Biological Films-Microscopical Investigations and Computer Simulations, Materials Science and Engineering, C 8-9, p451-462.

Rittmann,B.E., Manem,J.A., 1992, Development and Experimental Evaluation of a Steady-State, Multispecies Biofilm Model, Biotechnology and Bioengineering, V.39, p914-922.

Ross,N., Deschenes,L., Bureau,J., Clement,B., Comeau,Y., Samson,R., 1998, Ecotoxicological Assessment and Effects of Physicochemical Factors on Biofilm Development in Groundwater Conditions, Environmental Science and Technology, 32, p1105-1111.

Ross,N., Villemur,R., Deschenes,L., Samson,R., 2001, Clogging of Limestone Fracture by Stimulating Groundwater Microbes, Water Research, V35, Issue 8, pp. 2029-2037

Savant,C.J.Jr., Levy,E.C., 1962, Fundamentals of the Laplace Transformation, McGraw-Hill Book Company, Inc.

Schirmer,M., Butler,B.J., Roy,J.W., Frind,E.O., Barker,J.F., 1999, A Relative-Least-Square Technique to Determine Unique Monod Kinetics Parameters of BTEX Compounds Using Batch Experiments, Journal of Contaminant Hydrology, V37, pp69-86.

Shaw,J.C., Bramhill,N.C., Wardlaw,N.C., Costerton,J.W., 1985, Bacterial Fouling in a Model Core System, Applied and Environmental Microbiology, pp.693-701.

Smets,B.F., Grasso,D., Engwall,M.A., Machinist,B.J., 1999, Surface Physicochemcial Properties of Pseudomonas Fluorescens and Impact on Adhesion and Transport Through Porous Media, Colloids and Surfaces B: Biointerfaces, V14, pp121-139.

Spiegel,M.R., 1965, Schaum's Outline of Theory and Problems of Laplace Transforms, McGraw-Hill Publishing Company.

Sommer,H., Spliid,H., Holst,H., 1995, Nonlinear Parameter Estimation In Microbiological Degradation Systems and Statistic Test For Common Estimation, Environment International, V.21, No.5, pp551-556.

Srivastava,R., Brusseau,M.L., 1996, Nonideal Transport of Reactive Solutes in Heterogeneous Porous Media: 1.Numerical Model Development and Moments Analysis, Journal of Contaminant Hydrology, V24, pp117-143.

Stehfest,H., 1970, Algorithm 368. Numerical inversion of Laplace transforms, Comm. ACM 13, pp.479-49 (erratum 13, 624).

Suchomel,B.J., Chen,B.M., Allen,M.B., 1998, Network Model of Flow, Transport and Biofilm Effects in Porous Media, Transport in Porous Media, 30, pp.1-23.

Talbot,A.,1979, The accurate numerical inversion of Laplace transforms, J. Inst. Math. Appl., V23, pp.97-120.

Tanyolac,A., Beyenal,B., 1998, Prediction of Substrate Consumption Rate, Average Biofilm Density, and Active Thickness for a Thin Spherical Biofilm at Pseudo-Steady State, Biochemical Engineering Journal, 2, p207-216.

Taylor,S.W., Jaffe,P.R., 1990a, Biofilm Growth and the Related Changes in the Physical Properties of a Porous Medium. 1: Experimental Investigation, Water Resources Research, V26, No.9, pp2153-2159

Taylor,S.W., Jaffe,P.R., 1990b, Biofilm Growth and the Related Changes in the Physical Properties of a Porous Medium. 3: Dispersivity and Model Verification, Water Resources Research, V26, No.9, pp2171-2180

Taylor,S.W., Jaffe,P.R., 1990c, Substrate and Biomass Transport in a Porous Medium, Water Resources Research, V26, No.9, pp2181-2194

Tchobanoglous,G., Burton,F.L., 1991, Wastewater Engineering: treatment, disposal, and reuse. Metcalf & Eddy, Inc., 3rd ed., 1334 pp.

VanGenuschten,M.T., 1981, Non-equilibrium Transport Parameters from Miscible Displacement Experiments, Res.Rep.119, U.S. Department of Agriculture, U.S. Salinity Lab, Riverside, California.

VanGenuschten,M.T., Wierenga,P.J., 1976, Mass Transfer Studies in Sorbing Porous Media: Analytical Solutions, Soil Science Society of America Journal, V40, pp473-480.

Vandevivere,P., Baveye,P., 1992, Saturated Hydraulic Conductivity Reduction Caused by Aerobic Bacteria in Sand Columns, Soil Science Society of America Journal, 56, p1-12.

Vandevivere,P., Baveye,P., DeLozada,S.D., DeLeo,P., 1995, Microbial Clogging of Saturated Soils and Aquifer Materials: Evaluation of Mathematical Models, Water Resources Research, V.31, No.9, p2173-2180.

vanLoosdrecht,M.C.M., Eikelboom,D., Gjaltema,D., Mulder,A., Tijhuis,L., Heijnen,J.J., 1995, Biofilm Structures, Water Science and Technology, V.32, No.8, p35-43.

Vennard,J.K., Street,R.L., 1961, Elementary Fluid Mechanics, 5th Edition, John Wiley & Sons Inc.

Warner,J.W., Gates,T.K., Namvargolian,R., Miller,P., Comes,G., 1994, Sediment and Microbial Fouling of Experimental Groundwater Recharge Trenches, Journal of Contaminant Hydrology, 15, p321-344.

Wanner,O., Gujer,W., 1986, A Multispecies Biofilm Model, Biotechnology and Bioengineering, V28, p314-328.

Wanner,O., Reichert,P., 1996, Mathematical Modeling of Mixed Culture Biofilms, Biotechnology and Bioengineering, V.48, pp737-744.

Wik,T., 1999, Adsorption and Denitrification In Nitrifying Trickling Filters, Water Resources, V.33, No.6, pp1500-1508

Wilderer,P.A., Morgenroth,E., 2000, Influence of Detachment Mechanisms On Competition In Biofilms, Water Research, V.34, No.2, p417-426.

Zhang,T.C., Bishop,P.L., 1995, Density, Porosity and Pore Structure of Biofilms, Water Research, 28(11), p22

APPENDICES

APPENDIX A

SOURCE CODE AND SAMPLE INPUT, OUTPUT AND PLOT FILES

Input files have the extension .inp. The output files have the extension .out and the plot files have the extension .plt. Fortran source code has been developed in Fortran PowerStation 4.0 Microsoft Developer Studio and has the extension .for.

Source code, BIOFRAC.for:

```
PROGRAM BIOFRAC
C**********************************************************************
C
C       THIS CODE SIMULTES THE BACTERIAL ACCUMULATION IN FRACTURED
MEDIA
C       WITH RATE-LIMITED SORPTION. SORPTION IS DOMINANT TILL NLL
LAYERS OF
C       BIOFILM ARE ACCUMULATED. AT TIME=TAO WHEN NLL LAYERS OF
BIOFILM
C       ACCUMULATES AND THE SUBSTRATUM IS FULLY COVERED, THEN
SORPTION IS
C       DOMINATED BY ATTACHMENT AND DETACHMENT.
C       THE ADVECTION-DISPERSION EQUATION IS MODIFIED TO ACCOUNT FOR
C       BACTERIAL ACCUMULATION AND TRANSPORT IN A DISCRETE
FRACTURE.
C       THE ANALYTICAL SOLUTION IS IN LAPLACE SPACE AND INVERTED BACK
C       TO REAL SPACE BY USING DEHOOG ALGORITHM.
C
C
C    M. BEYZA YAZICIOGLU
C       2002
C**********************************************************************
C
```

```
C     LIST OF PARAMETERS
C*************************************************************************
C
C    C - CONCENTRATION OF BACTERIA IN AQUEOUS PHASE (M/L**3)
C        XBIGS - CONCENTRATION OF SORBED BACTERIA AT TIME TAO (M/L**3)
C        AVSORB - AVERAGE SORBED CONCENTRATION OF BACTERIA ALONG THE
FRACTURE (M/L**3)
C        ROWAV - AVERAGE AQUEOUS CONCENTRATION OF BACTERIA ALONG
THE FRACTURE (M/L**3)
C        XC0 - CONSTANT SOURCE CONCENTRATION OF BACTERIA
C                ENTERING THE FRACTURE (M/L**3)
C
C        TPRIME - FROM HEAVISIDE FNC. DURATION OF CONSTANT INPUT (T)
C        BDEC -  DECAY CONSTANT FOR EXPONENTIALLY RISING AND DECAYING
FUNCTION
C
C        V - AVERAGE VELOCITY OF FLUID IN FRACTURE (L/T)
C        ALP - DISPERSIVITY (L)
C        DL - LONGITUDINAL DISPERSION COEFF. (L**2/T)
C        XTWOB - FRACTURE APERTURE, 2b (L)
C        NFL - FRACTURE LENGTH (L)
C        ICOLUMN - LOCATION IN THE FRACTURE (L)
C        XCW - BACTERIAL CELL WIDTH (L)
C        XCL   - BACTERIAL CELL LENGTH (L)
C        XCH - BACTERIA CELL HIGHT (L)
C        NLL - NUMBER OF LAYERS OF SORBED CELLS ON ONE FRACTURE WALL
C        XCMASS - MASS OF ONE BACTERIAL CELL (M)
C
C        XK1 - RATE - LIMITED ADSOPRTION CONSTANT (1/T)
C        XK2 - RATE - LIMITED DESORPTION CONSTANT (1/T)
C        XKDET - DETACHMENT CONSTANT (1/T)
C        XKAT - ATTACHMENT CONSTANT (1/T)
C        XMAX - MAXIMUM SPECIFIC GROWTH CONSTANT OF BACTERIA (1/T)
C        XM - GROWTH CONSTANT OF BACTERIA (1/T)
C        XLAM - DECAY CONSTANT OF BACTERIA (1/T)
C        XKP - IRREVERSIBLE ADSORPTION CONSTANT (1/L)
C
C        T - TIME (T)
C        TSTOP - DURATION OF THE EXPERIMENT (T)
C        BKS - SATURATION RATE COEFFICIENT FOR BACTERIA (M/L**3)
C        BS - SUBSTRATE CONCENTRATION (M/L**3)
C        IXFT - F(T) = 1.F(T)=C0 OR
C                2.F(T)=HEAVISIDE STEP FUNCTION OR
C                3.F(T)=EXP.DECAYING SOURCE OR
C                4.F(T)=EXP. RISING SOURCE
C
```

```
C*************************************************************************
**
C       INPUT IS IN FILE BIOFRAC.INP
C       OUTPUT IS IN FILE BIOFRAC.OUT
C       PLOT FILE IS BIOFRAC.PLT
C*************************************************************************
**
C
      IMPLICIT DOUBLE PRECISION (A-H,O-Z)
      DIMENSION C(0:500,0:500),T(0:500)
      DATA IDATA/0/
C
C     OPEN FILES
C
C     BIOFRAC.INP PROVIDES INPUT PARAMETERS
C     BIOFRAC.OUT PROVIDES THE CALCULATED RESULTS
C     ===================================================
      OPEN(UNIT=7,FILE='BIOFRAC.INP',STATUS='UNKNOWN')
      OPEN(UNIT=8,FILE='BIOFRAC.OUT',STATUS='UNKNOWN')
      OPEN(UNIT=9,FILE='BIOFRAC.PLT',STATUS='UNKNOWN')
C
C
C     READ FROM INPUT FILE
C     ============================
          READ(7,1000) XC0
          READ(7,1000) TPRIME
          READ(7,1000) BDEC
          READ(7,1000) V
          READ(7,1000) ALP
          READ(7,1000) XTWOB
          READ(7,1001) NFL
          READ(7,1000) XFW
          READ(7,1000) XCW
          READ(7,1000) XCL
          READ(7,1000) XCH
          READ(7,1000) XCMASS
          READ(7,1001) NLL
          READ(7,1000) XK1
          READ(7,1000) XK2
          READ(7,1000) XKDET
          READ(7,1000) XKAT
          READ(7,1000) XMAX
          READ(7,1000) XLAM
          READ(7,1000) XKP
          READ(7,1000) BKS
          READ(7,1000) BS
```

```
      READ(7,1000) ERROR
      READ(7,1000) ALPHA
      READ(7,1000) TFACT
      READ(7,1001) NTERM
      READ(7,1000) TSTART
      READ(7,1000) TSTOP
      READ(7,1001) NT
      READ(7,1001) IXFT

C
C   CALCULATE DL, 2/2B, GROWTH CONSTANT,
C   CONCENTRATION AT THE END OF ADS-DES PERIOD
C   ==========================================
      DL=DCMPLX(V*ALP)
      XTWTWOB=DCMPLX(2.0D+0/XTWOB)
      XM=DCMPLX((XMAX*BS)/(BKS+BS))
      XCHECK=DCMPLX(2.0D+0*NLL*NFL*XFW/(XCL*XCW))

C
C   CHECK BIOFILM THICKNESS
C   HAS TO BE LESS THEN FRACTURE APERTURE
C   ================================
      XBIOTHICK=DCMPLX(2.0D+0*NLL*XCH)
      IF(XBIOTHICK.GT.XTWOB) THEN
      WRITE(*,3)
      ELSEIF (XBIOTHICK.EQ.XTWOB) THEN
      WRITE(*,4)
      ENDIF

C
C   INITIALIZE TIME VALUES
C   ================================
      RANGE=TSTOP-TSTART
      STEP=RANGE/DFLOAT(NT)
      SUM=TSTART
      DO 10 IROW=1,NT
      SUM=SUM+STEP
      T(IROW)=SUM
 10   CONTINUE

C
C   CALCULATE CONSTANTS FOR INVERSION
C   BIGT AND ATERM
C              AND
C   LOOP THROUGH TIME AND CALL THE NUMERICAL INVERTER
C   ================================================
```

```
      FXNNUMB=1.0
      XGAP=0

      DO 31 IROW=1,NT

            ROWAV=0.0D+0
            DO 30 ICOLUMN=1,NFL

            BIGT=TFACT*TSTOP
            ATERM=ALPHA-(DLOG(ERROR)/(2.D0*BIGT))

            CALL HOOG2(BIGT,ATERM,NTERM,T(IROW),C(IROW,ICOLUMN),
     *XC0,TPRIME,BDEC,ICOLUMN,V,DL,XTWTWOB,XK1,XK2,XKAT,XKDET,
  *XM,XLAM,XKP,XCATTAO,FXNNUMB,IXFT,XGAP)

            ROWAV=ROWAV+C(IROW,NFL)

30    CONTINUE

   ROWAV=DCMPLX(ROWAV*XC0/NFL)

      XAV=XK2-XM+XLAM
      AVSORB=DCMPLX((1.0D+0-CDEXP(DCMPLX(-
XAV)*T(IROW)))*XK1*ROWAV/XAV)

      ROWTOT=DCMPLX(AVSORB*2.0D+0**XCH*NFL*XFW/XCMASS)

      IF(ROWTOT.GE.XCHECK) THEN

        IF (FXNNUMB.EQ.1) THEN

          XGAP = T(IROW)

              XCATTAO=DCMPLX(ROWAV)

        ENDIF

        FXNNUMB=2

   ENDIF

C
C   CONSTRAIN THE OUTPUT
C   ========================
      IF(C(IROW,ICOLUMN).LE.1.0D-6) C(IROW,ICOLUMN)=1.0D-6
31    CONTINUE
```

```
C
C   INITIALIZE THE OUTPUT FILE (GIVES C/C0 VS T)
C   ============================================
    WRITE(8,5)
    WRITE(8,6) ALP,DL,XTWOB,NFL,XK1,XK2,XKDET,XKAT,XM,XLAM,XKP,
       *TSTOP,ROWAV,AVSORB,XGAP
C
C   WRITE THE SOURCE CONDITION
C   ==========================
    IF(IXFT.EQ.1) THEN
       WRITE(8,26)
       ELSE
       ENDIF
       IF(IXFT.EQ.2) THEN
       WRITE(8,27)
       ELSE
       ENDIF
       IF(IXFT.EQ.3) THEN
       WRITE(8,28)
       ELSE
       ENDIF
       IF(IXFT.EQ.4) THEN
       WRITE(8,29)
       ELSE
       ENDIF
       IF(IXFT.EQ.2) THEN
       WRITE(8,41) TPRIME
       ELSE
       ENDIF

C
C   OUTPUT FILE
C   ===========
    WRITE(8,7)
    WRITE(8,9)
    WRITE(8,8) (IROW,T(IROW),C(IROW,NFL),IROW=1,NT)

C
C   INITIALIZE PLOT FILE
C   ====================
    WRITE(9,20)
    WRITE(9,21) NT,IDATA
    WRITE(9,22) (T(IROW),C(IROW,NFL),IROW=1,NT)

C
```

```
C   END EXECUTION
C   ===========
      WRITE(*,*) ' '
      WRITE(*,*) ' Completed.....BITTI! ',ROWAV,AVSORB,XGAP,ROWTOT,
         *XCHECK
      WRITE(*,*) ' '

C
C   FORMAT STATEMENTS
C   =================
3       FORMAT(//' TOO MANY LAYERS OF BIOFILM. PLEASE REDUCE THE
NUMBER OF
     * LAYERS '//)
4       FORMAT(//' THIS BIOFILM THICKNESS WOULD CLOG THE FRACTURE,
PLEASE
     * RECUDE THE NUMBER OF LAYERS '//)
5     FORMAT(//' ACCUMULATION OF BACTERIA IN FRACTURED MEDIA: C VS. T '/
     */)
6     FORMAT(//'  ------------------------------------------------
     *-----'/
     *'   Dispersivity                    (l)  = ',F12.5,/
          *'      ------------------------------------------------------'/
     *'   Dispersion coefficient          (l**2/t)  = ',F12.5,/
          *'      ------------------------------------------------------'/
     *'   Fracture aperture               (l)  = ',F12.5,/
          *'      ------------------------------------------------------'/
     *'   Fracure length                  (l)  = ',I12.5,/
          *'      ------------------------------------------------------'/
     *'   Rate-limited adsorption constant   (1/t)  = ',F12.5,/
          *'      ------------------------------------------------------'/
     *'   Rate-limited desorption constant   (1/t)  = ',F12.5,/
     *'   ------------------------------------------------------'/
     *'   Detachment constant             (1/t)  = ',F12.5,/
          *'      ------------------------------------------------------'/
     *'   Attachment constant             (1/t)  = ',F12.5,/
          *'      ------------------------------------------------------'/
     *'   Maximum growth rate of bacteria    (1/t)  = ',F12.5,/
          *'      ------------------------------------------------------'/
          *'      Decay constant of bacteria         (1/t)  = ',F12.5,/
          *'      ------------------------------------------------------'/
     *'   Irreversible adsorption constant   (1/t)  = ',F12.5,/
          *'      ------------------------------------------------------'/
     *'   Duration of the experiment         (1/t)  = ',F12.5,/
          *'      ------------------------------------------------------'/
     *'   Average conc. along fract. @switch  (1/t)  = ',F12.5,/
          *'      ------------------------------------------------------'/
```

```
     *'   Average sorbed conc. @switch       (1/t) = ',F12.5,/
          *'   ----------------------------------------------------'/
     *'   Switch Time (XGAP)                 (1/t) = ',F12.5,/
          *'   ----------------------------------------------------'/)

7    FORMAT(//'        I        CONC.          TIME')
8    FORMAT(I12,7X,E12.4,7X,E12.4)
9    FORMAT('**************************************************')
20    FORMAT(' ACCUMULATION OF BACTERIA IN FRACTURED MEDIA: C/C0 VS.
T')
21   FORMAT(2I10)
22   FORMAT(2E12.4)
26      FORMAT('F(T)=C0')
27      FORMAT('HEAVISIDE STEP FUNCTION F(T)=C0*H(t-tprime)')
28      FORMAT('EXPONENTIALY DECAYING SOURCE F(T)=C0exp(-Bt)')
29      FORMAT('EXPONENTIALY RISING SOURCE F(T)=C0(1-exp(-Bt))')
41      FORMAT('TPRIME = '2F10.4)
42      FORMAT('WHERE B = '2F10.4)
1001 FORMAT(I15)
1000 FORMAT(E20.7)
        STOP
     END

C
C    **********************************************************************
C
C    FUNCTION TO BE INVERTED
C    ===================================
     FUNCTION FS(P,XC0,TPRIME,BDEC,ICOLUMN,V,DL,XTWTWOB,XK1,
         *XK2,XKAT,XKDET,XM,XLAM,XKP,XCATTAO,FXNNUMB,IXFT,XGAP)

     IMPLICIT DOUBLE PRECISION(A-H,O-Z)
     COMPLEX*16 FS,P,ARG1,ARG2,ARG3,ARG4,ARG5,ARGI,ARG6,ARG7
         COMPLEX*16 ALPHA,BETA,THETA,XBIGS,XS,PHI,ARGFIN

C
C    1ST EQUATION: BEFORE THE SWITCH
C    ================================

         IF (FXNNUMB.EQ.1) THEN

C
C    SOURCE CONDITION,
C    =================
          IF(IXFT.EQ.1)THEN
          ARG6=DCMPLX(XC0/P)
```

```
      ELSE
            IF(IXFT.EQ.2)THEN
            ARG6=DCMPLX(XC0*(CDEXP(-TPRIME*P))/P)
            ELSE
                  IF(IXFT.EQ.3)THEN
                  ARG6=DCMPLX(XC0/(P+BDEC))
                  ELSE
                        IF(IXFT.EQ.4) THEN
                        ARG6=DCMPLX(XC0-(XC0/(P+BDEC)))
                        ENDIF
            ENDIF
            ENDIF
      ENDIF



C
C   REDUCES TO OGATA BANKS WHEN ALL CONSTANTS ARE SET TO ZERO
C     ==========================================================


            ARG1=DCMPLX(P-XM+XK2+XLAM)
            ARG2=DCMPLX(XTWTWOB*P*XK1/ARG1)
            ARG3=DCMPLX(ARG2-XM+V*XKP+XLAM+P)
            ARG4=DCMPLX(V**2/(4.0D+0*DL**2)+ARG3/DL)
            ARG5=DCMPLX(V/(2.0D+0*DL))
            ARGI=DCMPLX(CDSQRT(ARG4))
            ARG7=DCMPLX(ARG6*CDEXP(ICOLUMN*ARG5)*
  *CDEXP(-ARGI*ICOLUMN))
     FS=DCMPLX(ARG7/XC0)

      ELSEIF (FXNNUMB.EQ.2) THEN

C   SOURCE CONDITION,
C   ==================
      IF(IXFT.EQ.1)THEN
      ARG6=DCMPLX(XC0/P)
      ELSE
            IF(IXFT.EQ.2)THEN
                  XHEAV=DCMPLX(XGAP-TPRIME)
                  IF(XHEAV.LT.0)THEN
                  XC0=0.0
                  ENDIF
            ARG6=DCMPLX(XC0*(CDEXP(-TPRIME*P))/P)
            ELSE
```

```
                    IF(IXFT.EQ.3)THEN
                    XC0=DCMPLX(XC0*CDEXP(DCMPLX(-BDEC*XGAP)))
                    ARG6=DCMPLX(XC0/(P+BDEC))
                    ELSE
                        IF(IXFT.EQ.4) THEN
                        XC0=DCMPLX(XC0*(1.0d+0-CDEXP(DCMPLX(-
BDEC*XGAP))))
                        ARG6=DCMPLX(XC0-(XC0/(P+BDEC)))
                        ENDIF
            ENDIF
            ENDIF
        ENDIF

C
C   FUNCTION 2
C    REDUCES TO NON - HOMOGENOUS OGATA BANKS WHEN CONSTANTS ARE
SET TO ZERO.
C    REDUCES TO OGATA BANKS WHEN CONSTANTS AND INITIAL CONDITION
ARE SET TO ZERO
C
================================================================
========
        ALPHA=DCMPLX(P/(P+XKDET-XM+XLAM))
        BETA=DCMPLX(XK2-XM+XLAM)
        XBIGS=DCMPLX((1.0D+0-CDEXP(-BETA*XGAP))*XK1*XCATTAO/BETA)
    PHI=DCMPLX(-XCATTAO+XTWTWOB*XBIGS*(ALPHA-1.0D+0))
        THETA=DCMPLX(XM-XLAM-P-XTWTWOB*P*XKAT/((P+XKDET-
XM+XLAM)))
        XS=DCMPLX(PHI/THETA)
        ARG1=DCMPLX(XS)
        ARG2=DCMPLX((-PHI+ARG6*THETA)/THETA)
        ARG3=DCMPLX(V**2-4.0D+0*DL*THETA)

            ARG4=DCMPLX(V-CDSQRT(ARG3))
            ARG5=DCMPLX(ARG4*ICOLUMN/2.0D+0/DL)
            ARGFIN=DCMPLX(ARG1+ARG2*CDEXP(ARG5))
            FS=DCMPLX(ARGFIN/XC0)


        ENDIF

        RETURN
    END

C
C   ****************************************
```

```
C
C   NUMERICAL INVERSION OF LAPLACE TRANSFORMS
C
C   ****************************************
    SUBROUTINE
HOOG2(BIGT,ATERM,NTERM,T,C,XC0,TPRIME,BDEC,ICOLUMN,V,
         *DL,XTWTWOB,XK1,XK2,XKAT,XKDET,XM,
     *XLAM,XKP,XCATTAO,FXNNUMB,IXFT,XGAP)
C    **********************************

C    SUBROUTINE FOR NUMERICAL INVERSION OF LAPLACE TRANSFORMS
C    USING THE QUOTIENT-DIFFERENCE ALGORITHM OF DE HOOG ET AL. (1982)

C    IMPLEMENTED BY: C.J. NEVILLE
C                SEPTEMBER 1989

C    NOTES: 1. THIS IS A DOUBLE PRECISION VERSION
C           2. THIS VERSION IS DESIGNED TO INVERT ANALYTICAL LAPLACE
C             TRANSFORMED EXPRESSIONS

C    DECLARATION OF VARIABLES
C    ========================
     IMPLICIT COMPLEX*16 (A-H,O-Z)
     DIMENSION D(0:40),WORK(0:40)
     DOUBLE PRECISION T,BIGT,ATERM,C,PI,FACTOR,ARGI,RESULT
     DOUBLE PRECISION XC0,TPRIME,BDEC,V,DL,XTWTWOB,XK1,XK2,XKAT,
        *XKDET,XM,XLAM,XKP,XCATTAO,FXNNUMB,XGAP
C

     PI   = 3.14159265358979323846264338327950D+00
     ZERO = DCMPLX(0.0D+00,0.0D+00)
     ONE  = DCMPLX(1.0D+00,0.0D+00)
     TWO  = DCMPLX(2.0D+00,0.0D+00)
     FACTOR = PI/BIGT
     M2=2*NTERM

C    CHECK THAT NTERM IS A MULTIPLE OF 2 (>= 2)
C    ==========================================
     IF(M2.LT.2) THEN
      WRITE(8,100)
     WRITE(*,100)
100     FORMAT(5X,'ERROR: NTERM MUST BE GREATER THAN OR EQUAL TO 2')
       RETURN
     ENDIF
     M2=(M2/2)*2
```

```
C   CALCULATE Z
C   ===========
    Z=DCMPLX(DCOS(T*FACTOR),DSIN(T*FACTOR))

C   CALCULATE THE PADE TABLE
C   ========================
    ARG0=DCMPLX(ATERM,0.0D+00)
    AOLD=FS(ARG0,XC0,TPRIME,BDEC,ICOLUMN,V,DL,XTWTWOB,XK1,XK2,
       *XKAT,XKDET,XM,XLAM,XKP,XCATTAO,FXNNUMB,IXFT,XGAP)/TWO

    ARGI=FACTOR
    A=FS(DCMPLX(ATERM,ARGI),XC0,TPRIME,BDEC,ICOLUMN,V,DL,
       *XTWTWOB,XK1,XK2,XKAT,XKDET,XM,XLAM,XKP,XCATTAO,FXNNUMB,I
XFT,
   *XGAP)

C   INITIALIZE THE TABLE ENTRIES
C   ----------------------------
    D(0)=AOLD
    WORK(0)=ZERO
    WORK(1)=A/AOLD
    D(1)=-WORK(1)
    AOLD=A

C   CALCULATE SUCCESSIVE DIAGONALS OF THE TABLE
C   -------------------------------------------
    DO 10 J=2,M2

C   INITIALIZE CALCULATION OF THE DIAGONAL
C   --------------------------------------
      OLD2=WORK(0)
      OLD1=WORK(1)
      ARGI=ARGI+FACTOR
        A=FS(DCMPLX(ATERM,ARGI),XC0,TPRIME,BDEC,ICOLUMN,V,DL,
       *XTWTWOB,XK1,XK2,XKAT,XKDET,XM,XLAM,XKP,XCATTAO,FXNNUMB,I
XFT,
   *XGAP)

C   CALCULATE NEXT TERM AND SUM OF POWER SERIES
C   -------------------------------------------
      WORK(0)=ZERO
      WORK(1)=A/AOLD
      AOLD=A

C   CALCULATE DIAGONAL USING THE RHOMBUS RULES
C   ------------------------------------------
```

```
      DO 20 I=2,J
        QLD3=OLD2
        OLD2=OLD1
        OLD1=WORK(I)

C       QUOTIENT-DIFFERENCE ALGORITHM RULES
C       ----------------------------------
        IF((I/2)*2.EQ.I) THEN
C          I EVEN: DIFFERENCE FORM
C          -----------------------
          WORK(I)=OLD3+(WORK(I-1)-OLD2)
        ELSE
C          I ODD: QUOTIENT FORM
C          --------------------
          WORK(I)=OLD3*(WORK(I-1)/OLD2)
        END IF
20      CONTINUE

C     SAVE CONTINUED FRACTION COEFFICIENTS
C     ------------------------------------
      D(J)=-WORK(J)
10    CONTINUE

C     EVALUATE CONTINUED FRACTION
C     ===========================
C     INITIALIZE RECURRENCE RELATIONS
C     -------------------------------
      AOLD2=D(0)
      AOLD1=D(0)
      BOLD2=ONE
      BOLD1=ONE+(D(1)*Z)

C     USE RECURRENCE RELATIONS
C     ------------------------
      DO 30 J=2,M2
        A=AOLD1+D(J)*Z*AOLD2
        AOLD2=AOLD1
        AOLD1=A
        B=BOLD1+D(J)*Z*BOLD2
        BOLD2=BOLD1
        BOLD1=B
30    CONTINUE

C     RESULT OF QUOTIENT-DIFFERENCE ALGORITHM
C     =======================================
      RESULT=DBLE(A/B)
```

```
C    CALCULATE REQUIRED APPROXIMATE INVERSE
C    ======================================
     C=DEXP(ATERM*T)*RESULT/BIGT
     RETURN
     END
```

Sample input file, BIOFRAC.inp:

```
1.0E+1      XC0: INITIAL CONCENTRATION OF BACTERIA (M/L**3)
5.0E+3      TPRIME: DURATION OF CONSTANT INPUT FOR HEAVISIDE (T)
1.0E+4      BDEC: EXPONENTIAL RISE OR DECAY CONSTANT
5.0E+0      V: GROUNDWATER VELOCITY (L/T)
5.0E-1      ALP: DISPERSIVITY (L)
5.0E-4      XTWOB: FRACTURE APERTURE (L)
10          NFL: FRACTURE LENGTH (L)
2.0E+0      XFW: FRACTURE WIDTH(L)
5.0E-6      XCW: BACTERIAL CELL WIDTH (L)
5.0E-6      XCL: BACTERIAL CELL LENGTH (L)
5.0E-6      XCH: BACTERIAL CELL HEIGHT (L)
1.0E-13     XCMASS: MASS OF ONE BACTERIAL CELL (M/CELL)
2           NLL: NUMBER OF BIOFILM LAYERS ON A SINGLE FRACTURE WALL
3.0E-0      XK1: ADSORPTION CONSTANT(1/T)
6.0E+0      XK2: DESORPTION CONSTANT(1/T)
4.0E+0      XKDET: DETACHMENT CONSTANT (1/T)
1.0E+0      XKAT: ATTACHMENT CONSTANT (1/T)
0.0E-0      XMAX: GROWTH CONST (1/T)
0.0E-0      XLAM: DECAY CONSTANT OF BACTERIA (1/T)
1.0E-5      XKP: IRREVERSIBLE ADSORPTION CONSTANT (1/L)
0.0E+0      BKS: SATURATION COEFFICIENT (M/L**3)
1.0E+0      BS: CONCENTRATION OF SUBSTRATE (M/L**3)
1.000E-6    ERROR:
0.000000    ALPHA:
0.799930    TFACT:
16          NTERM:
0.0E+0      TSTART: STARTING TIME
5.0E+3      TSTOP: STOP TIME (DAY)
100         NT: NUMBER OF TIME POINTS
IXFT: 1- C0 ; 2- HEAVISIDE ; 3- EXP DECAY ; 4- EXP RISE
```

Sample output file, BIOFRAC.out:

ACCUMULATION OF BACTERIA IN FRACTURED MEDIA: C VS. T

Dispersivity	(l) =	.50000
Dispersion coefficient	(l**2/t) =	2.50000
Fracture aperture	(l) =	.00050
Fracure length	(l) =	00010
Rate-limited adsorption constant	(1/t) =	3.00000
Rate-limited desorption constant	(1/t) =	6.00000
Detachment constant	(1/t) =	4.00000
Attachment constant	(1/t) =	1.00000
Maximum growth rate of bacteria	(1/t) =	.00000
Decay constant of bacteria	(1/t) =	.00000
Irreversible adsorption constant	(1/t) =	.00001
Duration of the experiment	(1/t) =	5000.00000
Average conc. along fract. @switch	(1/t) =	.99926
Average sorbed conc. @switch	(1/t) =	.49963
Switch Time (XGAP)	(1/t) =	2200.00000

F(T)=C0

I	CONC.	TIME
1	.5000E+02	.9924E-06
2	.1000E+03	.9928E-06
3	.1500E+03	.9932E-06
4	.2000E+03	.9936E-06
5	.2500E+03	.9940E-06

6	.3000E+03	.9943E-06
7	.3500E+03	.9946E-06
8	.4000E+03	.9949E-06
9	.4500E+03	.9952E-06
10	.5000E+03	.9955E-06
11	.5500E+03	.9957E-06
12	.6000E+03	.9960E-06
13	.6500E+03	.9962E-06
14	.7000E+03	.9969E-06
15	.7500E+03	.9995E-06
16	.8000E+03	.1011E-05
17	.8500E+03	.1057E-05
18	.9000E+03	.1208E-05
19	.9500E+03	.1646E-05
20	.1000E+04	.2779E-05
21	.1050E+04	.5427E-05
22	.1100E+04	.1110E-04
23	.1150E+04	.2239E-04
24	.1200E+04	.4341E-04
25	.1250E+04	.8034E-04
26	.1300E+04	.1420E-03
.		
.		
.		
99	.4950E+04	.9992E+00
100	.5000E+04	.9993E+00

Sample plot file, BIOFRAC.plt:

ACCUMULATION OF BACTERIA IN FRACTURED MEDIA: C/C0 VS. T

100	0
.5000E+02	.9924E-06
.1000E+03	.9928E-06
.1500E+03	.9932E-06
.	
.	
.	
.4750E+04	.9987E+00
.4800E+04	.9988E+00
.4850E+04	.9989E+00
.4900E+04	.9991E+00
.4950E+04	.9992E+00
.5000E+04	.9993E+00

APPENDIX B

COMPARISON OF OGATA-BANKS SOLUTION TO PHASE I AND NON-HOMOGENOUS OGATA-BANKS SOLUTION TO PHASE II

B.1 Comparison of Ogata Banks Solution and the code OGATA to Phase I solution and the code BIOFRAC

In order to develop a differential equation to account for transport of solutes in porous media, a flux of solute into and out of a fixed volume element is considered. Advection and hydrodynamic dispersion are the physical processes that control this flux. The principal equation that descirbes these processes is called the advection-dispersion equation. The one dimensional form of the advection-dispersion equation for transport of solutes in saturated, homogenous, isotropic, steady-state, uniform flow is (Freeze et al., 1979):

$$D\frac{\partial^2 c}{\partial x^2} - v\frac{\partial c}{\partial x} = \frac{\partial c}{\partial t} \qquad \text{(B.1)}$$

where D coefficient of hydrodynamic dispersion, c is concentration of solute, v is velocity, x is linear coordinate direction taken along the flow line and t is time. The initial and boundary conditions are:

$$c(x,0) = 0$$

(B.2)

$$c(0,t) = c_0$$

(B.3)

$$c(\infty,t) = 0$$

(B.4)

where c_0 is the initial source concentration.

The equation, boundary conditions and the solution were presented by Ogata and Banks in 1961. Thus the solution is referred to as the Ogata-Banks solution.

Equation B.1 is a non homogenous, partial differential equation. In order to eliminate the time derivative Laplace transform can be used. The application of Laplace transform results in:

$$\frac{p\bar{c} - c(x,0)}{D} = \frac{\partial^2 \bar{c}}{\partial x} - \frac{v}{D}\frac{\partial \bar{c}}{\partial x}$$

(B.5)

$$\bar{c}(0,p)=\frac{c_0}{p}$$

(B.6)

$$\bar{c}(\infty,p)=0$$

(B.7)

where $\bar{c}$ is the concentration in Laplace space and p is the Laplace variable. If equation B.2 is submitted into equation B.5, the resulting equation in standard form is:

$$\frac{\partial^2\bar{c}}{\partial x}-\frac{v}{D}\frac{\partial\bar{c}}{\partial x}-\frac{p}{D}\bar{c}=0$$

(B.8)

which is an ordinary differential equation with the solution:

$$\bar{c}(x,p)=A\left\{\exp\left[\frac{vx}{2D}+\sqrt{\frac{v^2}{D^2}+\frac{4p}{D}}\frac{x}{2}\right]\right\}+B\left\{\exp\left[\frac{vx}{2D}-\sqrt{\frac{v^2}{D^2}+\frac{4p}{D}}\frac{x}{2}\right]\right\}$$

(B.9)

where A and B are integration constants that can be found by substituting equations B.6 and B.7 into equation B.9. The resulting solution in Laplace space is:

$$\frac{\bar{c}}{c_0} = \frac{1}{p}\left\{\exp\left[\frac{vx}{2D} - \sqrt{\frac{v^2}{D^2} + \frac{4p}{D}}\frac{x}{2}\right]\right\}$$

(B.10)

In order to verify the analytical solution for Phase I, the solution is compared to equation B.10. The Phase I solution presented is:

$$\bar{c}(x,p) = \bar{f}(p)\left\{\exp\left(x\frac{v - \sqrt{v^2 + 4D\alpha}}{2D}\right)\right\}$$

(B.11)

where

$$\alpha = vk_p + \lambda - \mu + p + \frac{2}{2b}\left(p\frac{k_1}{p - \mu + k_2 + \lambda}\right)$$

(B.12)

In case of advection-dispersion equation, the additional processes in Phase I do not exist. Thus irreversible adsorption, decay, growth, rate-limited adsorption and rate-limited desorption constants are set to zero which results in:

$$\alpha = p$$

(B.13)

When B.13 is substituted into equation B.11 and the source function is set to constant source cncentration , that is:

$$\bar{f}(p) = c(0, p) = \frac{c_0}{p}$$

(B.14)

the equation B.11 becomes:

$$\bar{c}(x, p) = \frac{c_0}{p}\left\{\exp\left(x\frac{v - \sqrt{v^2 + 4Dp}}{2D}\right)\right\}$$

(B.15)

which is exactly the same equation as equation B.11.

Following the verification of the analytical solution, equation B.11 is coded using Fortran 77. The breakthrough curves, using the codes OGATA and BIOFRAC, are generated using the flowing parameters:

Constant source concentration	50 gr m^{-3}
Groundwater velocity	5.0 m day^{-1}
Dispersivity	0.5 m

Duration	6.5 days

Table B.1 Input data

The irreversible adsorption, growth, decay, rate-limited adsorption and rate-limited desorption coefficients are set to zero in code BIOFRAC. The resulting two breakthrough curves show perfect agreement with each other, which verifies that the code BIOFRAC (Figure 3.1).

B.2 Comparison of Non-Homogenous Ogata Banks Solution and the code NHOGATA to Phase II solution and the code BIOFRACII

Phase II solution is a non-homogenous partial differential equation since the initial conditions for sorbed and aqueous phases are not zero. In order to make the advection-dispersion equation (B.1), a non-homogenous equation for verification purposes, the initial condition (B.2) has to change to:

$$c(x,0) = S$$

(B.16)

where S is an arbitrary concentration value. The advection-dispersion equation in Laplace space is:

$$\frac{p\bar{c} - c(x,0)}{D} = \frac{\partial^2 \bar{c}}{\partial x} - \frac{v}{D}\frac{\partial \bar{c}}{\partial x}$$

(B.17)

as presented before. When equation B.16 is substituted into equation B.17, the resulting equation is:

$$\frac{\partial^2 \bar{c}}{\partial x} - \frac{v}{D}\frac{\partial \bar{c}}{\partial x} - \frac{p}{D}\bar{c} = -\frac{S}{D}$$

(B.18)

which is a non-homogenous differential equation that can be solved using the method of variation of parameters. The general solution in Laplace space is:

$$\bar{c}(x,p) = \frac{S}{p} + E\left\{\exp\left(\frac{1}{2}\frac{v - \sqrt{v^2 + 4Dp}}{D}x\right)\right\} + F\left\{\exp\left(\frac{1}{2}\frac{v + \sqrt{v^2 + 4Dp}}{D}x\right)\right\}$$

(B.19)

where E and F are inegration constants. When the boundary conditions are applied, the final solution is:

$$\bar{c}(x,p) = \frac{S}{p} + \frac{c_0 - S}{p}\left\{\exp\left(\frac{1}{2}\frac{v - \sqrt{v^2 + 4Dp}}{D}x\right)\right\}$$

(B.20)

In order to verify the analytical solution for Phase II, the solution is compared to equation B.20. The Phase II solution presented is:

$$\bar{c}(x,p)=\frac{\phi}{\theta}+\frac{-\phi+\bar{f}(p)\theta}{\theta}\exp\left\{\frac{1}{2}\frac{\left(v-\sqrt{v^2-4D\theta}\right)}{D}x\right\}$$

(B.21)

$$\theta=\mu-\lambda-p-\frac{2}{2b}\frac{pk_{at}}{p-\mu+\lambda+k_{\det}}$$

(B.22)

$$\phi=-c_\tau+\frac{2}{2b}\left(\frac{p}{p+k_{\det}-\mu+\lambda}-1\right)\left(\frac{k_1c_\tau}{k_2-\mu+\lambda}\left[1-\exp\left(-\left(k_2-\mu+\lambda\right)\tau\right)\right]\right)$$

(B.23)

where

$$c(x,0)=c_\tau \qquad \text{(B.25)}$$

In case of non-homogenous advection-dispersion equation, the additional processes in Phase II do not exist. Thus decay, growth, attachment and detachment constants are set to zero which results in:

$$\theta = -p$$

(B.26)

$$\phi = -c_\tau$$

(B.27)

When B.25 and B.26 are substituted into equation B.21 and the source function is set to constant source concentration , that is:

$$\bar{f}(p) = c(0, p) = \frac{c_0}{p}$$

(B.27)

the equation B.21 becomes:

$$\bar{c}(x,p) = \frac{c_\tau}{p} + \frac{c_\tau + c_0}{p} \exp\left\{\frac{1}{2}\frac{\left(v - \sqrt{v^2 - 4D\theta}\right)}{D}x\right\}$$

(B.28)

which is exactly the same equation as equation B.20.

Following the verification of the analytical solution, equation B.20 is coded using Fortran 77. Similarly, Phase II solution B.21 is coded separately and named BIOFRACII. The breakthrough curves, using the codes NHOGATA and BIOFRACII, are generated using the flowing parameters:

Constant source concentration	50 gr m^{-3}
Groundwater velocity	5.0 m day^{-1}
Dispersivity	0.5 m
Duration	6.5 days
c_τ = S = Value that makes the equations non-homogenous	10

Table B.2 Input data

The irreversible adsorption, growth, decay, attachment and detachment coefficients are set to zero in code BIOFRACII. The resulting two breakthrough curves show perfect agreement with each other, which verifies that the code BIOFRAC (Figure 3.2).